Sensing and haptic technologies for applications in medical robotics

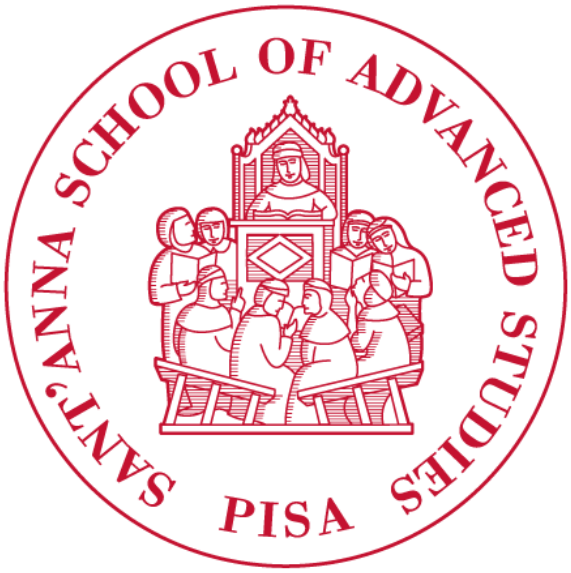

June 2018

Candidate
Renato Caliò

Supervisor
Calogero Maria Oddo

Tutors
Gastone Ciuti
Christian Cipriani
Paolo Dario

Abstract

The sense of touch is crucial in humans for understanding the world and interacting with it. It gives consistency to what otherwise would remain just a shape, and it is therefore of primary importance in our everyday life. Being deprived of such faculty is highly disabling for those individuals who have incurred in a hand loss, making artificial limb substitution even more challenging. Also in robotics, the importance of tactile information is considered essential for enabling dexterous manipulation.

In medical environments, the introduction of **minimally invasive surgery** (MIS) does not allow the surgeons to avail of the sense of touch. On one hand, MIS has significantly reduced invasiveness in surgical procedures, making the patient recovery much faster. However, on the other hand, physicians can not avail of tactile information, making manipulation tasks more difficult and, in certain cases, diagnoses based on indirect estimations (*e.g.* visual inspection instead of palpation).

In the last decades, physiology studies have shed light on the characteristics of the human sense of touch allowing a better understanding of the basic working principles in nature. Engineering research has put lot of effort in translating this knowledge in order to mimic the human sensory capabilities, achieving important results both in sensory restoration and robotics. Physiologists proved that the sense of touch is able to convey highly complex information. This paves the way to technological solutions for improving **sensory substitution**, availing of the scientific awareness of human touch capabilities. It is well known that individuals, who are subject to sight or hearing loss, use touch to substitute the lost sense. Haptic technology can help improving the condition of disabled individuals and make assistive aids more effective.

The present work of thesis concerns the two topics of: *i)* haptic feedback in medical and surgical scenarios; and *ii)* technologically-aided sensory substitution through tactile stimulation. Our effort has been therefore split to pursue two complementary results: *i)* proving a robotic device for capsule endoscopy able to discern tactile cues for diagnosis purposes, and *ii)* developing a haptic stimulation technology for sensory substitution, applicable in assistive device for sensory impaired people and in virtual reality for training and remote control.

Thesis outline

Introduction on haptics provides a summary about physiology of the human sense of touch and the state-of-the-art of artificial tactile sensing. The technology here presented concerns mainly sensors for robotics and prosthetics, presenting at the end the MEMS-based tactile sensor, originally developed for prosthetics, that has been involved in the scientific works later presented in **Part A** of this thesis.

Part A focuses on the development of a robotic capsule for colonoscopy equipped with a tactile tri-axial sensor. **Chapter 2** gives an overview of the state-of-the-art in capsule endoscopy, defining the scope of the related scientific works, presented in the subsequent sections. **Chapter 3** shows a case study involving the proposed tactile robotic capsule for closed-loop force control during locomotion in an endo-luminal environment. In **Chapter 4** we present a study involving the tactile robotic capsule for autonomous classification of non-polypoid tumours (NPT) by assessing the hardness of rubber inclusions in a soft silicone matrix.

Part B concerns the research work carried out in the field of tactile stimulation for sensory substitution. In particular, **Chapter 5** provides a state-of-the-art analysis of sensory substitution devices for deaf or visually impaired people. **Chapter 6** discusses a method we developed to encapsulate piezoelectric actuators in order to improve their integrability and performances for tactile stimulation. The encapsulated sensors are then characterized. Furthermore, we presented a psychophysical test conducted with a haptic glove embedding two of such sensors. In **Chapter 7** we show a study involving a haptic glove and a vibro-

tactile wrist-band used in the context of a virtual reality environment. The technology is conceived for applications in remote control, sensory substitution and surgical tele-operation, thus representing the bridge linking **Part A** and **Part B** of the present work of thesis.

Finally, the **Conclusions and future perspective**, of the work presented, are discussed in the last chapter.

Contents

Introduction on haptics

Tactile sensors define a category of devices able to acquire information related to physical touch. Their scope spans normal and shear forces, vibration, stiffness, texture and temperature measurements. The maturation of this technology has been anticipated for over 40 years [1, 2]. Anyhow, initial issues related to design criteria, lack of standard benchmarks to assess reliability of the sensors and high cost, delayed this technology to establish until the 1990s [3]. Since the early stages of research, targeted applications were seen in medical robotics and industrial automation. In the last decades, the research trend in the field of tactile sensing has been constantly increasing, as shown in TABLE I. This chapter consists of a brief introduction on the physiology of the human sense of touch, in Section 1.1, in order to summarize the scientific knowledge in this matter, and a short overview on the state-of-the-art of artificial tactile sensing, in Section 1.2, which also represents the basis of the work presented later, in PART-A of this thesis.

TABLE I
PAPERS PUBLISHED PER DECADE, STARTING FROM 1970, USING THE SEARCH TERMS "TACTILE AND SENSORS".

Year	Scopus	IEEE	Springerlink
1970-1979	41	11	7
1980-1989	522	167	35
1990-1999	703	640	200
2000-2009	1751	1300	394
2010-2018	3461	2452	1074

1.1. Physiology of human sense of touch

The sense of touch represents our interface to explore the physical world, to shape it and manipulate it. Highly accurate description of mechanical events is possible thanks to the mechano-receptive afferents innervating the glabrous skin. In the last decades, the characteristics of these units and their role have been studied in order to allow a better understanding of perception and motor functions in human. About 17,000 mechanoreceptors innervate the glabrous skin of the human hand [4, 5]. They are classified in two categories, based on the nature of their response to sustained step indentation of the skin. Slowly adapting units exhibit a sustained discharge to constant stimuli. Fast adapting units have, on the other hand, a more pronounced sensitivity to dynamic events. Both groups are further divided in two sub-categories, based on their receptive fields. Fast adapting type I (FA I, also called RA I) and slowly adapting type I units (SA I), having small and well defined receptive fields, and fast adapting type II (FA II, or RA II) and slowly adapting type II (SA II) characterized by wider fields with diffuse borders [6]. Type I afferents terminate superficially in the skin, and they have higher density in the fingertips. The population of FA I is larger than SA I (respectively 43 % and 25 % of the 17 000 tactile units), reflecting the importance of extracting dynamic features from mechanical events. To give a better idea, FA I reach innervation densities of 140 units per cm^2 on the fingertips, whereas SA I units are around 70 per cm^2 [7]. The end organs of FA I and SA I units are called, respectively, Meissner's corpuscles and Merkel's discs [8]. FA II and SA II units terminate deeper in dermal and subdermal tissues, and are less dense and more uniformly distributed. They constitute, respectively, the 13 % and 19 % of the tactile receptors. Their endings are named are Pacinian corpuscles (FA II) [9] and Ruffini endings (SA II) [10]. Figure 1 illustrates the location of the four types of receptors. Figure 2 shows the receptive fields and the characteristic discharge of each type of mechano-receptors. It has been proved that primary sensory neurons transmit information by their firing rates (see neural spike train in Figure 2C). Anyhow, evidences show that relative timing of the first impulses in individual units of ensembles of afferents conveys information about the direction of fingertip force and the

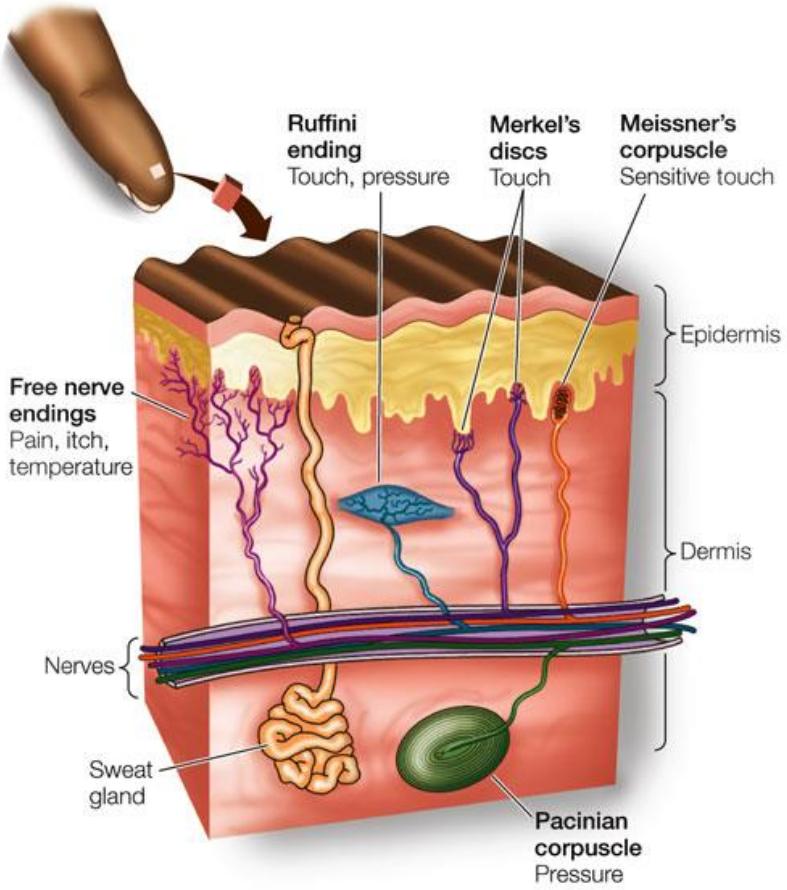

Figure 1 – Representation of glabrous skin section illustrating the different types of mechanoreceptive endings and their position [image from Life Science of Biology - 8th Edition - 2007 Sinauer Associates]

shape of the surface contacting the fingertip [11]. Manipulation of everyday objects is a complex task, which involves not just single, but a population of afferents all over the fingertip, highlighting the importance of patterns of firing in ensembles of tactile afferents [12]. The curvature of objects influences firing rates in most FA‑I, SA‑I and SA‑II afferents [13]. Whereas SA‑II afferents probably provide coarser information about object shape [5]. Changes in either surface shape or force direction can alter the first‑spike latency of individual afferents. For a code based on relative spike timing to be effective, sufficient numbers of afferents must be recruited. This is ensured by the high density of afferents, especially in the fingertips. It has been estimated that the firing activity of five FA I afferents is enough to discriminate different surface curvatures and force directions. While, a double amount of SA I is necessary for a corresponding reliability, because of a larger variability in first-spike latency [12]. The relative timing of impulses presumably also contains information

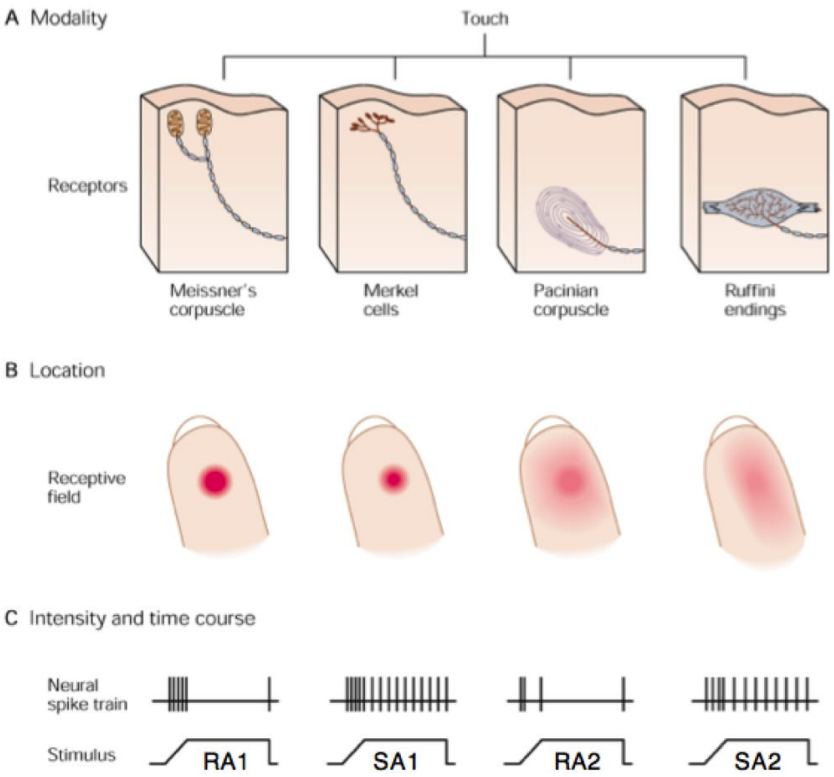

Figure 2 – Schematic representation of the four types of receptors based on their receptive fields and the response to sustained step indentation of the skin [image from Barrett, Kim E. "Ganong's review of medical physiology. 2010."]

about other crucial initial contact parameters, such as the frictional condition and contact events that occur between held objects and other objects. The lack of a consistent relationship between the latencies for response onsets and firing rates in tactile afferents suggests that these two codes in fact provide independent information about tactile events. It is possible that different codes are used by different processes. For example, relative spike timing may primarily support fast stimulus classification in the control of action, which operates on rapidly varying signals. Firing rates, by contrast, might preferentially support perceptual mechanisms that operate under less time pressure and, often, on steadier signals. Furthermore, the fact that the two codes seem to convey similar information but in apparently independent ways suggests that they represent complementary monitoring systems.

1.2. Artificial tactile sensing

A hand loss is an unfortunate and highly disabling event that strongly affects the quality of life of an individual. Although hand prosthetics has reached notable technological advances in the last years [14-16], restoring the sense of touch is fundamental to allow a close to natural sensation of the artificial limb, and to enable dexterous manipulation [17]. As in humans, the sense of touch in robots would contribute to improve their interaction with the surrounding environment. As a consequence, lot of effort has been put in developing systems capable of mimicking the human sense of touch. In particular, two aspects have been focused: the development of artificial sensitive skin (both synthetic skin and bio-artificial skins), and the transduction mechanism. Microelectronics related materials (silicon and glass), plastic and polymeric materials (*e.g.*, polydimethylsiloxane, PDMS) have been used, as well as hybrid artificial-biological microstructures (BioMEMS), which can be fabricated with different classes of artificial, bio-artificial, and bio-engineered materials. Biological components such as proteins, cells and tissues can also be used [18, 19]. Using soft materials as an artificial skin is useful to protect the embedded tactile sensors. Furthermore, the high conformability of the material helps increasing the contact area and the contact friction coefficient of the sensing system, thus improving grasp stability [20]. Thorough

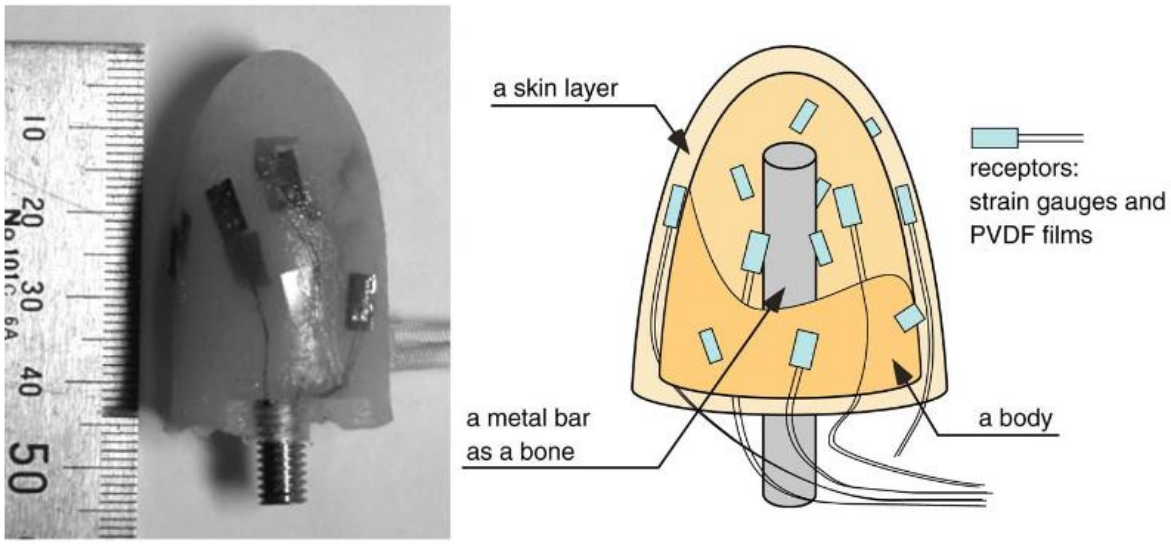

Figure 3 – Anthropomorphic soft fingertip picture (left) and its cross sectional sketch (right), developed by Hosoda et al. [24]

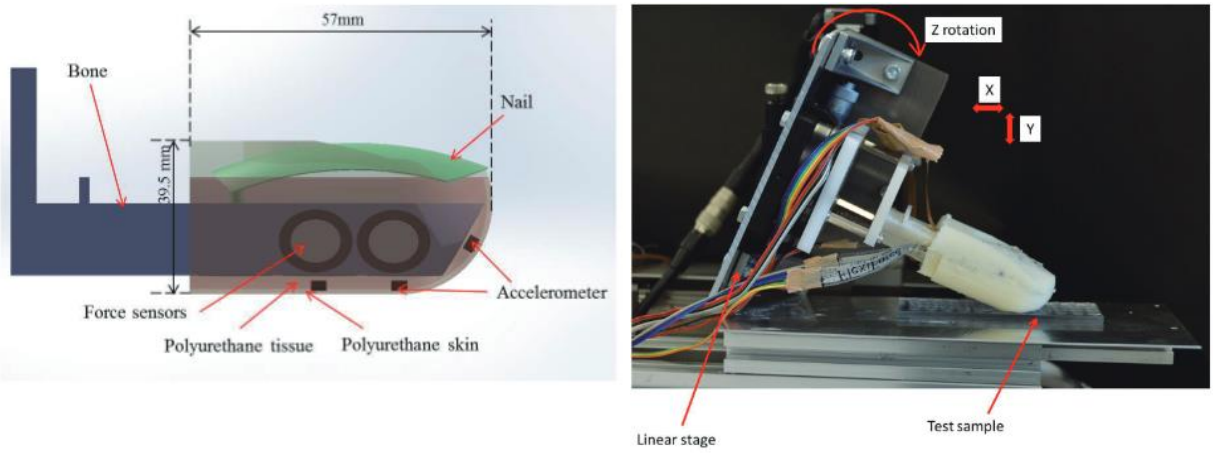

Figure 4 – Biomimetic fingertip embedding accelerometers and force sensors, proposed by Chaturanga et al. [26]

reviews of tactile sensors technology for the design of the skin and transduction mechanisms, either with synthetic or bio-hybrid approaches, have been published [3, 19, 21-23]. Hereafter, we mention few examples that we find interesting for the sake of the present dissertation. In 2006, Hosoda et al. demonstrated an anthropomorphic soft fingertip embedding strain gauges and piezoelectric sensors, arranged randomly at different depths and locations [24]. The fingertip structure consists of a metallic bone, two silicon rubber layers of different hardness and the receptors: strain gauges and PVDF (polyvinylidene fluoride). As for humans, the device is meant to learn to acquire meaningful information from the receptors in order to detect slippage and object textures. The authors conducted experiments of discrimination by pushing and/or rubbing the object. Figure 3 shows a picture and a cross section of the device. Ho et al. developed a tactile hemispherical soft fingertip with size similar to that of a human thumb. The sensor is a micro-scaled force/torque sensor able to output one component of force and two components of torque simultaneously. It is embedded in a polyurethane rubber hemispherical dome. The sensor was used for texture recognition and incipient-slip detection [25]. Chaturanga et al. presented in 2012 a biomimetic fingertip for humanoid robots. The fingertip has a bone, covered with a polyurethane rubber layer that mimics tissue and another polyurethane layer with a different hardness, which mimics human skin layer. It embeds three accelerometer and seen force sensors. It was used for detecting micro-vibrations and force modalities, and it was able to identify different types of surface textures [26]. Figure 5 shows a rendering of

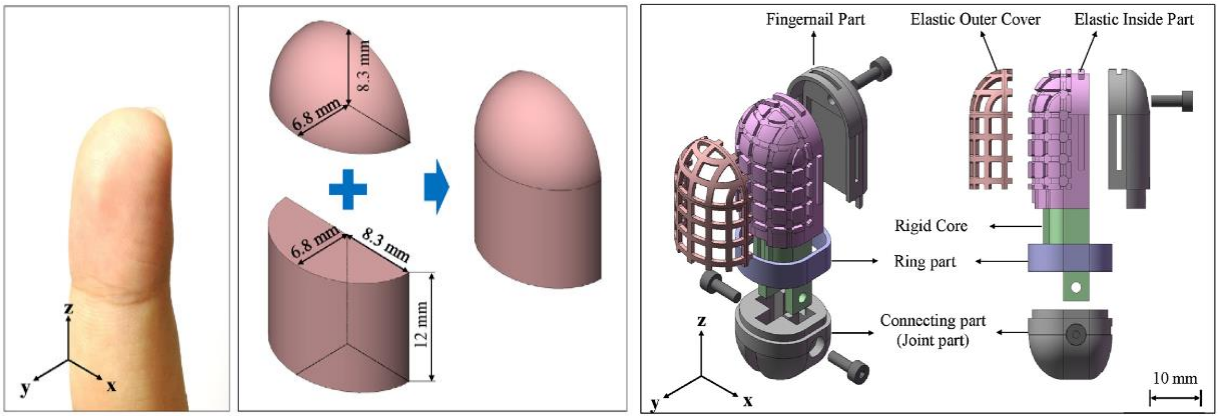

Figure 5 – 3D-curved shaped robotic fingertip by Kim et al. [27]

the device and the set-up used for testing. Kim et al. fabricated and tested a robotic fingertip with a 3D-curved shape resembling a human finger. It embeds a flexible grid with 37 contact-resistance sensing points shaped to match the fingertip structure (Figure 5). The device senses both force and location simultaneously. The slip information can also be extracted indirectly by tracking the change of the center of the contact point [27]. In 2015, Park et al. presented a microstructured ferroelectric skin, inspired to human fingertips, to discriminate static and dynamic pressure and temperature stimuli.[28]. The authors fabricated fingerprint-like patterns and interlocked microstructures in ferroelectric films (graphene oxide sheets in PVDF matrix), resembling epidermal-dermal microridges of human fingers, in order to enhance the piezoelectric, pyroelectric, and piezoresistive sensing of static and dynamic mechanothermal signals (Figure 6).

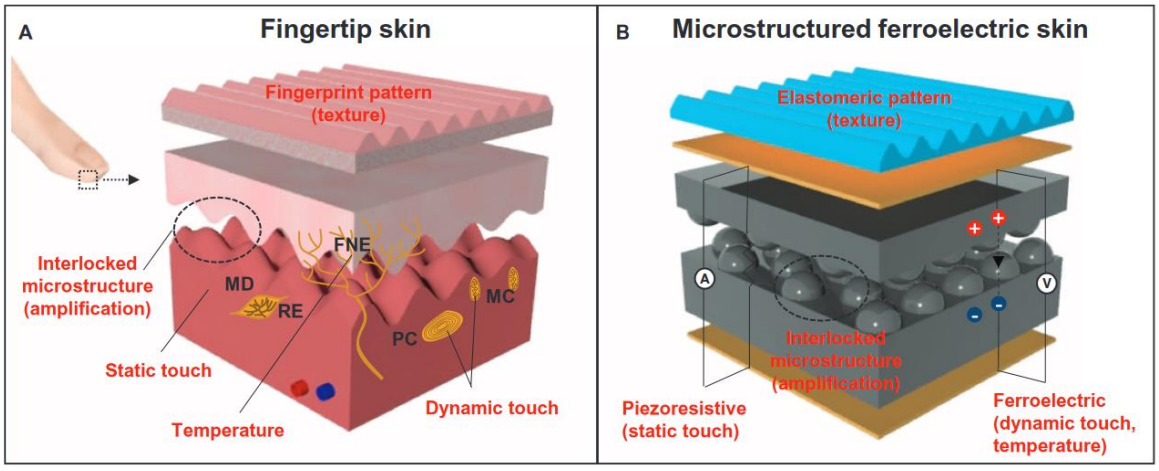

Figure 6 – Microstructured ferroelectric skin resembling the human fingertip anatomy presented by Park et al. [28]

The sensor was tested for simultaneous monitoring of pulse pressure and temperature of artery vessels, detection of acoustic signals, and discrimination of surface textures. In 2008, after patenting the technology, Wettels et al. presented a tactile sensor array, called BioTac®, aiming at mimicking the mechanical properties of the receptors in the human fingertip. The device consists of a rigid core and conductive fluids contained within an elastomeric skin. Electrodes, placed on the surface of the rigid core, are used to read impedance changes when an external force deforms the fluid path [29, 30]. The device was later refined by adding thermistors for temperature readings [31]. BioTac® is now commercialized by Sintouch® LLC. In 2005, a piezo-resistive MEMS micro tri-axial force sensor (called microTAF) was demonstrated by Beccai et al. [32]. The sensor consists of a central pillar which mechanically deflects four piezo-resistive channels when in contact with an external body. It has been integrated in artificial fingertips for roughness encoding and surface discrimination [33-35] (Figure 7). In 2014, it has been integrated in a prosthetic finger to restore tactile sensory feedback to an amputee subject [36].

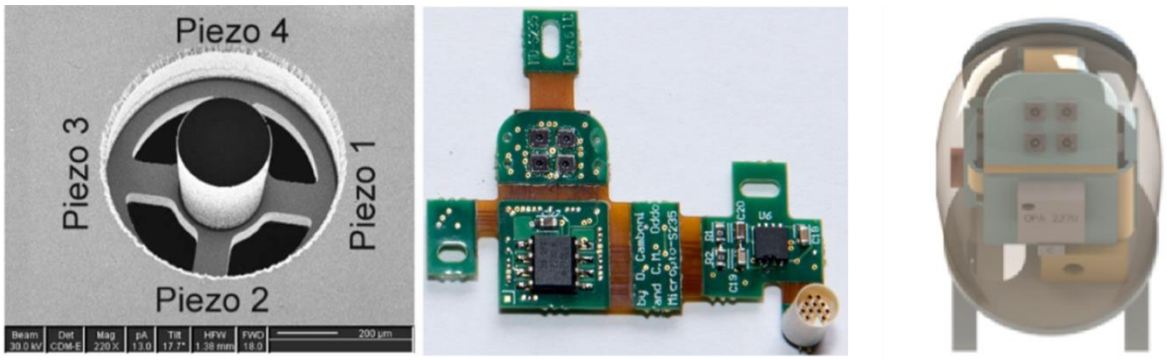

Figure 7 –MicroTAF sensor proposed by Beccai et al. (left), circuit for prosthetic fingertip containing an array of 4 microTAF (center) and 3D rendering of prosthetic fingertip (right) [36]

PART A – Capsule endoscopy

Chapter

2. State-of-the-art on capsule endoscopy[1]

Digestive diseases are a major burden for society and healthcare systems, and with an aging population, the importance of their effective management will become critical. Healthcare systems worldwide already struggle to insure quality and affordability of healthcare delivery and this will be a significant challenge in the midterm future. Wireless capsule endoscopy (WCE), introduced in 2000 by Given Imaging Ltd., is an example of disruptive technology and represents an attractive alternative to traditional diagnostic techniques. WCE overcomes conventional endoscopy enabling inspection of the digestive system without discomfort or the need for sedation. Thus, it has the advantage of encouraging patients to undergo gastrointestinal (GI) tract examinations and of facilitating mass screening programmes. With the integration of further capabilities based on micro-robotics, *e.g.* active locomotion, embedded therapeutic modules, haptic feedback, WCE could become the key-technology for GI diagnosis and treatment.

This chapter presents an overview on WCE and describes the state-of-the-art of current endoscopic devices with a focus on research-oriented robotic capsule endoscopes enabled by microsystem technologies. The purpose is to present the scope where the works on

[1] The present chapter is adapted from the journal paper "Ciuti, G., Caliò, R., Camboni, D., Neri, L., Bianchi, F., Arezzo, A., Koulaouzidis, A., Schostek, S., Stoyanov, D., Oddo, C. M., Magnani, B., Menciassi, A., Morino, M., Schurr , M. O., & Dario, P. (2016). Frontiers of robotic endoscopic capsules: a review. Journal of Micro-Bio Robotics, 11(1-4), 1-18."

tactile endoscopy presented later in chapters 3 and 4 takes place, as well as the scientific need behind.

2.1. Introduction

Cancer is a major cause of morbidity and a leading cause of mortality worldwide, accounting for 8.2 million deaths in 2012, with 14.1 million new cases and 32.6 million people living with cancer (diagnosed in the previous 5 years) [37]. Moreover, death from cancer is projected to rise to over 13 million by 2030 [38]. In the digestive tract, the most common cancers occur in the oesophagus, stomach and colorectum. Colorectal cancer (CRC), in particular, accounted for 1,360,000 new cases in 2012, being the third most common cancer in men (746,000 cases, 10 % of the total) and the second in women (614,000 cases, 9.2 % of the total) worldwide. Furthermore oesophageal cancer accounted for 456,000 new cases worldwide in 2012 (3.2 % of the total) and stomach cancer for 952,000 new cases (6.8 % of the total) in 2012, making it the fifth most common malignancy worldwide. Differently, cancers of the small bowel are rare, representing only about 3 % of new cases per year with respect to CRC [37]. As demonstrated by the aforementioned statistics, colorectal cancers represent the most significant pathology within the gastrointestinal (GI) tract; for this reason, particular attention has been devoted to CRC in this review. A significant aspect is related to its diagnosis and treatment. In particular, it is worth mentioning that the survival rate of CRC patients can reach almost 90 % –when diagnosis is made at an early stage– falling to less than 7 % for patients with advanced disease. Several screening tests are effective in reducing CRC incidence and/or mortality, and population screening has been rolled out in Europe and in the United States, mostly for patients older than 50 years or for those with a family history of CRC [39-41]. However, CRC screening programmes can be life-saving only if reliable and with high adherence, which is directly related to invasiveness and consequent discomfort (as low participation rates dilute the intrinsic efficacy of CRC screening).

To date, conventional colonoscopy is considered to be the most effective method for CRC diagnosis and it represents the gold standard for the evaluation of colonic disease due to its

ability to visualise the inner surface of the colon, acquire biopsies and treat pre-neoplastic, early and stage neoplastic lesions. However, invasiveness, patient discomfort, fear of pain, and –more often than not– the need for conscious sedation limit the take-up of screening colonoscopy [42]. The technology behind standard colonoscopy consists of a long, semi-rigid insertion tube with a steerable tip (stiff if compared to the colon), which is pushed by the physician from the outside. As a result of this driving approach, scope looping occurs during the insertion phase leading to pain and potential tissue damage or even perforation (e.g., 0.1–0.3 % for diagnostic procedures in colonic tissue) [43].

On the other hand, wireless capsule endoscopy (WCE), which has been established in the last decade, represents an appealing alternative to traditional endoscopic techniques [44]. WCE enables inspection of the entire GI tract without discomfort or the need for sedation, thus avoiding many of the potential risks of conventional endoscopy. Therefore, it can encourage patients to accept GI tract examinations without concerns of pain or invasiveness. However, current WCE models are passive devices and their motion relies on natural bowel peristalsis, which implicates the risk of failing to capture images of significant regions, since the practitioner cannot control capsule/camera orientation and motion [45]. For this reason, they are commonly used for inspecting the small bowel (even if small bowel cancer is much less frequent than CRC, but not approached with standard endoscopes), seeking for sources of occult bleeding. The small bowel, in fact, has a virtual lumen that does not require insufflation for distension for a proper inspection in most cases and does not need navigation to focus on points of interests. Unlike the small bowel, the large bowel requires proper distension for inspection and navigation in order to allow visual orientation. Therefore, capsule endoscopy should integrate active motion. When applied to the examination of the large bowel, robotic endoscopic capsules and innovative robotic endoscopes may overcome the drawbacks of pain and discomfort, but they still lack in reliability, diagnostic accuracy and –overall– fail due to their inherent inability to combine therapeutic functions with common screening aims [46-48]. Furthermore, these techniques (mainly for robotic endoscopes) are often difficult to learn and master; hence, strict dependence on the operator's skills introduces subjectivity to the procedure and consistent

relevant costs for the healthcare systems willing to deliver a standardised procedure [49, 50].

2.2. Medical needs and clinical issues

Technology should help in further promoting CRC screening and allow, as a consequence, a tailored and less invasive treatment. However, the aforementioned factors limit the acceptance of conventional colonoscopy-based screening protocols. For these reasons, different techniques have been proposed, such as the combination with faecal occult blood test (FOBT), in order to reduce the number of colonoscopies. Nevertheless, this approach is burdened by a high rate of false negative results. Another alternative is based on computed tomography (CT) of the colon; however, it requires ideal bowel preparation and considerable X-ray exposure [42].

Direct visualisation of the colonic mucosa is preferred in order to detect subtle mucosal alterations, as in inflammatory bowel diseases, as well as any flat or sessile colonic lesions. Nevertheless, standard colon WCE shows insufficient sensitivity in detecting colonic lesions even after a major technology upgrade [51]; furthermore, the intense bowel preparation required, together with the fact that it is not possible to perform a biopsy, deprives colon WCE from getting the lead in the field [52]. An ideal diagnostic tool for the colon should

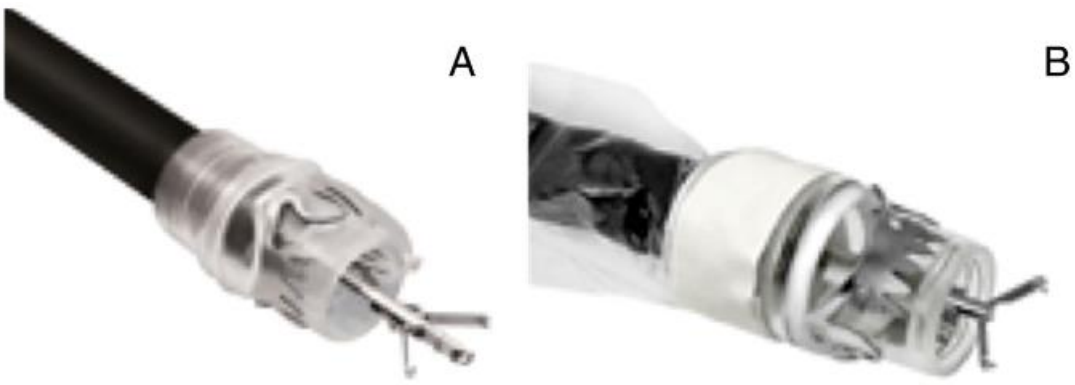

Figure 8 – a) OTSC®; and b) FTRD® system by Ovesco Endoscopy AG (Courtesy of Ovesco Endoscopy AG, Tübingen, Germany)

provide direct visualisation and pain-free navigation through a sufficiently distended colon. This can be achieved by avoiding pressure on the bowel wall when advancing as well as avoiding extensive uncontrolled painful distension of the colon and/or loop formation. Regarding lesion visualization, the medical device should be reliable in detecting lesions at least >5 mm, which are characterized by increased potential for dysplasia, and this of course includes the areas behind bowel folds, which are often unexplored with conventional endoscopy, despite the wide angle of vision, and/or the use of transparent caps [53].

2.3. Commercial solutions: main current approaches

Wolf and Schindler are the fathers of modern GI endoscopy. They pioneered the inspection of the GI tract with semi-flexible endoscopes in 1868. Nowadays, flexible scopes are considered the mainstream endoscopic tools; they enable reliable diagnoses in the GI tract showing also therapeutic and surgical capabilities. However, since scopes are still rather rigid instruments, there are high chances of traumatic procedures, also owing to the manoeuvring mechanism, which limits patients' tolerability and acceptance of the diagnostic technique. Moreover, pain or sedation-related issues limit the pervasiveness of a mass-screening campaign, which is a high public health priority, making patients reluctant to undergo endoscopy. Only mass screening guarantees the appropriate selection of who should undergo endoscopy to ensure early detection and treatment of asymptomatic pathologies, with particular attention to CRC.

As said, diagnosis and treatment in the GI tract are dominated by the use of flexible endoscopes. A few large companies, namely Olympus Medical Systems Co. (Tokyo, Japan), Pentax Medical Co. (Montvale, NJ, USA), Fujinon, Inc. (Wayne, NJ, USA) and Karl Storz GmbH & Co. KG (Tuttlingen, Germany), cover the majority of the market in flexible GI endoscopy. With respect to new technologies, this field is rapidly emerging, as flexible endoscopes are considered a platform for advanced diagnostic and therapeutic procedures.

In recent years, new imaging modalities aiming to enhance conventional white light endoscopy have been adopted in clinical routine and are constantly being further developed. The most prominent imaging enhancement technologies are narrow band imaging (NBI) by Olympus, i-Scan by Pentax, flexible spectral imaging colour enhancement (FICE) by Fujinon, autofluorescence imaging (AFI) by Olympus, and confocal laser endomicroscopy (CLE) by Pentax. Literature shows that enhanced imaging modalities can have an added value in the diagnosis of various pathologic entities with positive effects on accuracy, sensitivity and

Figure 9 – a) PillCam®SB3 (Given Imaging); b) PillCam®COLON2 (Given Imaging); c) PillCam®UGI (Given Imaging); d) PillCam®PATENCY (Given Imaging) - Courtesy of Medtronic, Inc.; e) EndoCapsule (Olympus); f) OMOM capsule (Chongqing Jinshan Science & Technology) - Reprinted from Intest Res 2016;14(1):21-29 with permission; g) MiroCam (Intromedic); and h) CapsoCam (CapsoVision)

specificity as well as time and cost of the procedure [54-58].

The field of interventional endoscopy is also constantly evolving. Recent developments, such as over-the-scope clips (OTSC®), enable endoscopists to perform more complex and radical procedures, and even spare patients from surgery through a less traumatic endoscopic intervention [59] (Figure 8a). The FTRD® system by Ovesco Endoscopy AG (Tübingen, Germany) enables endoscopic full-thickness resection in the colorectum in an effective manner [60] (Figure 8b). Such novel procedures extend the field of application of endoscopic devices well into the surgical domain.

The FDA approval of the first WCE has led to a novel diagnostic technology in endoscopy, especially for small bowel diagnosis. At the time of the present publication, four companies dominate the WCE market. The family of PillCam® WCEs (PillCam® SB3, PillCam® Colon2, PillCam® UGI, and PillCam® PATENCY) was developed over the years leading to the first WCE introduced by Given Imaging, Ltd. (Yoqneam, Israel), and is currently marketed by Medtronic, Inc. (Dublin, Ireland). Further players in the WCE field are Olympus, Co. (Tokyo, Japan) with the EndoCapsule, IntroMedic, Co., Ltd. (Seoul, South Korea) with the MiroCam, the Chinese group Chongqing Jinshan Science & Technology,Co.,Ltd.withtheirOMOMcapsule, and CapsoVision, Inc. (Saratoga, CA, USA) with the 360° panoramic HD image CapsoCam capsule. The most representative commercial capsules are depicted in Figure 9. Main target diseases are obscure GI bleeding (OGIB) and assessment or mapping for newly diagnosed Crohn's disease (CD). Furthermore, other indications include surveillance of small intestinal polyposis syndromes or tumours as well as assessment of response and/or clinical complications of celiac disease [61, 62]. Moreover, two-headed capsules further target the oesophagus and the colon for CRC screening [51]. Latest developments that have been introduced into the market are essentially improvements of previous WCE devices, both in terms of technology (e.g., higher resolution, longer battery lifetime) and/or application (*e.g.*,movement-sensitive control of frame acquisition frequency, changes of capsule size to promote sensitivity in colon screening). However, novel technologies need to combine the low invasiveness and high patient comfort of wireless endoscopic devices with novel, more

powerful technological features in order to address widespread improvements in CRC diagnosis and treatment [63].

2.4. System architecture of a robotic capsule

A robotic capsule platform consists of at least six primary modules: *i)* locomotion, *ii)* localization, *iii)* vision, *iv)* telemetry, *v)* powering and *vi)* diagnosis and treatment tools (Figure 10). However, most robotic endoscopic capsules, developed to date, include only a subset of the aforementioned modules due to size constraints. Technological integration is challenging, however, thanks to current progresses in microsystem technologies and micromachining, as well as in interface and integration, modern devices can embed most of these modules and provide both diagnostic and treatment functionalities. The following subsections will illustrate the above-mentioned modules of an endoscopic capsule.

2.4.1. Locomotion

Locomotion is a crucial aspect that must be considered when designing a robotic endoscopic capsule. WCEs can be active or passive, depending on whether they have controlled or noncontrolled locomotion. Passive locomotion currently dominates the market (*e.g.*, PillCam® WCEs). Active locomotion is still primarily at research level, but it has great

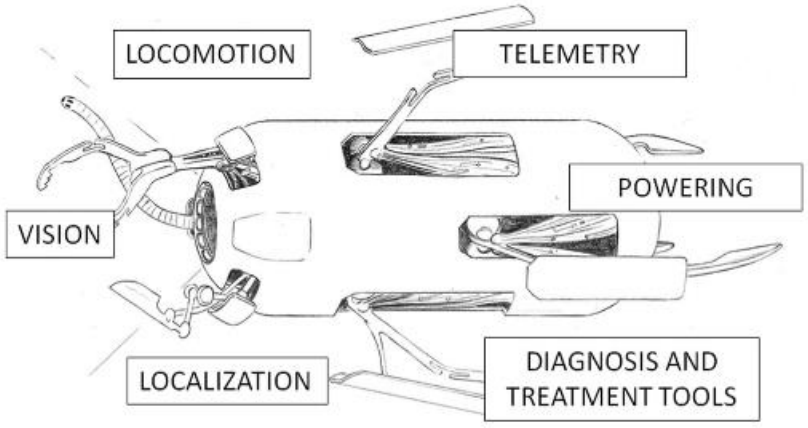

Figure 10 – System architecture of a robotic capsule

potential, since it would enable the clinician to manoeuvre the device for precise targeting. However, the main issue is related to technological integration. It is difficult to embed a locomotion module into a swallowable capsule because of the size of actuation and power constraints. For instance, the power consumption of a legged capsule device is about 400 mW only for motors, consequently requiring the integration of a high capacitance and also bulky battery [64].

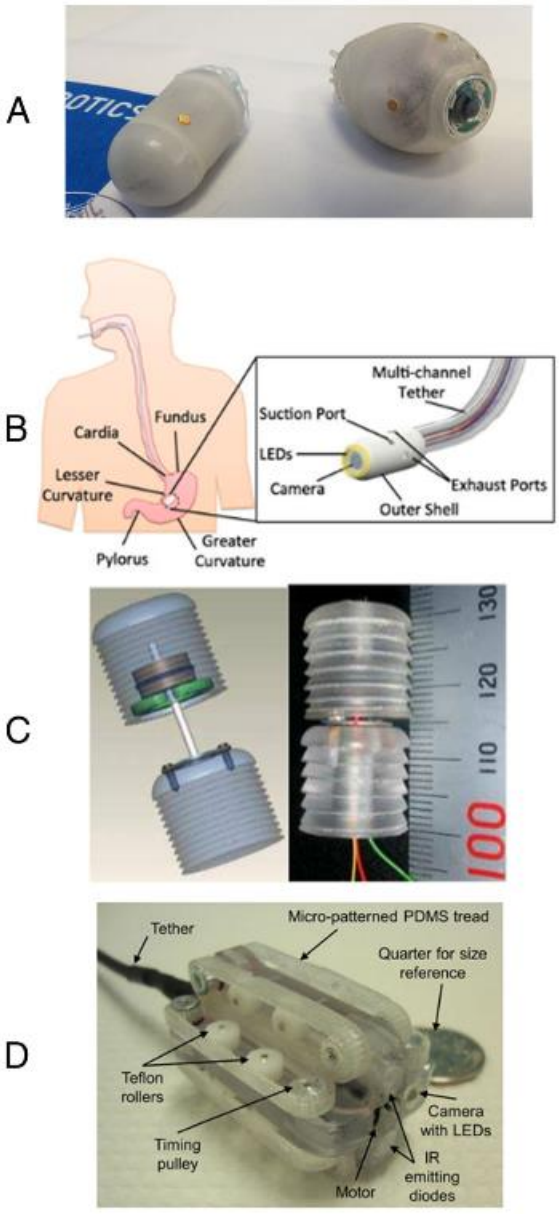

Figure 11 – Internal locomotion platforms: a) Swimming capsule by Tortora et al. (left) and by De Falco et al. (right); b) water jet-based soft-tethered capsule by Caprara et al.; c) earthworm-like locomotion device by Kim et al.; and d) wired colonoscopic capsule with micro-patterned treads by Sliker et al.

Two main strategies allow the implementation of active locomotion in an endoscopic swallowable capsule: one consists in embedding on-board a miniaturized locomotion system(s), *i.e.* internal locomotion; the other requires an external approach, i.e. external locomotion. This latter approach generally relies on magnetic field sources.

Internal Locomotion

Different internal locomotion approaches have been investigated in literature and the most significant solutions will be presented and analysed in this paragraph. An interesting active capsule system for gastroscopy was developed by Tortora et al. [65] (Figure 11a-left). The submarine-like robotic capsule exploits four independent miniaturized propellers actuated by DC brushed motors; placed in the rear part of the capsule, propellers are wirelessly controlled to guarantee 3D navigation of the capsule in a water-filled stomach. An advanced version of this capsule, which embeds a camera module, has been developed by De Falco et al. [66] (Figure 11a–right). Other possible bio-inspired approaches of swimming in a water-filled stomach cavity include flagellar or flap-based swimming mechanisms [67, 68]. Caprara et al. recently developed an innovative approach for stomach inspection that consists of a soft-tethered gastroscopic capsule; the camera capsule is oriented by means of water jets provided by a multichannel external water distribution system (Figure 11b)[69].

Several mechanisms based on internal locomotion approaches have been developed for targeting the entire intestine (*i.e.*, large and small bowel). A mechanism, which is bio-inspired by an earthworm-like locomotion approach, was developed by Kim et al. [70, 71] (Figure 11c); it consists of cyclic compression/extension shape-memory alloy (SMA) spring actuators and anchoring systems based on directional micro-needles. Another bio-inspired solution for internal locomotion was proposed by Li et al. [72]. It exploits a mechanism mimicking cilia extension using six SMA actuated units, each provided with two SMA actuators for enabling bidirectional motion. A paddling-based technique, for crawling in the intestine, was proposed by Park et al. [73]. The capsule uses multiple legs that travel from the front to the back of the capsule, in contact with the tissue, allowing directional propulsion along the lumen. Sliker et al. developed a wired colonoscopic capsule composed of micro-patterned treads [74]. The capsule drives eight polymer treads simultaneously

through one single motor (Figure 11d). Interaction of the treads (located on the outer surface of the capsule) with the tissue guarantees propulsion of the capsule device. Bio-inspired leg-based capsules were also developed by The BioRobotics Institute of the Scuola Superiore Sant'Anna in Italy. Increasingly sophisticated legged robot prototypes using embedded brushless motors (*i.e.*, 4 legs [64], 8 legs [75],and 12 legs [76, 77]), were developed starting from a first generation SMA-based solution [78]. Legged capsules demonstrated effective bidirectional control, stable anchorage and adequate visualization of the lumen without the need for insufflation. Finally, electrical stimulation of the GI muscles was proposed as a method for roughly controlling capsule locomotion or at least to stop it by generating a temporary restriction in the bowel [79, 80]. Although internal locomotion has significant advantages, such as the local distension of the tissue (*i.e.*, no insufflation is required for accurate visualization of the lumen), it comes with a dramatic drawback: the excessive internal encumbrance needed to attain the size of an ingestible capsule (*e.g.*, due to the presence of actuators, transmission mechanisms and high-capacity power modules).

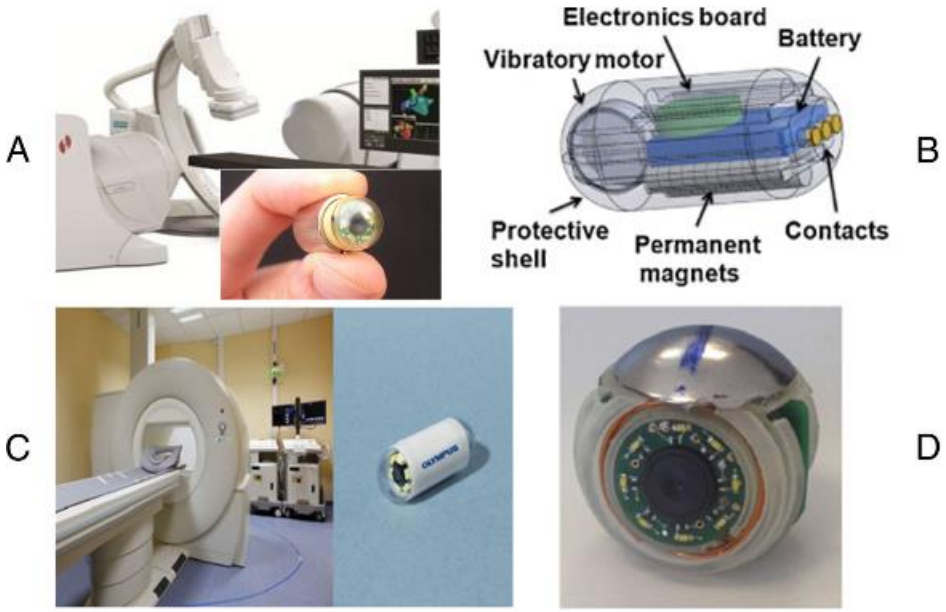

Figure 12 – External locomotion platforms: a) GI tract exploration platform developed by Carpi et al. exploiting the Stereotaxis system; b) magnetically-driven capsule with vibration by Ciuti et al.; c) gastric examination platform developed cooperatively by Olympus Inc. and Siemens AG Healthcare; and d) SUPCAM endoscopic capsule (©2015 ucarini G, Ciuti G, Mura M, Rizzo R, Menciassi A. Published under CC BY 3.0 license. Available from: http://dx.doi.org/0.5772/60134)

External locomotion

The external locomotion approach uses permanent magnets or electromagnets and entails external field sources that interact with internal magnetic components, which are embedded in the capsule, to provide navigation and steering. The benefit of the external approach is that there are no on-board actuators, mechanisms and batteries, thanks to a small-integrated magnetic field source, i.e. in most cases a permanent magnet. Given Imaging Ltd. investigated the use of a handheld external permanent magnetic source to navigate a capsule in the upper GI tract using a customized version of PillCam Colon, which integrates a permanent magnet, as part of the European FP6 project called "Nanobased Capsule-Endoscopy with Molecular Imaging and Optical Biopsy (NEMOproject)" [81].

Carpi et al. exploited a cardiovascular magnetic navigation system (Niobe, Stereotaxis, Inc., St. Louis, MO, USA) for the robotic navigation of a magnetically modified endoscopic capsule, *i.e.* a PillCam SB, Given Imaging Ltd., for gastric examination [82, 83] (Figure 12a). An active locomotion approach based on permanent magnets (outside and inside the capsule) was proposed by Ciuti et al. [84, 85]. The platform combines the benefits of magnetic field strength and limited encumbrance with accurate and reliable control through the use of an anthropomorphic robotic arm. Tested in a comparative study, colonoscopy using this novel robotically-driven capsule was feasible and showed adequate accuracy compared to conventional colonoscopy [86]. This approach was investigated in the framework of the FP6 European Project called "Versatile Endoscopic Capsule for GI TumOr Recognition and therapy (VECTOR project)" [87]. A significant derivative technology from the VECTOR project consisted of a soft-tethered magnetically-driven capsule for colonoscopy [88]; the device represents a trade-off between capsule and traditional colonoscopy combining the benefits of low-invasive propulsion (through "front-wheel" locomotion) with the multifunctional tether for treatment. Ciuti et al. also proposed a magnetically-driven capsule with embedded vibration mechanisms (*i.e.*, motor with an asymmetric mass on the rotor) which allow progression of the capsule along the lumen and reduced friction [89] (Figure 12b). Mahoney and Abbott addressed a permanent magnetic based actuation method for helical capsules by optimizing magnetic torque while minimizing magnetic

attraction [90]. The same authors demonstrated the 5-DOF manipulation of an untethered magnetic device in fluid [91].

A novel endoscopy platform for gastric examination was developed by Olympus Inc. and Siemens AG Healthcare (Erlangen, Germany). The system combines an Olympus endoscopic capsule (31 mm in length and 11 mm in diameter with two 4 frames per second (fps) image sensors) and a Siemens magnetic guidance equipment, composed of magnetic resonance imaging and computer tomography. A dedicated control interface allows the navigation of the capsule system with five degrees of freedom (*i.e.*, 3D translation, tilting and rotation) [92] (Figure 12c).

A hand-guided external electromagnetic system is at the basis of the robotic endoscopic platform developed during the European FP7 project called "New cost–effective and minimally invasive endoscopic device able to investigate the colonic mucosa, ensuring a high level of navigation accuracy and enhanced diagnostic capabilities (SUPCAM project)" [93, 94]. The external electromagnetic source navigates a colonoscopic spherical-shape capsule provided with an internal permanent magnet, able to perform a 360° inspectionthrough inner camera rotation (Figure 12d). A significant limitation of the external magnetic locomotion approach is the difficulty in obtaining effective visualization and also locomotion in a collapsed environment. Solutions for local tissue distension were proposed by several researchers, as reported in [95, 96].

2.4.2. Localization

Capsule position and orientation are necessary to locate the lesions in the GI tract, determine future follow-up treatment and provide a feedback for capsule motion (in the case of active locomotion). For this reason, an accurate localization system is crucial for WCE [97]. Commercially available WCEs employ different localization strategies, *e.g.* Given Imaging patented a localization method in 2013 based on a single electromagnetic sensor coil [98], instead Intromedic's localization method relies on electric potential values [99].

One of the methods used for localization consists of capturing images from the capsule: each region of the GI tract is identified by anatomical landmarks [100]. Spyrou et al. proposed an image-based tracking method using algorithms for 3D reconstruction based on the registration of consecutive frames [101].

Several research teams have instead focused on localization techniques based on magnetic fields and electromagnetic waves. Low-frequency magnetic signals can pass through human tissue without any attenuation [102], plus, magnetic sensors do not need to be in the line of sight to detect the capsule [103]. However, precision decreases if a ferromagnetic tool is unintentionally inserted into the workspace [104]; also, the size of the permanent magnet is restricted by the dimensions of the capsule, which also limits the accuracy of results [105]. Moreover, if a magnetic actuation strategy is implemented, it is possible that an undesired interference with the magnetic localization system may occur. Weitschies et al. were the first to equip a capsule with a permanent magnet for passive capsule endoscopy [106, 107]. A 37-channel superconducting quantum interference device (SQUID) magnetometer was used to record the magnetic field distribution over the abdomen, for several time intervals. The resolution of the position was approximately a few millimetres and the temporal resolution was in the order of milliseconds. Wu et al. [108] developed a wearable tracking vest consisting of an array of Hall-Effect sensors. This was used to track a capsule provided with a Neodymium magnet. The array was around 40 cm × 25 cm × 40 cm (length × width × height) in order to cover the stomach and small intestine area of a normal human body. Instead, Plotkin et al. [109] used a large array (8x8 matrix) of coplanar transmitting coils. At the beginning of the procedure, a complete transmitting array is sequentially activated to obtain the initial position of the receiving coil, which is enclosed inside the capsule. Only a sub-array of 8 coils is used in the following tracking stages. The authors report a 1-mm, 0.6° tracking accuracy. Another approach was proposed by Guo et al. [110] who used three external energized coils fixed on the patient's abdomen. The coils were arranged to excite three axes magneto-resistive sensors inside a capsule that measured the electromagnetic field strength. This method is based on the principle of magnetic dipole. The position and orientation errors reported 6.25–36.68 mm and 1.2–8.1° in the range of 0–0.4 m.

Several approaches are possible for the application of active actuation systems. The Olympus group [111] proposed a plurality of magnetic field detecting devices. They were placed on the patient's body to detect the strength of the magnetic field in the coil of the capsule, and were induced by an external magnetic field device. The operating frequency lies in the range of 1 kHz to 1 MHz to avoid absorption of the living tissue. This technique has an accuracy of under 1 mm when the resonant circuit is placed within 120 mm from the detecting coil array.

Similar ideas were proposed by Kim et al. [112], who used magnets inside an endoscopic capsule. An external rotating magnetic field forced the capsule to rotate. Three hall-effect sensors inside the capsule were employed to measure the position and the orientation of the capsule. The authors state that the largest position detection error is less than 15 mm, and the maximum orientation detection in the pitching direction is within −4° and 15°.

Salerno et al. proposed a localization system, compatible with external magnetic locomotion, based on a triangulation algorithm. It uses a custom on–board triaxial magnetic sensor to detect the capsule in the GI tract. Position errors reported are of 14 mm along the X axis, 11 mm along the Y axis (where X and Y are in the plane of the abdomen) and 19 mm along the Z axis. Salerno et al. [113] also developed an online localization system (working at 20 Hz) embedding a 3D Hall sensor and a 3D accelerometer with pre-calculated magnetic field maps describing the external-source magnetic field. The authors reported a position error of less than 10 mm when the localization module and the external magnet are at a distance of 120 mm.

The localization algorithm presented by Di Natali et al. [87, 114] is compatible with magnetic manipulation. It is a real-time detection strategy employing multiple sensors with a pre-calculated magnetic field map. The proposed approach showed a position detection error below 5 mm, and angular error below 19° within a spherical workspace of 15 cm in radius. The same authors proposed a Jacobian-based iterative method for magnetic localization in robotic capsule endoscopy. Overall refresh rate was 7 ms, thus enabling closed-loop control strategies for magnetic manipulation running faster than 100 Hz. The average localization

error, expressed in cylindrical coordinates was below 7 mm in both the radial and axial components and 5° in the azimuthal component [115].

Electromagnetic wave methods are also used alongside these approaches. Radio frequency has been widely used for locating an object in both outdoor and indoor environments achieving an accuracy of hundreds of millimetres [116]. Given Imaging Inc. integrated this method of localization in the PillCam®SB system. Eight sensors placed in the upper abdomen receive the strength of signals emitted by the capsule. The average position error is 37.7 mm and the maximum error is 114 mm [117].

Medical practices suggest other approaches that are currently used in the clinical procedure. Among these approaches is the application of medical imaging. X-rays can also be exploited to track an object, e.g. an endoscopic capsule placed inside the digestive tract [82]. The gamma scintigraphy technique is used as well to visualize the position of the Enterion capsule, a drug-delivery-type capsule, in real time [118]. The MRI system was proposed by Dumoulin et al. to track interventional devices in real time [119].

2.4.3. Vision

The main purpose of a CE is of course to obtain images of the internal anatomy. Therefore, imaging capabilities, in terms of modality, sensor characteristics and illumination, are among the most important features that must be considered when designing these systems [120, 121]. A variety of solutions have been proposed featuring a range of capabilities. They will be considered in this section: *i)* sensor resolution, *ii)* sensor location, *iii)* field-of-view (FoV), *iv)* illumination and *v)* modality.

Sensor temporal and spatial resolution

Both temporal frames per second (fps) and spatial number of pixels are important resolution criteria for imaging. Temporal resolution determines the information that the capsule can cover while travelling through the patient. If this is too low there is a risk of omitting gastrointestinal regions from the examination. Typical commercial systems originally

operated at 2–3 fps only a few years ago [122], however, faster systems above 16 fps are the more recent standard [123], often with variable fps control settings.

Spatial resolution determines the quality of diagnosis that can be achieved for site analysis. This can be particularly important if the texture or appearance of the gastrointestinal surface is used for diagnosis or staging of the disease. This functionality could be particularly important for pathologies such as Barret's oesophagus where image texture is an indicator of disease progression. The typical spatial resolution for early capsule platforms was approximately 360×240 pixels, however, new systems are able to achieve higher resolutions [123, 124].

Sensor location

The position of the sensor and lens determines the region imaged by the travelling capsule. Since most devices are designed with a predicted travel direction in the long axis of the capsule, the majority of image sensors are mounted at the tip of the capsule. More recently, capsules integrating multiple cameras have been developed and can potentially acquire images looking forward and backwards, such as PillCam® Colon 2 and UGI capsules. Similar results may also be achieved through lens design [125]. In particular, microlens arrays or lenticular lens arrays, which have been demonstrated in laparoscopic surgery [126], could be used to provide a multi-view image using a single sensor to maintain a small device footprint. Different configurations, where a side viewing sensor is used, have also been explored because looking forwards is not always the clinically optimal configuration [127]. Side viewing capabilities can potentially map the entire surrounding lumen around the capsule and ensure a continuous monitoring functionality, which can also be important for mapping algorithms.

Field-of-view

The limited workspace within the gastrointestinal system means that the distance between the capsule and the tissue is very small. This requires capsules to provide a wide field of view in order to observe a sufficient image of the tissue walls. Typically the FoV of capsules ranges between 140° and 170°. However, different setups have been explored, for example the

CapsoCam capsule presents a new concept with a 360° panoramic lateral view with four cameras [127].

Illumination

Image quality is inherently governed by the illumination and sensor capabilities of the endoscopic capsule. Illumination is typically provided by LED sources configured to provide white light images, which are most commonly used for interpretation by the physician. Adaptive illumination strategies have recently been under investigation for achieving optimal image quality while preserving battery power based on image processing [128]. Different strategies can be employed to conserve power, e.g. the brightness of the image can be used to estimate the distance from the surface under observation because illumination power is a function of distance. The overall image brightness can then be adapted to maintain diagnostic image quality.

Modality

White light (WL) is the main modality for WCE imaging because it is the most well understood signal for interpretation by physicians. Nevertheless, molecular imaging has been explored by a number of teams and projects [129]. Autofluorescense capsule prototypes have been explored [130] for potentially detecting disease without an on-board camera [131, 132]. NBI potentially exposes useful subsurface vessel information that can characterize disease [133]; details are reported in previous paragraphs. The type of light and the 2D or 3D image modalities of the capsule have also been explored. It is possible that multiple 2D images can potentially offer a 3D reconstruction of the video, which could allow more accurate lesion classification [134-137].

Stereoscopic systems have already been developed, such as the one developed in 2013 by Simi et al. for laparoscopic procedures [138]. A new concept of capsule with a stereo camera system for colonoscopy will be investigated by the authors within the Endoo EU project (www.endoo-project.eu). Modalities that can penetrate deeper within tissue walls are also under exploration, for example in the UK SonoPill project [45]. It is likely that new methods

for manufacturing microarrays for sensing ultrasound will play an important role in enabling such sensing capabilities [139].

2.4.4. Telemetry

How to transmit and receive data is a central topic in WCE technology. A high data rate telemetry system is essential to allow high-resolution imaging. Due to size constraints and technological limitation of wireless communication, the telemetry subsystem is often a bottleneck in capsule design. Robotic endoscopic capsules can employ radiofrequency transmission, human body communication, or can also integrate a data storage system, thus avoiding wireless communication [140]. Human body communication technology uses the human body as a conductive medium. It requires less power than radiofrequency communication, but involves a large number of sensor electrodes on the skin [141]. Wireless capsules using radiofrequency communication are attractive because of their efficient transmission through the layers of the skin. This is especially true for low frequency transmission (UHF-433 ISM and lower) [142]. However, low frequency transmission requires large electronic components. Given Imaging's capsules embed a Zarlink's transceiver, and transmit 2.7 Mb/s at 403–434 MHz [46]. A part of its recent research focuses on developing impulse radio ultra-wideband antennas (IR-UWB) for WCE [143-145]. A CMOS system employing an ON-OFF keying modulation, with a superetherodyne receiver, is presented in [146]. A low power transmitter working in the ISM 434 MHz band is discussed in [147]. It is designed using CMOS 0.13 µm technology and consumes 1.88 mW.

2.4.5. Powering

Power management is a major challenge in WCE, because of dimension constraints and high consuming components, such as LEDs [148]. Capsules are usually powered by silver oxide button batteries. Two or three of them allow up to 15 h operation [140]. Lithium ion polymer batteries, as well as thin film batteries, are promising solutions to enhance power density and reduce battery dimensions [46].

Wireless power transfer has also been investigated. In particular, RF power transfer is highly suitable for medical devices, since it is non-invasive and non-ionizing [148]. An inductive power system, operating at 1 MHz and able to supply 300 mW, is presented in [149]. A portable magnetic power transmission system is demonstrated in [150]. The system was also tested on a pig and showed an energy conversion efficiency of 2.8 %. An inductive-based wireless recharging system is presented in [151]. It can provide up to 1 W power and is able to recharge a VARTA CP 1254 battery in 20 min. In [152] an analytical comparison among simple solenoid, pair of solenoids, double-layer solenoids, segmented-solenoid, and Helmholtz power transmission coils (PTCs) is carried out with a FEM simulation. It shows that the segmented solenoid PTC can transfer the maximum amount of power.

2.4.6. Diagnosis and treatment

Progress in micro-electromechanical systems (MEMS) technologies have led to the development of new endoscopic capsules with enhanced diagnostic capabilities, in addition to traditional visualization of mucosa (embedding, *e.g.* pressure, pH, blood detection and temperature sensors). However, current capsule endoscopes lack treatment module(s), thus requiring a subsequent traditional endoscopic procedure. Developing clinical capsules with diagnostic, interventional and therapeutic capabilities, such as biopsy sampling, clip release for bleeding control, and/or drug delivery, will allow WCE to become the mainstream endoscopic mode. This section is divided into two categories: *i)* diagnosis and *ii)* treatment, as reported below.

Diagnosis

With regard to image-based diagnosis and derived algorithms for enhanced diagnosis, even if a full 3D map of the distance covered by the diagnostic imaging device is not achieved, 3D surface shape at specific time instants provides important diagnostic information. In particular, these shape cues can be used to identify polyp structures; indeed methods for automatically identifying and analysing them have been developed [153, 154]. While 3D methods based on shading or multiple views are interesting, the most clinically relevant advances for computational processing of WCE images have been based on 2D data.

Specifically, automated abnormality detection and highlighting have been investigated and proposed [155-157]. These methods benefit significantly from recent developments in machine learning and especially convolutional neural networks which have shown to be highly capable of addressing detection and segmentation problems. Training data for machine learning methods is still a challenge, however, the community is moving towards addressing this issue, for example with the recent EndoVis challenge at MICCAI 2015 [37].

With regard to enhanced diagnostic inference from capsule images, various methods have been proposed to enhance the image; however, none have yet taken into account strong appearance and surface tissue shape priors. Enhancing image quality and information is critical to reduce the chances of missing potential adenocarcinomas (currently estimated around 6 %) [158, 159]. Quick view function is important for allowing practical analysis of capsule videos, which can be lengthy [160].

Apart from image enhancement, powerful diagnostic accuracy molecular imaging in gastrointestinal endoscopy has recently emerged as an exciting technology encompassing different modalities that can visualize disease-specific morphological or functional tissue

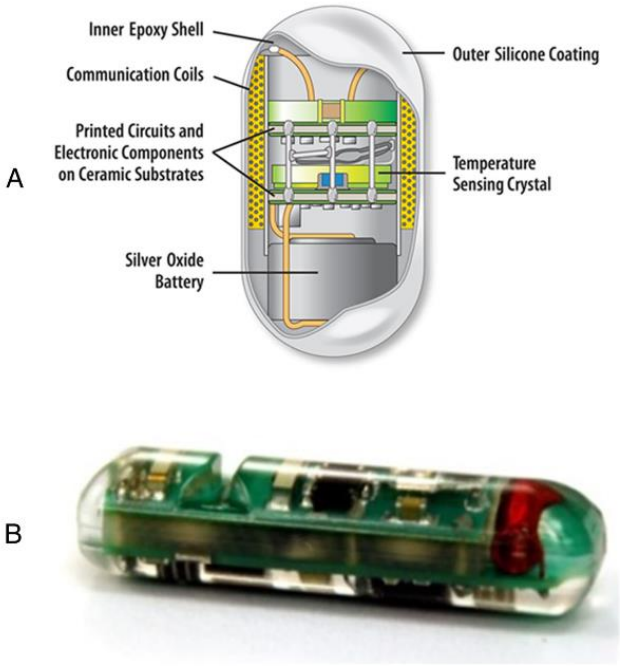

Figure 13 – a) CorTemp by HQ Inc. (Palmetto, FL, USA); and b) HemoPill acute, Ovesco Endoscopy AG (Tübingen, Germany)

changes based on the molecular signature of individual cells [122, 161].

However, it is worth mentioning that a huge number of endoscopic capsules have been designed with embedded sensing capabilities, most of them already available on the market.

Gonzalez-Guillaumin et al. [162] developed a wireless capsule for the detection of gastro-oesophageal reflux disease. It embeds impedance and pH sensors, and uses a magnetic holding solution for surgical fixation. Johannessen et al. developed a wireless multi-sensor system (Lab-in-a-Pill capsule) equipped with a control chip, a transmitter, and sensors for pH, conductivity, temperature and dissolved oxygen [163]. The FDA-approved Bravo capsule for pH monitoring (produced by Given Imaging Ltd.) is a device for evaluating gastroesophageal reflux disease [164]. The OMOM pH capsule (JinShan Science & Technology Co., Ltd., Chonqing, China) is a wireless pH monitoring system not approved by FDA. It needs to be anchored in the oesophagus and is able to transmit pH data to an external recorder. The SmartPill capsule by Given Imaging Ltd. is a FDA-approved capsule for assessment of GI motility. It measures several physiological parameters (e.g., pH, pressure and temperature) while travelling through the GI tract [165]. CorTemp by HQ Inc. (Palmetto, FL, USA) is a FDA-approved capsule for internal body temperature measurement, with ±0.1 °C accuracy (Figure 13a). The working principle is based on a quartz crystal, embedded into the capsule, whose vibration frequency varies with temperature. Consequently, a magnetic flux is established, and a low-frequency signal flows through the body [166, 167]. In the attempt to provide less-invasive procedures for imaging of the GI tract, Check-Cap (Mount Carmel, Israel) is a wireless capsule, which uses low-dose radiation to obtain the 3D reconstructed image of the colon. It could mitigate the need for bowel preparation [168]. The HemoPill acute by Ovesco Endoscopy AG (see Figure 13b) is a wireless capsule able to detect acute bleeding in the upper GI tract. It contains an optical sensor able to detect blood in the organ content in concentrations as low as 1 % [169].

Treatment

Several research groups developed endoscopic capsules with embedded modules for GI tract treatment. Valdastri et al. developed a capsule for treating bleeding in the GI tract, which is

able to electrically release an endoscopic clip (Figure 14a) [170]. Kong et al. developed a wireless capsule for biopsy. It consists of a rotational tissue cutting razor fixed to a torsional spring, constrained by a paraffin block [171]; a more advanced version of the device was developed and presented in [172].

Simi et al. developed a wireless capsule for biopsy. It employs magnetic fields for stabilization of the capsule and enables reliable sampling during the biopsy (Figure 14b) [173]. A novel biopsy method using deployable microgrippers released in the stomach from a capsule robot has been proposed by Yim et al. [174]. The capsule is positioned in the stomach by means of a magnetic system. The microgrippers fold and collect small biopsies when triggered by body heat. The capsule then collects the microgrippers using a wet adhesive patch.

The system developed by Quaglia et al. (Figure 14c) [175] exploits a spring mechanism based on SMA for unlocking a bench compressed by a super elastic structure in order to release a bioadhesive patch. Several other robotic capsules for drug delivery have been developed by

Figure 14 – a) Therapeutic wireless endoscopic capsule with an endoscopic clip for treating bleeding in the GI tract produced by Valdastri et al.; b) Magnetic-driven biopsy capsule produced by Simi et al.; c) Therapeutic capsule for bioadhesive patch release produced by Quaglia et al.; d) Soft-tethered therapeutic capsule colonoscope developed by Valdastri et al.; e) and f) Capsule for photodynamic therapy of Helicobacter pylori bacterium by Tortora et al.

different research groups. A significant example is the one developed by Woods et al. that consists of a micro-positioning mechanism for targeted drug delivery and a holding mechanism used for resisting against peristaltic contractions [176]. An exhaustive review of drug delivery systems for capsule endoscopy has been written by Munoz et al. [177].

Tortora et al. developed a capsule for the photodynamic therapy of Helicobacter pylori bacterium consisting in a swallowable device including LEDs and a battery and able to deliver light at specific wavelengths the Helicobacter is sensitive to [178]. A robotic capsule able to provide several therapeutic functionalities was developed by Valdastri et al. (Figure 14d) [88]. The soft-tethered capsule colonoscope features a compliant multilumen tether for suction, irrigation, insufflation or access for standard endoscopic tools (*e.g.*, polypectomy snares, biopsy forceps, retrieval baskets and graspers). Gorlewicz et al. proposed a method for obtaining tissue distension. It consists of a tetherless insufflation system, based on a controlled phase transition of a small volume of fluid (stored on-board the capsule) to a large volume of gas, emitted into the intestine [95].

Finally, artificial touch is an enabler of research progression towards minimally invasive surgery (MIS) in medical robotics, with particular respect to operational safety, automation of interventional procedures, capability to reproduce haptic feedback and characterization of tissues for diagnostic purposes [3, 179]. Over the last years, tactile sensing has demonstrated major breakthroughs in the domain of hand neuro-prosthetics [17, 21, 35, 36, 180-182], and there is relevant literature showing the benefits (*e.g.*, considering duration and effectiveness of operations) of force and tactile sensing technologies as valuable tools in robot–assisted surgery [183]. Various research projects have addressed the integration of the sense of touch in surgical or diagnostic tools [184, 185] and shown the feasibility of using artificial touch for tumour localization [186-189]. However, the integration of tactile sensing in robotic tools for medicine is still an open research topic, requiring several advances prior to clinical application and socio–economic impact. Furthermore, though endoscopic or MIS tools endowed with tactile sensorization have been developed [190],only very recent and preliminary technologies [191], within the framework of the EndoVESPA EU project,

integrate an artificial sense of touch in dedicated tools for robotic capsules [192], mainly as a consequence of miniaturization constraints.

2.5. Capsule endoscopy patents

A large number of patents of capsules for digestive endoscopy have been filed worldwide, underlining the interest for these novel devices and field of medical application. It is not possible to provide an exhaustive and detailed patents' analysis in this manuscript, but the main topics of interest will be highlighted in order to understand, in some cases, the industrial trends. Inventors and companies are particularly trying to improve the features and techniques of these challenging devices, which require high technology and particular attention to patients' comfort and physicians' requests.

For these reasons, over the last years different aspects of this topic have been studied and developed, such as: *i)* wireless capsule, *ii)* magnetic guidance, *iii)* imaging, *iv)* power source, *v)* energy management, *vi)* localization and locomotion mechanism, *vii)* drug delivery, and *viii)* biopsy. Different companies, such as Olympus, Co., Given Imaging, Ltd, Siemens AG, and university research groups have invested time and resources to develop new ideas for these devices and achieve interesting technological solutions. Some of these are dedicated to improve imaging information obtained from cameras located on the capsule. They use thermal imaging cameras or an internal radiation unit that detects radioactivity drugs injected into the body. In fact, imaging processing makes it possible to increase contrast in the gastrointestinal tract for particular pathologies and morphologies. For example, the use of infrared or other frequencies of the electromagnetic spectrum allows details that are not visible through the spectrum to be analysed. Physicians can thus improve their diagnosis and better respond to disease evolution. Another area under examination is the optical section, which includes lenses and image sensors (*e.g.*, CMOS, CCD). Recent developments have focused on enhancing the image captured from the capsule by using multiple image sensors for a spherical view [193] or on using images sensors at the front end and the rear end of the capsule. The use of ultrasound and Doppler principles is a challenging topic for engineers

and researchers, allowing them to incorporate these technologies within the capsules and generate different kind of images and details of the examined tract. The majority of patents on capsule endoscopy focuses on new methods for performing locomotion and tracking the position of the capsule. More specifically, they describe new techniques that employ magnetic guidance - leading to magnetic interaction and capsule motion management improvement [194] - or that use an ultrasound positioning system. Power efficiency is another topic that is under examination, especially for wireless capsules that need to reduce energy consumption and guarantee all features and functions over the entire duration of the exam (*e.g.*, self-charging method for the charging of a power source by an external electric field). Moreover biopsy mechanisms have been developed to permit the capsule to collect tissues samples and so improve exam efficiency and complexity. This is achieved by using electro-mechanical solutions to collect and store the sample inside the capsule [195].

All these new features and ideas are interesting and some of them promise to bring real and tangible aid to the evolution of endoscopy with clear advantages for both patients and clinicians.

2.6. Discussion

Although the introduction of WCE in clinical practice at the start of the millennium led to shock waves of change in the field of GI endoscopy, over the last few years, progression has significantly slowed down with respect to the research advancements and thus expectations: this is indirectly even demonstrated by the fact that, since 2009, the number of new patent applications are decreasing [37]. Since the appearance of the first capsule endoscope, several IT and robotics research groups around the globe have proposed a variety of methods, including algorithms for detecting haemorrhage and lesions, reducing review time, localizing the capsule or lesion, assessing intestinal motility, providing wireless endoscopic capsule control through accurate magnetic models, locomotion and therapy, and enhancing video quality. Even though research is prolific (as measured by publication activity), the technological industrial-oriented progress made during the past 5 years can only be

considered as marginal (with respect to clinical needs and research-oriented outcomes). Nevertheless, WCE has the potential to become the leading screening, diagnostic and therapeutic technique for the entire GI tract [137]. Moreover, the use of a robotic miniaturized device that promises to offer targeted therapy (*e.g.*, used as a smart active carrier to drug delivery) has been a long-term fascination and –why not– unfulfilled dream of the medical profession and the patients alike. For a device to create the next innovative robotic solution for non-invasive diagnosis and therapy in the research field of WCE, the aforementioned modules (*e.g.*, powering, telemetry, diagnosis and treatment) should be addressed and properly integrated. Several similarities could be drawn from the field of medicine/gastroenterology and other sciences as well bio-mimetic/bio-inspired approaches, such as the spider/insect, worm and fish-like capsules that are promising approaches not only with respect to navigation within the digestive tract, but also for treatment (*e.g.*, haemostatic clips or drug delivery, biopsies or small dissections) [45]. Chimeric devices that combine the best of both worlds, *i.e.* conventional and wireless GI endoscopy, seem a promising next step (as in the Endoo EU project). Therefore, following this approach, we believe that GI endoscopy in the third decade of the new millennium will become a success story of screening efficacy and minimal –if any– discomfort. This should be provided by an enhanced version of the capsule-based platform and allied technologies, which should allow, e.g. improved image-based capabilities with assistive algorithms [196], and active locomotion [85]. As aeronautical engineering –for more than a century now– has not significantly moved away from the conceptual design/idea of the aviation pioneers, the external capsule-like shell of the device - with optimizations of materials and shape [45, 197]- will not change drastically over time. Instead, the speed (and accurate control of the device), the functional characteristics (image definition, illumination, 3D reconstruction, tactile sensing and therapeutic embedded tools for targeted therapy and in situ drug delivery) and the indications for obtaining it will change over time. We believe that the era of assistance or –in some extreme cases– automation (in diagnosis and therapy), an era of universal, equitable, high-quality GI endoscopy is finally here.

Chapter

3. Closed-loop force control for capsule endoscopy[2]

Discomfort in traditional endoscopy can be mainly ascribed to the lack of measurement and control of the force applied to the gastrointestinal wall. This is what prevents CRC mass screening programmes to become real. Hand-guided control of conventional scopes is painful and can potentially cause tissue damage because of looping, and in the worst case can lead to perforation (*i.e.*, 0.1–0.3 % for diagnostic procedures in the colonic tract) [198]. Capsule endoscopy represents today the alternative procedure to avoid pain and discomfort of traditional colonoscopy. However, one of its major drawbacks is the passive locomotion, which does not allow either a specific investigation on critical areas, leading to false negatives, or therapeutic treatment.

Magnetically-driven capsules is one of the most promising and mature technologies, in the field of active capsule endoscopy, aiming at going beyond invasiveness and discomfort typical of traditional endoscopes [199]. However, magnetically-driven systems require a precise localization system for implementing a closed-loop control for robot-assisted navigation [87, 200-202].

In this chapter, we present a magnetically-driven endoscopic capsule equipped with a dense array of MEMS tactile sensors [35, 203, 204], already introduced at the end of Section 1.2 , which is here preliminarily used as a force sensor module for enhancing closed-loop control. This system can allow an improved magnetic link control, serving as a redundant system

[2] The contents of this chapter are adapted from the conference paper "Caliò, R., Camboni, D., Ortega Alcaide, J., Oddo, C. M., Carrozza, M. C., Menciassi, A., Ciuti, G., Dario, P., Robotic endoscopic capsule for closed-loop force-based control and safety strategies. 2017 IEEE International Conference on Cyborg and Bionic Systems (CBS 2017)"

beside magnetic localization techniques, and it avoids exceeding the upper limit of magnetic attraction forces for safety purposes [205].

The sensors embedded into the capsule allow online force readout. A closed-loop force control for real-time safety strategy has been implemented. Moreover, fine force readout enhances capsule navigation, allowing optimization of the contact condition and thus diminishing friction with the endo-luminal wall. The presented system will be tested in the future to prove capabilities as tactile tool for remote palpation, providing the physician with texture and stiffness information during endoscopic procedure.

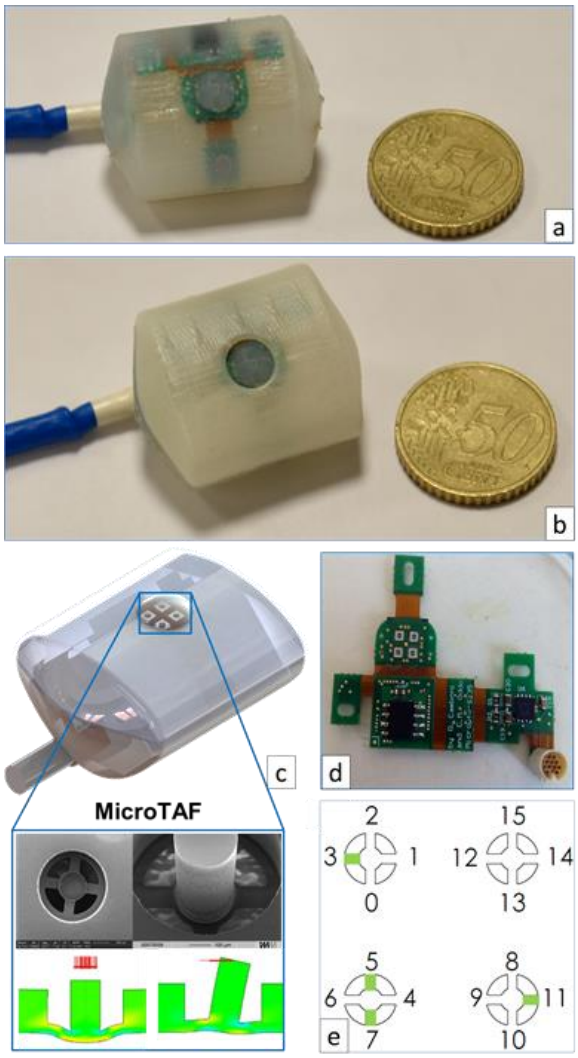

Figure 15 – a) Tactile endoscopic capsule, b) capsule with 3D printed cover, c) capsule rendering with detail of MEMS sensors, d) electronics embedded in the capsule, and e) sensors map showing the 4 channels in use.

3.1. Materials and methods

The tactile endoscopic capsule dimension is 33 mm (l), 26 mm (w), and 17 mm (h). It is equipped with a 2x2 array of MEMS tactile sensors. Each sensor consists of 4 piezo-resistive channels at the roots of a cross-shaped structure, with a central pillar. Further details on the sensors and their fabrication process can be found in [203, 204]. The MEMS array is covered with a soft circular dome of 7 mm in diameter made of Dragon Skin® 10 in order to protect the array and distribute the applied force on it (Figure 15). In the present study, a selection of four piezo-resistive channels of the capsule has been used, for the sake of data order reduction (Figure 15e). The capsule also integrates a N50 NdFeB permanent magnet with dimensions 12 mm (l), 8 mm (w), and 8 mm (h). The rest of the system consists in: *i)* a robotic platform with a 6-DOFs anthropomorphic manipulator (Comau Racer 5-0.80, Comau, Grugliasco, Italy), mounting a cylindrical-shape N52 NdFeB permanent magnet (length 80 mm and diameter 90 mm) on its end-effector (Figure 16a); and *ii)* a control and processing unit (National Instruments IC-3173, National Instruments, Austin, TX, USA) which receives

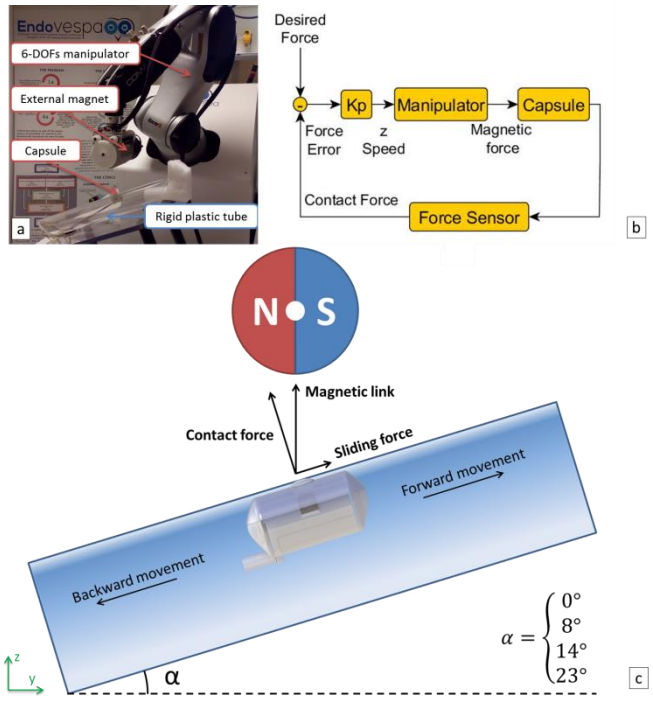

Figure 16 – a) Robotic test bench, b) block diagram of the system, and c) schematic representation of the experimental setup and test protocol.

the tactile sensors output and updates the robot trajectory, accordingly (Figure 16b). The IC-3173 control unit reads the MEMS array at a frequency of 380 Hz and implements two control loops. The high level force control loop takes the sensors readout as an input and implements the control strategy, with a loop time of 20ms. The low level control loop generates the acceleration curves based on the high level control loop output and communicates with the robot controller every 2 ms. The robot controller then manages the motor drivers with a loop time of 400µs. The experimental procedure starts inserting the capsule in a rigid plastic tube (55 mm diameter and 370 mm length). The magnetic end-effector is over but distant from the capsule, which is not in contact with the tube wall. The magnet at the end-effector of the robotic arm is moved towards the capsule (varying z) to establish the magnetic link.

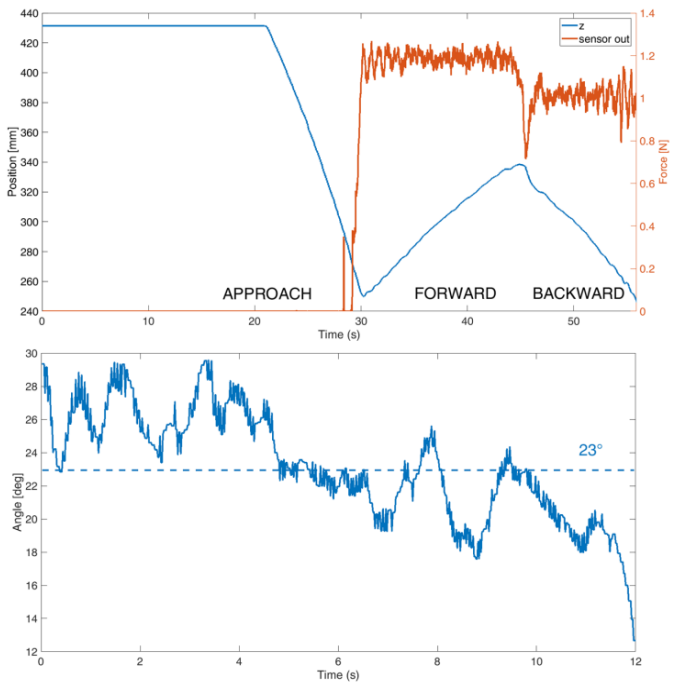

Figure 17 – (top) Z movement of the manipulator and norm of the force sensors during the 23° inclination test, and (bottom) angle variation during forward movement.

The capsule is considered in contact when at least one sensor of the array overcomes 0.25 N of estimated contact force (all the reference values have been selected after a preliminary experimental pilot test). The capsule is then moved by the robotic manipulator until the end of the tube with a predetermined constant speed of 25 mm/s, by means of the established

magnetic link (Figure 16c). The z distance is automatically adjusted during locomotion in order to maintain a constant contact force between the capsule and the tube wall. The capsule stops moving only if the contact condition is lost; in this case only z is varied in order to re-establish a magnetic link with the capsule. The height of the end-effector is adjusted using a preliminary closed-loop proportional controller (with Kp 0.25) following the block diagram presented in Figure 16. The desired target force was selected to be 1.1 N after qualitatively evaluating in a pilot test its suitability for a continuous motion. This value is compatible with the maximum force the large bowel can sustain, which is 13.5 N [205]. When the capsule reaches the end of the tube it goes back to the initial position. The forward/backward path is performed three times per configuration. A series of four tests has been performed setting the tube at four different angles with respect to the x-y horizontal plane, i.e., 0°, 8°, 14° and 23°.

3.2. Results

TABLE II summarizes the data obtained from the experiments. The results have been averaged on the three trials performed per each configuration. The norm of the force sensors is well maintained at the target force in all the configurations tested, with small variations during each single trial. The manipulator's Cartesian coordinates have been used for a control calculation of the angle trajectory, in order to assess the effectivity of the system to follow the path. The angle mean value gives a good estimation of the actual tube inclination, meaning that the manipulator accurately maintains, in average, a constant distance with the capsule in order to guarantee the desired contact force. The significant value of standard deviation is given by the continuous adjustment due to small variations of contact conditions and non-smooth sliding of the capsule, mainly caused by stick and slip on the tube wall. This is confirmed by the high frequency of the angle adjustment, which also explains the high values of standard deviation of the angle trajectory control calculation but it also points out the responsive reaction of the control system. It is possible to notice in Table 1 that the mean angle trajectory is always slightly higher during the backward

movement. This is because when the forward movement ends, the manipulator starts moving in the opposite direction and it needs to go beyond the capsule to make it move backward (*i.e.* to create the required magnetic gradient to allow the capsule movement). In this tract the manipulator moves away from the tube because of the increasing magnetic force, and therefore the backward movement has an initial condition of a certain distance from the tube, making it perform a descent movement with a higher equivalent angle than expected.

Figure 17 shows the movement of the robot along the z axis and the norm of the sensor output while sliding in the tube. The robot first approaches the tube in order to establish a magnetic link with the capsule, thus stopping the vertical descent at the contact condition at the imposed force. Then the movement starts and the capsule goes up until the end of the tube and then returns to the initial position.

The sensor output slightly oscillates around the force threshold value, while sliding. It is

TABLE II
ANGLE TRAJECTORY ESTIMATED FROM THE ROBOT OUTPUT, ANGLE ADJUSTMENT FREQUENCY AND NORM OF THE FORCE SENSED BY THE USED FOUR SENSORS OF THE ARRAY. FRW: FORWARD; BCK: BACKWARD

Angle test		Sensors force readout		Angle trajectory control calc.		Angle adj
		Mean [N]	Std dev [N]	Mean [deg]	Std dev [deg]	Mean [Hz]
0°	frw	1.1	0.04	0.5	3.1	5.4
	bck	1.1	0.06	0.6	4.2	2.1
8°	frw	1.13	0.07	7.9	2.4	3.8
	bck	1.08	0.06	9.2	5.8	3.4
14°	frw	1.15	0.05	15.0	5.1	9.3
	bck	1.04	0.06	15.9	2.8	10.3
23°	frw	1.19	0.06	22.6	3.5	10.8
	bck	1.03	0.08	25.1	4.9	7.9

worth noting that, as expected, the force sensor readout is always higher than the target value while ascending and lower while descending. This is because, *e.g.*, while ascending the robot attempts a horizontal movement causing a force increase until the control reacts and corrects the trajectory. A fast variation in the force readout happens when the robot changes direction in order to come back to the beginning of the tube.

3.3. Discussion

This work presents a novel device based on an array of MEMS tactile sensors for controlling forces and then pressure applied on the wall of a rigid plastic tube, which represents a simplified scenario of endoscopy, with a straight path and without obstacles. These preliminary tests are meant to assess the system capabilities for improving closed-loop manoeuvrability and implementing safety measures. It is worth noting that the device is robust enough to work properly with a subset of channels among the 16 available. The system will be tested in a more realistic environment resembling compliance and obstacles of a real intestinal tract. Extensive tests will also be performed in combination with the capsule localization strategy that is under development by the authors within the Endoo EU project [206]. These experiments also represent a first assessment of the capabilities of such a system, which can be developed to work also as a tactile probe for remote palpation in endoscopic procedures, providing the physician with a new tool for diagnosis, beside the established vision-based techniques. It can also serve for online monitoring of the force against the colon wall thus paving the way to a painless procedure.

Chapter

4. Non-polypoid colorectal tumour detection through hardness and curvature classification[3]

Medical literature highlights the importance of detecting non-polypoid tumours (NPT) in colorectal endoscopy, in particular laterally spreading lesions larger than 10 mm. NPTs can be flat, slightly elevated or slightly depressed, exhibiting submucosal invasion, even in the case of small neoplasms [207]. Colorectal lesions present higher elastic modulus compared to non-cancerous tissues [208], as well as characteristic vascular patterns and sub-mucosal pit-patterns, generally observed through magnified endoscopy, narrow band imaging (NBI) or chromo-endoscopy [37, 209, 210]. However, chromo-endoscopy has a long learning curve, requiring at least 200 lesions to become competent [210]. Clinical studies have reported high sensitivity and specificity for these techniques. A study conducted on 200 colorectal polyps reported a sensitivity and specificity of 90.5 % and 89.2 % for NBI with magnification, and of 91.7 % and 90 % respectively, for magnifying chromo-endoscopy [211]. On the other hand, NPTs are difficult to detect for inexperienced physicians [207]. Besides optical imaging techniques, a branch of research has developed ultrasound pills, able to

[3] The contents of this chapter are adapted from the work ready for journal submission "Caliò, R.*, Camboni, D., Massari, L., D'Abbraccio, J., Mazomenos, E., Stoyanov, D., Menciassi, A., Carrozza, M. C., Dario, P., Ciuti, G., & Oddo, C. M. (2018). Endoscopic tactile capsule for non-polypoid colorectal tumor detection through hardness and curvature classification. IEEE Transaction on Biomedical Engineering"

detect gastro-intestinal tumours, as well as other diseases/conditions of the oesophagus, by involving piezoelectric micro electro-mechanic systems (MEMS) [139, 212].

The characteristic elastic modulus and submucosal pit pattern of colorectal tumours inspired the design of tactile devices for tumour detection in endoscopic procedures [3, 213-215]. The introduction of robotically-assisted minimally invasive surgery techniques (MIS) put emphasis on the development of haptic feedback tools, in order to provide surgeons with remote palpation [216-219]. One branch of research has focused specifically on the development of force sensor devices. Among these, optical-fibre distal force sensors have been developed, mainly for laparoscopy, because of their high dimension scalability when employed as uniaxial force sensors. Polygerinos *et al.* designed a force sensor for cardiac catheters, which can measure up to 0.8 N, from 0 to 10 Hz, and has an external diameter of 3 mm [220]. Puangmali *et al.* developed a 3-axis distal force sensor with 10 mm diameter, which is able to resolve 0.02 N within 3 N range [221]. Xie *et al.* proposed a probe with 14 tactile sensing elements, at a 2.5 mm spacing and 14 mm diameter, having a resolution of 0.05 N [222].

Other researches have focused on detection of hardness variations in soft tissues. Gwilliam *et al.* published a study comparing human and robotic sensing capabilities (employing a capacitive sensor), while localizing lumps in soft tissues. Their results show that the tactile sensor outperforms the human finger [223]. Ahn *et al.* proposed a palpation method, for prostate cancer detection, inspired by actual finger sweeping motion [224]. Ahmadi *et al.* built a beam-type optical sensor to measure the distribution of force in order to detect hardness in tissues. The device was pushed onto the test phantom, with a sustained force of 10 N [225]. Jia *et al.* demonstrated the capabilities of an elastomeric-based device, called GelSight, to detect lumps down to 2 mm diameter. However, this result was achieved by pressing the device onto the tissue with a force of 25 N [226] (unbearable for a human bowel, which would perforate applying a force of 13.5 ± 3.7 N on a surface of about 3.5 mm^2 [227]). Chuang *et al.* presented a miniaturized piezoelectric tactile sensor for hardness detection, which can fit into an endoscope, thanks to its small diameter of 1.4 mm. The drawback is that the piezoelectric working principle limits the device to dynamic forces. Also,

they drove the sensor with 12 N at 1 Hz by employing a shaker, even if the resulting force applied to the tissue was 0.6 N [228, 229]. In 2014, Arian *et al.* used a sensor resembling an artificial finger, called BioTac® to detect artificial tumors, in the form of rubber inclusions into a silicone matrix, and provide haptic feedback to the user. The authors reported an average accuracy of 72 %, but applying a force of 25 N to the phantom [186]. It's worth mentioning the work of Beccani *et al.*, who presented a wireless device for tissue palpation in laparoscopy [189, 230]. The tool is deployed and manoeuvred by means of a trocar. The sensing element consists in a magnetic field sensor, which localizes the tool based on an external magnet source. This allows estimating the reaction pressure and the indentation depth on the tissue. The device is able to detect lumps in soft tissue, and was demonstrated in both synthetic and *in-vivo* conditions showing 5% and 8% errors, respectively.

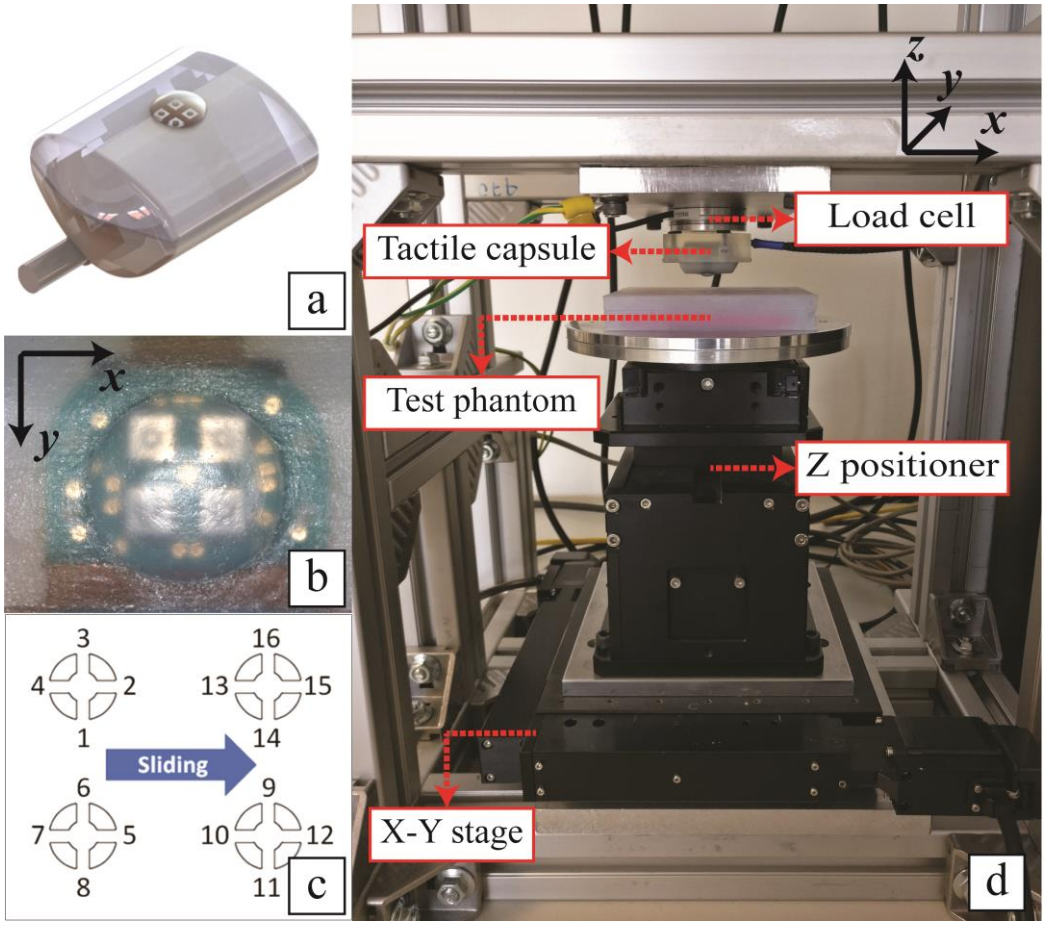

Figure 18 – a) rendering of the tactile capsule; b) microscope photograph of the array of MEMS sensors embedded into the capsule; c) layout of the four MEMS sensors and sixteen channels, with in green those used in this study; d) experimental set-up composed of three micrometric stages programmatically controlled with a LabVIEW routine, a 6-axis load cell, the tactile capsule and a test phantom.

Machine learning techniques have been employed for classification of hard inclusions in soft tissues. Nichols *et al.* presented a method to segment hard inclusions, using a Gaussian discriminant classifier. Its accuracy of segmenting 25 mm length inclusions was above 95 % [231]. Hui *et al.* employed the BioTac® finger and acquired two datasets from a silicone sample embedding hard lumps. They showed that a Gaussian model trained on one dataset performs poorly on the other one. Therefore they proposed a binary pairwise comparison technique to match the two datasets and achieved 80 % accuracy [232]. Winstone *et al.* introduced a bio-inspired tactile device, called TacTip, which measures its deformation due to the interaction with an object. The device consists in a deformable layer equipped with internal pins, which movement is optically detected. The authors demonstrated the device capabilities in classifying bumps of different size, shape and hardness [191, 233, 234]. They also compared a Support Vector Machine classifier (SVM) and a Classifier Neural Network (CNN) and obtained 81 % and 77 % accuracy, respectively, in detecting 36 mm silicone protuberant inclusions [206].

This chapter reports a work with an endoscopic tactile capsule for automatic detection and

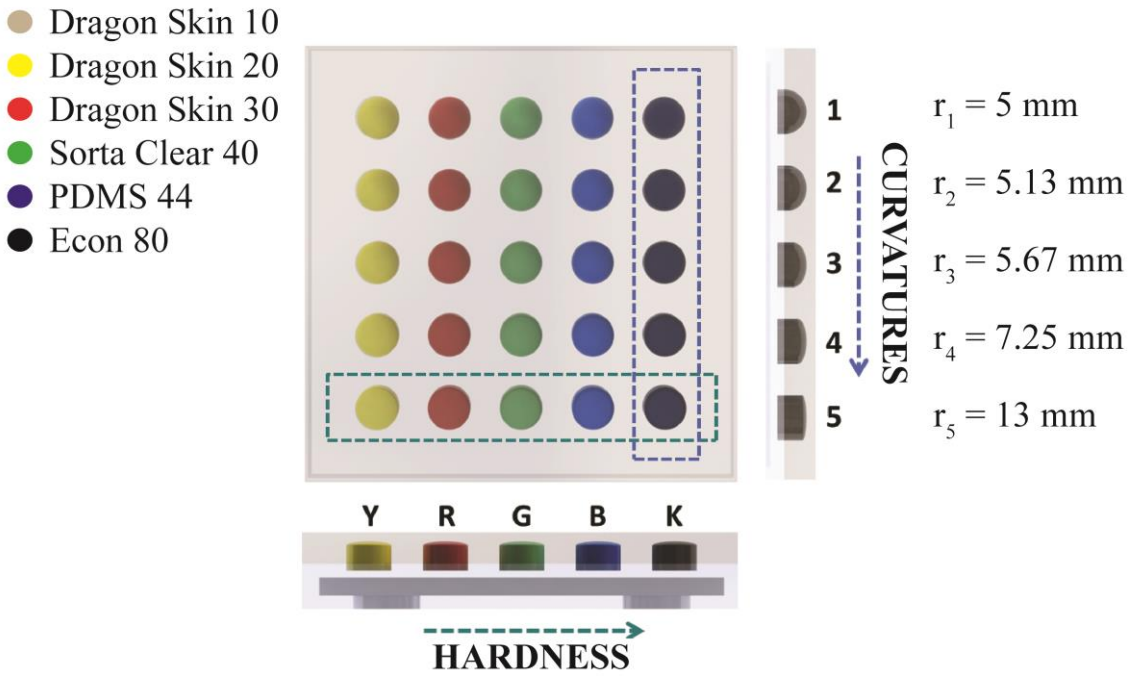

Figure 19 – Graphical representation of the silicone test phantom embedding rubber inclusions with different hardness and curvature. The Dataset 1 has been acquired by scanning the rows of the phantom, Dataset 2 scanning the columns.

classification of NPTs in colonoscopy. The device has been previously presented by the authors for force control during endoscopic navigation [235]. It is based on a MEMS tri-axial force sensor, originally developed in our lab for limb prostheses [203]. In 2006 a different device employing the same sensor was used for MIS applications, in a preliminary study of tactile tool for fetal surgery which proved the reliability of the sensor [236]. Here we employ it to classify, with machine learning techniques, variation of hardness and curvature in a silicone phantom with embedded rubber inclusions. Such inclusions are drowned in the phantom, avoiding protuberant bumps, and having size of 10 mm in order to resemble NPTs [207]. The robotic capsule scans the phantom by sliding on it, and not just indenting vertically, in order to be consistent with a realistic magnetically-driven endoscopic procedure [84, 85]. The normal force applied on the tissue while sliding is 0.4 N, which is in line with what reported in literature for capsule endoscopy [237]. Then, we train a 3 weighted k-nearest neighbor (3-wkNN) for classification and normalize the sensors output with the bias force applied to the tissue using a custom normalization model. The parameters of the normalization model have been chosen based on a particle swarm optimization (PSO). We have used different datasets for training and testing, thus addressing the issue of algorithm robustness discussed by Hui *et al.* in [232], and significantly outperforms the literature.

4.1. Methods

4.1.1. Tactile capsule and experimental set-up

The tactile capsule consists of an array of four tri-axial force MEMS sensors, with their conditioning electronics, and a 3D-printed body hosting a N50 NdFeB permanent magnet with dimensions 12 mm (l), 8 mm (w), and 8 mm (h). The capsule is covered with Dragon Skin® 20 silicone (Smooth-on, PA, USA), which has the shape of a circular dome over the sensors array (Figure 18a). The capsule dimension is 33 mm (l), 26 mm (w), and 17 mm (h). Each MEMS force sensor is composed by a central pillar which mechanically deflects four piezoresistive channels when in contact with an external body [203, 238] (Figure 18b and

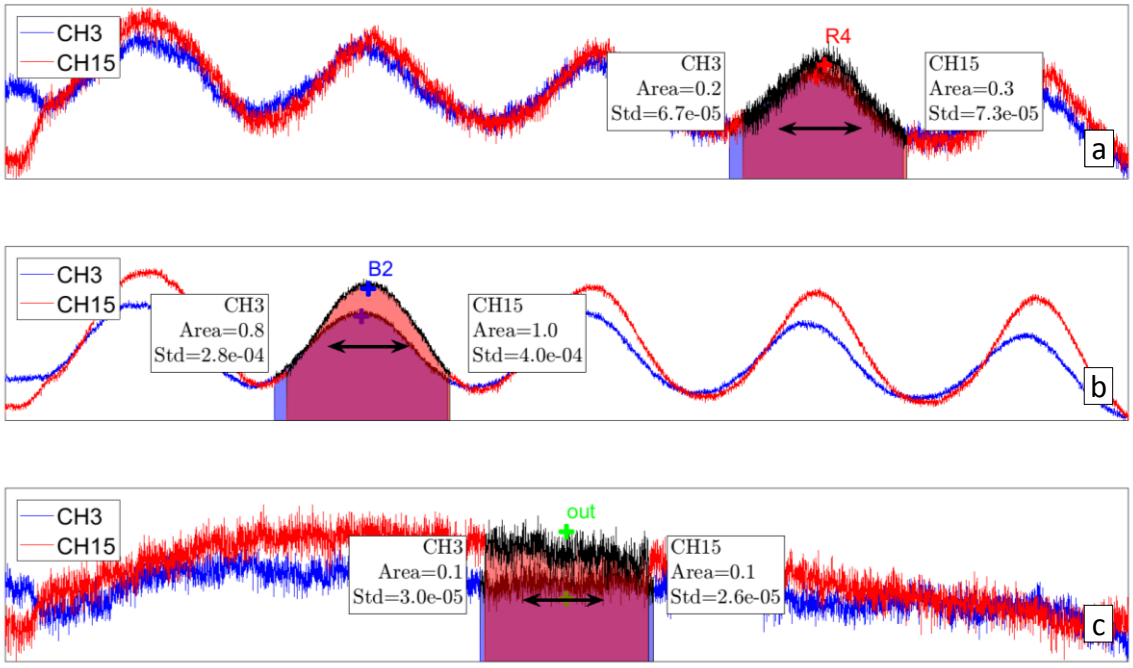

Figure 20 – Feature representation on example raw data from channels 3 and 15. Three different scanned lines, with highlighted inclusionsa) dragon skin 30, curvature 4 (R4), b) PDMS, curvature 2 (B2) and c) no inclusion (out).

Figure 18c). Out of the sixteen channels available, we selected the most informative ones, based on a static pilot test in idle condition. Thus, we have used only nine channels in the present work, *i.e.* channels 1, 3, 5, 7, 10, 11, 12, 13 and 15.

The test phantom is composed of Dragon Skin® shore 10A (Smooth-on, PA, USA) with dimensions 100 mm (l), 100 mm (w), and 17 mm (h). It embeds five lines of rubber inclusions (which are drowned, to have no superficial bumps) with increasing hardness according to Figure 19: DragonSkin® shore 20A (yellow line, marked with the Y letter - Smooth-on, PA, USA), DragonSkin® shore 30A (red line, R - Smooth-on, PA, USA), SORTA-Clear® shore 40A (green line, G - Smooth-on, PA, USA), PDMS shore 44A [239] (blue line, B - Sylgard 184, Dow Corning, USA) and Econ® shore 80A (black line, K - Smooth-on, PA, USA). Each rubber inclusion has circular shaped base with 10 mm diameter, height of 5 mm, centre to centre distance of 17 mm with the neighbors, and it is placed at 7 mm depth. Referring to Figure 19, each column corresponds to a different radius of curvature, increasing according to the numeration, going from a semi-sphere (1) to a cylinder (5).

The capsule is mounted on a 3D-printed support, and it is fixed while the test phantom moves below it. A 6-axis load cell (Nano 43, ATI Industrial Automation, Apex, NC, USA) is placed just over the capsule, in order to measure the force the capsule undergoes, in parallel with the MEMS sensors (Figure 18d). The test phantom is moved by a set of three motorized micrometric stages: an 8MTF-102LS05 *x-y* stage and an 8MVT120-25- 4247 vertical positioner, (Standa, Vilnius, Lithuania). These are programmatically controlled by a LabVIEW routine.

4.1.2. Test protocol

The test phantom is moved vertically, along *z*, to approach the capsule (Figure 18d). The indentation stops when a threshold force of 0.4 N is reached, based on the load cell measures. Then, after a pause of 2 s, it starts sliding, moving in position control along *x* for 85 mm, with a speed of 5 mm/s. The phantom is horizontally scanned: one scan for each line of rubber inclusions, plus one on a line without any inclusions (hereafter called *out*). This protocol is repeated five times.

Two datasets are acquired by placing the test phantom in two different configurations.

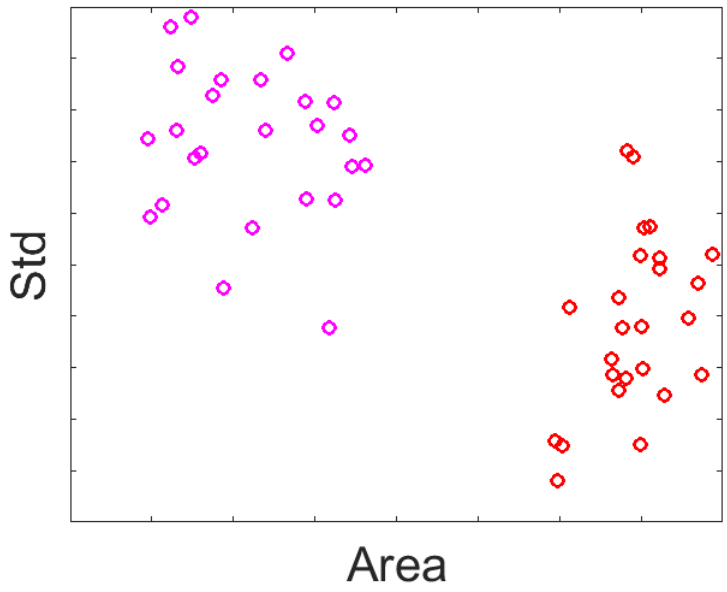

Figure 21 – Representation of feature associated to inclusions R (dragon skin 30), extracted from channel 1. In red: data from Dataset 1; and in magenta: Dataset 2.

TABLE III
CLASSIFIERS ACCURACY COMPARISON

Classifier	Hardness			Hardness and Curvature		
	DS 1	DS 2	DS 1,2**	DS 1	DS 2	DS 1,2**
Quadratic SVM	100	100	100	98.7	94.7	93
Cubic SVM	100	100	100	98.7	92.7	91
Gaussian SVM	100	99.3	100	98	88	93.3
Linear Discrim.	99.3	100	95.7	98.7	91.3	76.7
1-kNN	100	100	100	96	83.3	92.7
3-wkNN*	**100**	**100**	**100**	**96.7**	**94.7**	**94.7**
10-wkNN	100	99.3	100	94.7	86.7	89.3

* This result was achieved by using 7 channels of the 9 available (removing channels 10 and 12).
** Result obtained without bias force normalization, by merging the two Datasets.

According to Figure 19, the *Dataset 1* (DS 1) is obtained scanning the rows of the test phantom, *i.e.*, for each sliding the capsule runs on inclusions of different material (different hardness) but with same curvature. By rotating the phantom of 90 degrees, the *Dataset 2* (DS 2) is acquired by sliding on the columns of Figure 19, thus experiencing inclusions of same material but different curvature. Each dataset contains 30 slides per iteration of the protocol (from the 25 different rubber inclusions of the test phantom, plus five related to the line *out*). This sums up to 150 considering that the protocol is repeated five times.

4.1.3. Data pre-processing and features extraction

The acquired data are processed off-line with Matlab® (MathWorks, Inc., MA, USA). For each sliding, the array corresponding to the voltage output of each MEMS channel is programmatically divided in five parts (hereafter named *inclusions*), in order to isolate the peaks contained (see Figure 20a). Even the line with no rubber inclusions, previously named *out*, is divided in five parts. All the arrays have same length and the peaks of the inclusions are located in the middle of the arrays. The minimum value of the whole sliding is subtracted to each of them, and they are labeled according with the naming given to the rubber

inclusions in Figure 19, *i.e.*, a letter for the material and a number for the curvature (*e.g.*, Y4 stands for DragonSkin® shore 20, curvature 4).

Two features are associated to each *inclusion*: *i)* the area and *ii)* the standard deviation. These values are related to the hardness and the curvature of the material, respectively. Such features are used as predictors for the classification algorithm. Figure 20 shows some examples of raw voltage outputs, from channels 3 and 15 (single *inclusions* are highlighted, and the label associated to them and the related features are reported).

4.1.4. Normalization with the bias force

As expected, either little imperfections in positioning the phantom, or small variations in the indentation force can lead to significative changes in the *inclusion* features. Figure 21 shows how the features vary in the two datasets. The two groups should ideally overlay, being representations of the same items. However, since the capsule is moved in position control, the bias force fluctuation can be important, leading to such misalignment. For this reason, it is important to normalize the features with the bias force to which the capsule is subject. The load cell readings are used for this purpose. The bias force is assumed to be the minimum value, in the *inclusion*, of the F_x and F_z components. Because of slight asymmetries in the sensing part of the capsule (the circular dome is not perfectly centered on top of the sensors array, as it can be seen from Figure 18(b), the following model of normalization with the force has been adopted:

$$\begin{aligned} \overrightarrow{F_i} &= a_i\overrightarrow{F_x} + b_i\overrightarrow{F_z} \\ Area_i|_{norm} &= Area_i/(c_iF_i)^m \\ Std_i|_{norm} &= Std_i/(d_iF_i)^n \end{aligned} \qquad (1)$$

where the *i* subscript stands for the channel number. So, for each channel *i*, the normalization force F_i is given by a different combination of F_x and F_z. But also, the two features (*i.e.*, area and standard deviation) have a different relation with the applied force, which is described by the coefficients c_i, d_i, and m, n, which are constant for all channels.

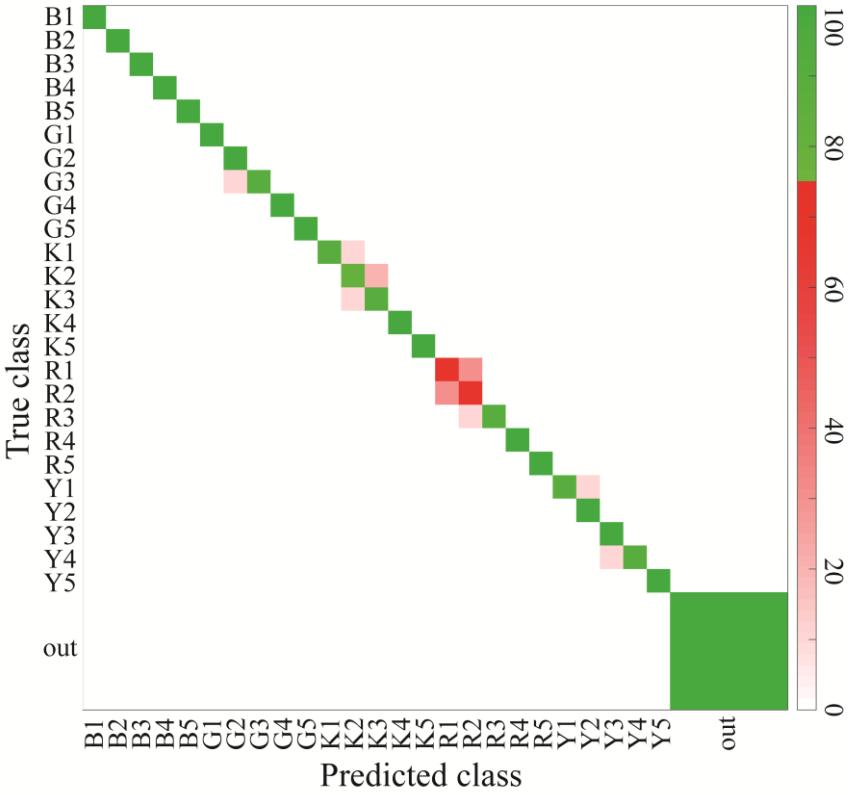

Figure 22 - Accuracy (94.7%) of training and validation of a 3 neighbors weighted k-NN classifier for hardness and curvature discrimination, trained with both the Curvature and Hardness Datasets (5-fold cross-validation). Channels 10 and 12 have been removed to improve performances.

Particle Swarm Optimization is adopted to solve this multi-dimensional problem. Nine more variables are added to enable the algorithm to switch off a number of channels in order to improve the performances. After each iteration, the classifier is trained according to the subset of channels in use, and the classifier loss resulting from the test is used as cost function. Upper and lower bounds x_U and x_L have been set to 1 and 0.01 for all the 47 variables, except *m* and *n*, which upper bound has been chosen to be 3 (zero has been excluded to avoid division by zero). The other PSO parameters are: *i)* number of iterations 1000, *ii)* population size 50, *iii)* inertia coefficient *w* 0.72, *iv)* cognitive acceleration and social acceleration coefficients, c_1 and c_2, 1.49 [240].

4.1.5. Classification algorithm

Two type of classification tests have been conducted: *i) Hardness classification*, involving six classes, which refer to the five different types of material plus the *out* (ignoring the

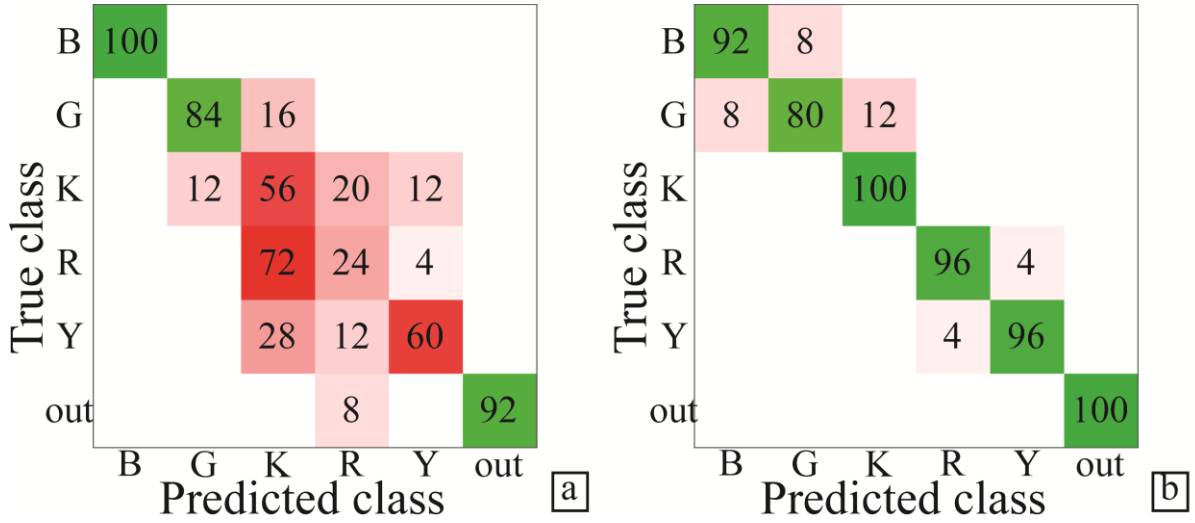

Figure 23 - Accuracy of a 3-wk-NN classifier for hardness discrimination (channels in use: 11, 12 and 15), trained with Dataset 1 and tested with Dataset 2: a) without bias force normalization (69 % accuracy), and b) with bias force normalization (94 % accuracy).

curvature information), and *ii) Hardness and curvature classification*, considering all the twenty six classes resulting by aggregating material and curvature information, plus *out*. These tests are performed on the single datasets (DS 1 and DS 2), and also merging the two (DS 1,2).

Several supervised classification algorithms have been considered as potential candidate. More specifically, we have compared: Support Vector Machine (SVM), with quadratic, cubic or Gaussian kernel; Linear Discriminant; k-nearest neighbors (kNN) and weighted k-nearest neighbors (wkNN). For kNNs we have performed an exhaustive comparison by varying the number of neighbors from 1 to 10, and also considering all the possible combinations of channels subset (which for 9 channels means 511 combinations). The algorithms have been compared based on a 5-fold cross-validation, without involving the force normalization. Then, the best classifier has been trained on DS 1, and tested on DS 2, by applying the bias force normalization.

TABLE IV
PSO OPTIMUM SOLUTION

Parameter	Channel 11	Channel 12	Channel 15
a	0.01	0.17	0.01
b	1	1	1
c	0.43	1	0.74
d	0.93	0.87	0.7
m		2.41	
n		1.51	

The channels that have been disabled by the optimization process are not reported in the table.

4.2. Results

4.2.1. Classifiers' comparison

The results of the classifiers comparison are summarized in TABLE III. The Quadratic SVM and the 3-wkNN achieved the best performances. Although the two have comparable results in terms of accuracy, the kNN is much faster because of lower computational cost. Therefore, we chose the 3-wkNN, which would be more suitable for a future real-time application of the classification method. The *Hardness classification* obtained by merging both the datasets (DS 1,2) has a 100 % accuracy, after a 5-fold cross-validation. Introducing the curvature information, and therefore enlarging the number of classes to twenty six, the *Hardness and Curvature classification* with the 3-wkNN classifier has 94.7 % accuracy. Figure 22 shows a confusion matrix of this classificatio n test. It is worth noting that the errors refer only to neighbor curvatures, e.g., R2 is mistaken with R1 or R3, but neither with R5, nor with items of other materials. This result has been obtained by removing channels 10 and 12, which improves the performance. *Out* occurrency is five times higher than the other items, justifying the different size in the confusion matrices of Figure 22 and Figure 24.

4.2.2. Classification with bias force normalization

A 3 w-kNN *Hardness classifier* (on six classes) trained on Dataset 1 and tested on Dataset 2, and applying the bias force normalization, has 94% accuracy (Figure 23b). The model described in (1), with the parameters defined by the PSO involves only the channels 11, 12 and 15. The complete solution of the PSO is summarized in TABLE IV. It is worth noting that a 3-wkNN classifier, without bias force normalization, using all the 9 available channels has 47 % accuracy, and restricting to the channels selected by the PSO, but without normalization, has 69 % accuracy (Figure 23a). This confirms that different sets of acquisition, having different bias forces, are not consistent if not normalized. Anyhow, enlarging the same classifier to twenty six classes, taking into account the curvature information, the accuracy drops down to 31.5 % (Figure 24). Even running a new PSO, we don't go over 49 %.

4.3. Discussion

The results we have obtained with this system, combining the proposed device and the chosen classification method, gives almost perfect results in terms of *Hardness classification*. On the other hand, the *Hardness and Curvature classification* test, which showed promising results after a 5-fold cross-validation, didn't obtain the expected results by involving the bias force normalization.

Anyhow, the optimization process has been affected by stagnation. The problem we tried to solve has 47 dimensions and the local minima are at least 511 (equal to all the possible channels combinations) times the number of classes we want to discriminate. So going from the six classes of the *Hardness classification* to the twenty six of the *Hardness and Curvature classification*, the local minima almost increase fivefold. The PSO algorithm tends to converge quite quickly to the swarm minimum, leaving potentially out of the search the real global minimum.

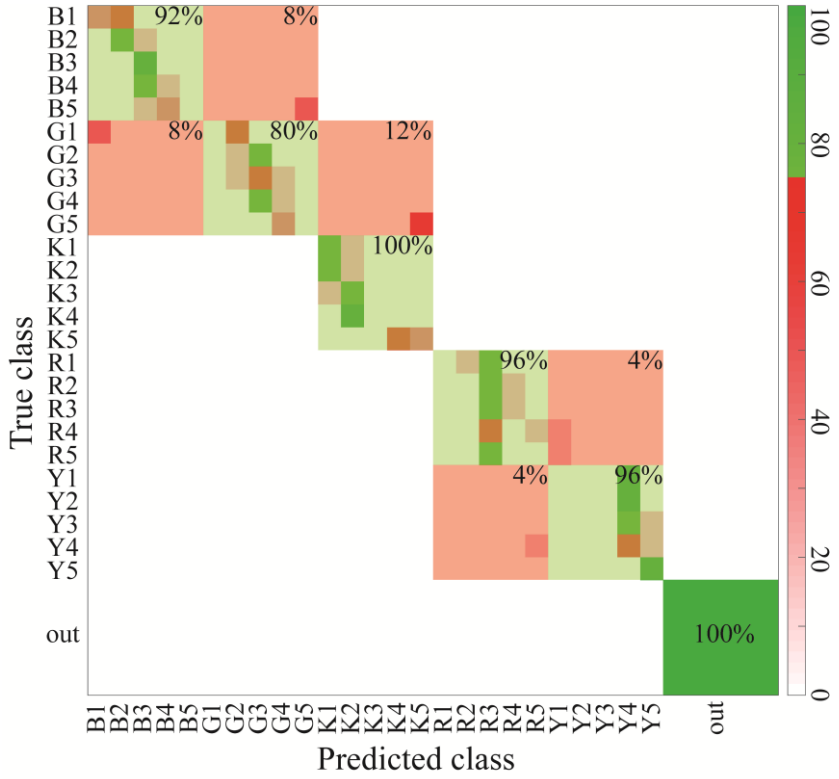

Figure 24 - Accuracy (31.5%) of training and validation of a 3 neighbors weighted k-NN classifier for hardness and curvature discrimination, trained with both the Curvature and Hardness Datasets (5-fold cross-validation). Channels 10 and 12 have been removed to improve performances.

Nonetheless, shown in Figure 24 do not present errors related to *out*, which is always discriminated from all the other items. Furthermore, we can see that the items are misclassified only with neighbors.

In this work an endoscopic tactile capsule for NPT detection based on hardness and curvature classification has been introduced. Our prototype is based on an array of piezoresistive MEMS force sensors. The device has been used for a proof of concept in a synthetic environment. There is potentiality for further scalability of the system, to make it compatible with the standards of colonoscopy. The results show a good accuracy, up to 94%, in discriminating different inclusions in a soft tissue, based on hardness. The method developed can be easily translated into a real-time algorithm in order to perform future tests in operative conditions.

In the real application scenario we foresee for our device, the tactile capsule is magnetically pulled by an external robotic arm equipped with a permanent magnet mounted on its tip.

The capsule will be navigated by the physician towards a suspected lesion, which will be eventually recognized with the help of image-based tools, and then a classification based on hardness will evaluate whether the tissue is tumorous or not. However, in such case the capsule would be subject to jumps and lumen occlusions that would make its movement unstable. A model that generalizes the sensors reading with the bias force makes the hardness classification robust and allows training the classifier with a subset of indentation forces, since the bias force model can generalize the output to a generic indentation force. The model we obtained with a heuristic optimization shows good results for the purposes of this study, *i.e.*, discriminating areas with different hardness while sliding onto a surface. So, even if the curvature information is not correctly classified, the device reliability is not compromised. Furthermore, in the realistic scenario, the magnetic localization system plays a central role. The localization output will provide the F_x and F_z components to the normalization model, and therefore the tactile system reliability will be strongly affected by the magnetic localization accuracy.

For this application we also believe that more detailed modelling of the tissue stiffness ranges and distribution of this value could add stronger priors to our classification method. This would necessitate further studies measuring and understanding this physiological value.

PART B - Haptic–assistive technologies

Chapter

5. State-of-the-art on haptic–assistive technologies[4]

Sensory substitution aids are able to mitigate in part the deficits in language learning, communication and navigation for deaf, blind and deaf–blind individuals. Tactile sense can be a means of communication to provide some kind of information to sensory disabled individuals. Hereafter, there is a review of haptic sensory substitution technologies for deaf, blind and deaf–blind individuals. The literature search has been performed in Scopus, PubMed and Google Scholar databases using selected keywords, analysing studies from 1960s to present. Search on databases for scientific publications has been accompanied by web search for commercial devices. However, a lack of acceptance of the available haptic assistive technologies emerges. Future research shall go towards miniaturized, custom-designed and low-cost haptic interfaces and integration with personal devices such as smartphones for a major diffusion of sensory aids among disabled. The present chapter are adapted from [241].

This chapter is an introduction for the works presented later in the manuscript. It defines the scope of our work and serves as comparison with the results we achieved.

[4] This chapter is adapted from the journal paper "Sorgini, F., Caliò, R., Carrozza, M. C., & Oddo, C. M. (2017). Haptic-assistive technologies for audition and vision sensory disabilities. Disability and Rehabilitation: Assistive Technology, 1-28."

5.1. Introduction

Individuals with disabilities of physical senses may have auditory, visual or tactile impairments, also in combination among them. Those with tactile impairments are often

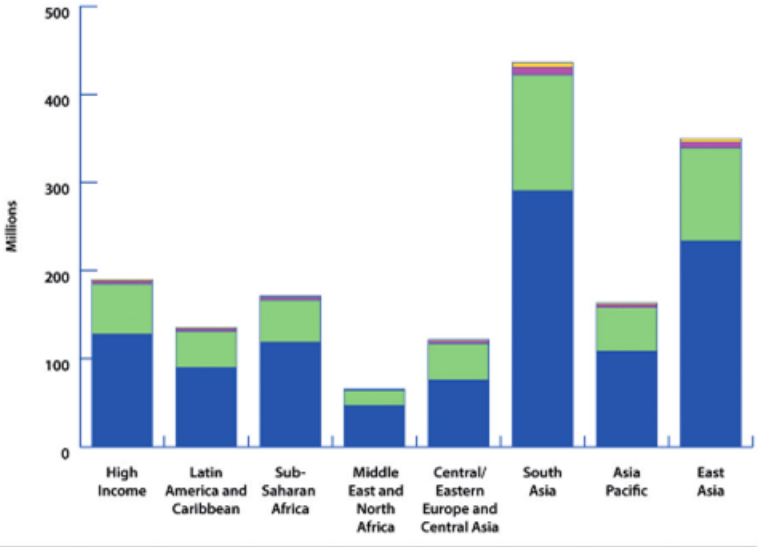

	High Income	Latin America and Caribbean	Sub-Saharan Africa	Middle East and North Africa	Central/ Eastern Europe and Central Asia	South Asia	Asia Pacific	East Asia
Profound Hearing Impairment (>80 dB)	1.78	1.64	1.72	0.52	1.73	5.29	1.94	3.84
Severe Hearing Impairment (65-79 dB)	3.27	2.85	3.03	0.94	3.02	9.09	3.38	6.83
Moderate Hearing Impairment (35-64 dB)	56.77	40.92	47.79	17.06	41.07	131.48	49.41	105.44
Slight Hearing Impairment (20-34 dB)	128.09	89.95	118.77	47.15	76.04	290.56	108.76	233.84

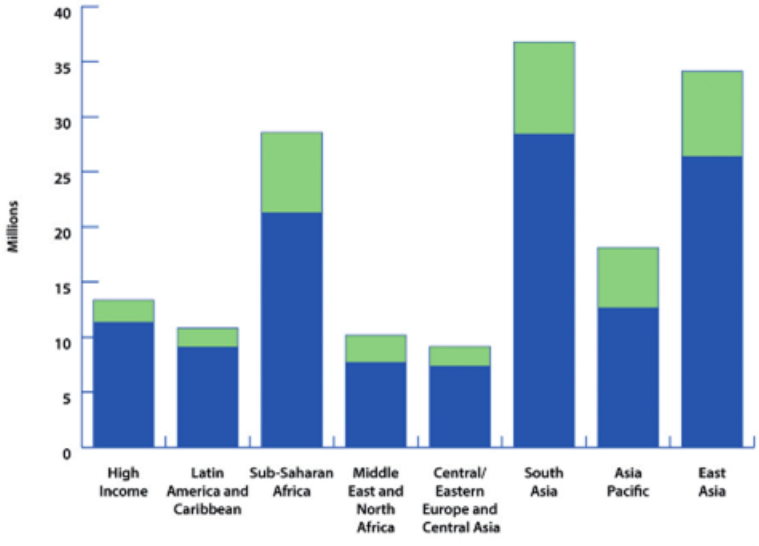

	High Income	Latin America and Caribbean	Sub-Saharan Africa	Middle East and North Africa	Central/ Eastern Europe and Central Asia	South Asia	Asia Pacific	East Asia
Total Vision Impairment	2.02	1.72	7.28	2.48	1.79	8.34	5.46	7.73
Low Vision Impairment	11.34	9.08	21.28	7.69	7.35	28.43	12.65	26.39

Figure 25 – Distribution of audition (top) and vision (bottom) disabilities in world sub-regions, according to the World Health Organization (WHO).

upper- or lower-limb amputees as a consequence of vascular diseases, cancer or accidents [242, 243]. More rarely, lack of touch sensitivity is not related to limb loss but is caused by rare pathologies such as neuro-degenerative disorders [244, 245], or the ageing process [246]. But hereafter, we consider the cases in which tactile afference is functional and can be used in combination with assistive technologies in order to mitigate the effects associated to deficits of the other physical senses. Hence, in the following, we address the cases of a lack or a significant deficit of audition, vision or both these senses. Such sensory disabilities can appear either by birth, or later due to pathologies or events that may occur during the life. Causes include rare pathologies, malformations, accidents or the natural ageing process. According to the World Health Organization (WHO), sensory disabilities affect the 5.3% of the world population for audition impairments and the 9.3% for vision impairments [241, 247-250]. The most frequent cases are those involving children and elderly [251]. There are many degrees of sensory impairments and most persons who experience these disabilities can make adaptations that lead to a partial reduction of the impact of their disability in everyday life, also in the workplace. Figure 25 shows the distribution of audition and vision disabilities across world regions according to WHO statistics, and also reports the degree of impairment. To the best of our knowledge, data referring to world distribution of deaf-blindness cannot be precisely estimated because of the difficulty in collecting reliable information on combined sensory disabilities. Sensory substitution systems can in part cover the communication and interfacing gap caused by sensory disabilities.

A sensory substitution system converts information related to a sense in a language understandable by another sense. The tactile sense can be a means of communication for auditory or visual information, or both, via sensory substitution aids. As a matter of fact, the tactile system is a communication channel since it possesses a relatively high density of mechano-tactile receptors that can act as parallel access points to transduce, convey and process information [252]. Hereafter, we review static and dynamic tactile displays used for communication, for relaying alerting messages, for navigation and the perception of environmental information such as sounds and presence of objects in the surroundings. Substitutive stimulation can be achieved by means of static indentations, vibrations or

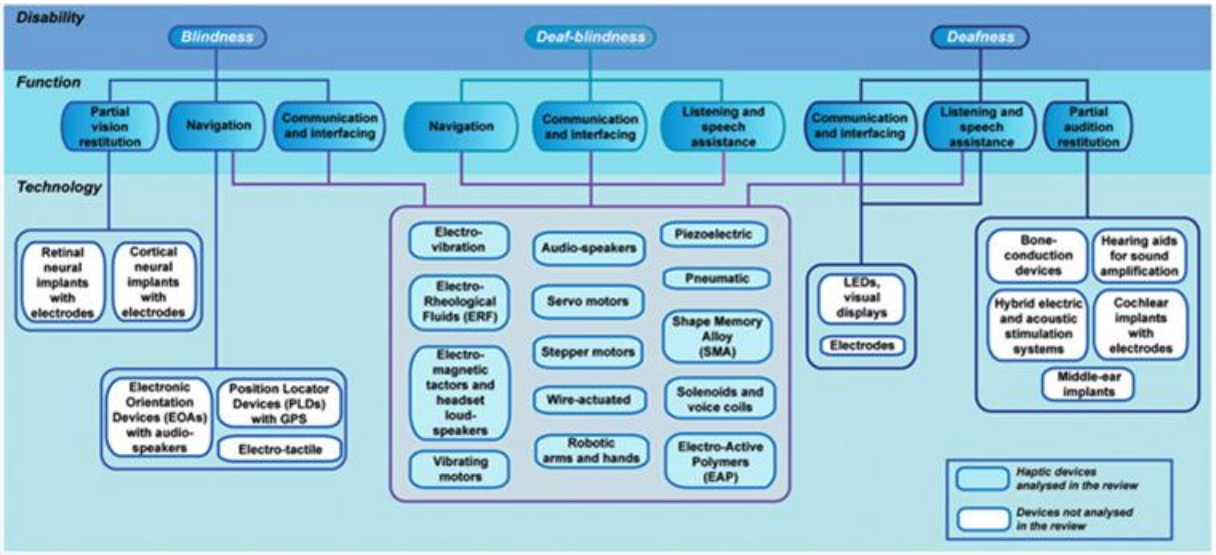

Figure 26 – Taxonomy of reviewed haptic sensory substitution systems for audition and vision sensory disabilities.

sliding on the surface of the skin. A schematic representation of existing sensory substitution aids is systematized in Figure 26, in which light blue rectangles represent the haptic technologies discussed in the present review. We classify sensory substitution systems based on the disability they address, and then we discern by targeted functionalities and used actuation technologies.

5.1.1. *Tactile communication methods*

Persons with single sensory disabilities such as deaf and blind can communicate and interface with the surroundings by means of codified languages (sign language for the deaf and Braille alphabet for the blind individuals). Communication can be harder for deaf–blind persons, because of the lack of both visual and audition senses. Codified communication methods involving tactile sense are then required. In both deaf/hard of hearing and deaf–blind communities the availability of a sign language as the only way of communication can lead to a linguistic isolation from the non-impaired. In fact, most of non-disabled people do not understand sign language and interpreters are expensive and not always available [253]. Sign languages for deaf and hard of hearing persons are based on visual sign patterns instead of sounds to transmit information. Characters and concepts are communicated using hand shapes, and also hands, arms and body orientations, but also with movements combined

with facial expressions [254]. Braille alphabet is the first method used to access written information by the majority of visually impaired people, yet not all blind individuals are able to understand Braille language [255]. In this code, characters are expressed using a cell of six dots put in three parallel rows. With 64 combinations, these cells can be used to express letters, numbers, punctuation marks and complex concepts [256]. Deaf or hard of hearing people also affected by visual impairments use sign languages among their communities. However, they are slower in signing or fingerspelling in comparison with people with the single hearing disability. Furthermore, some deaf–blind people with restricted peripheral vision may prefer the interlocutor to sign in a limited space at chest level, with the adaptation of some signs located at waist level. Nevertheless, the most common communication method among deaf–blind persons remains the tactile sign language.

In the last decades, several tactile languages were codified across different countries. Using tactile sign language, deaf–blind individuals place one hand, or both, on the speaker's hands. This allows deaf–blind people feeling shapes and movements, meaning characters and concepts. However, deaf–blind individuals with residual vision sometimes prefer to place their hands on the speaker's wrists, leaving the interlocutor's hands free to move. In this way, they can use their residual vision beside tactile sense to grasp what the other is saying. Fingerspelling, which is easier to learn than the sign language, is instead preferred by the visually impaired who became deaf later in life, or by deaf persons that only rely on speech reading, *i.e.*, lip-reading. The Print-On-Palm method consists instead in hand-writing letters on the interlocutors' hand palms. Tadoma is instead a tactile lip-reading where the interlocutor's thumb is placed on speaker's lips, while fingers lay along his/her jawline. It can also be performed via different hand positioning methods. Tadoma allows the deaf–blind person to catch the speaker's lips movement together with throat vibrations, and it is also used by persons with severe hearing impairments to improve their remaining hearing. It has been proved that Tadoma facilitates speechreading and language learning [257]. Other tactile languages, called manual alphabets, allow the word spelling on deaf–blind individuals hand palm. The most common are Lorm and Malossi. In the former, each letter corresponds to a particular sign or location on the palm of the interlocutor [258], in the latter, the palm is

touched following sequences associated with characters [259]. Another communication method is particularly used in Japan and is called Finger-Braille. In this case, users' fingers are used as keys of a Braille typewriter. The six Braille dots can be represented on the index, middle and ring fingers of both hands (two-handed Finger-Braille method) or using the distal interphalangeal joints and proximal interphalangeal joints of the index, middle and ring fingers on a single hand (one-handed Finger-Braille method) [260, 261].

For visually and hearing impaired subjects, haptic displays target the substitution of missing senses with somatosensory stimuli, taking advantage of the tactile sense. Haptic displays can be static or dynamic. In the former class, the actuation is achieved with mechanical pins statically positioned to form Braille characters, while in the latter the skin is stimulated by a dynamic mechanical action. Complex information can be conveyed by tactile icons, namely tactons. Tactons are abstract messages used to communicate information in a non-visual manner via the tactile sense. They are short tactile messages obtained through the variation of the parameters of cutaneous perception (*i.e.*, frequency, amplitude and duration of the stimulation), and are delivered to the skin via haptic actuators [262, 263]. Tactons are structured to be easily memorized, intuitive and able to induce abstraction for expert users. They encode information thanks to the variation of parameters such as frequency, amplitude, waveform and duration of the tactile pulse. The selection of the body area to stimulate is crucial since discrimination capabilities of human skin are a consequence of mechanoreceptors density.

5.2. Haptic technologies for deaf individuals

Haptic aids for deaf persons concern devices dedicated to "listening and speech assistance" and "communication and interfacing" purposes (Figure 26). The former devices play the specific role of audition substitution, partly allowing deaf individuals to listen through the tactile sense and to learn how to speak and modulate their voice properly. The latter devices can enhance social interactions between deaf persons and not impaired people, with the purpose of catching attention and feel sounds through the skin. A list of hearing aids is

presented in [241], with specific focus on actuation principles. In the next section, a discussion about deaf-oriented technologies will follow the guideline presented in Figure 26, first analysing “listening and speech assistance” aids and then going through “communication and interfacing” devices, with aggregation based on actuation technologies.

5.2.1. *Listening and speech assistance aids*

The development of listening and speech assistance devices started in the second half of 1900, when the researches carried out by Geldard led to the formulation of a tactile-based language similar to a tactile Morse code, the Vibratese. In these years, improvements in the prototyping of assistive devices consisted mainly in the development of wearable aids, often based on the transposition of the basic components of the speech, like the signal frequency and energy, in haptic information. Recent researches have shown that the human voice can be classified in two key acoustic components: the fundamental frequency and the formants. The fundamental frequency is the rate of vocal folds vibration, and is controlled with the variation of the tension and length, or surfaces area, of the vocal folds. Formants are instead the resonant frequencies of the vocal tract, responsible of the variation of vocal timbre, and are altered depending on the vocal tract length [264]. Thus, speech can be considered a wide-band variable-frequency signal generator (represented by the vocal folds) driving a certain number of variable-frequency resonant filters (activated by the vocal tract).

Vibrating motors

Vibrating motor technology is the most used in haptic applications. The actuation principle is based on the rotation of an eccentric mass thanks to the activation of an electrical winding. Vibrating motors are characterized by a wide range of physical dimensions, ranging from millimetres to centimetres, thus they can be integrated within wearable devices where non-invasiveness is essential. The variability of their actuation parameters like transmitted power, vibration frequency and supplying voltage make them suitable for the transmission of haptic information via customizable waveforms. The first wearable devices based on Vibratese language were actuated by means of vibrating motors. In the one experimented by Geldard, the tactile code was transmitted on users’ trunk via five vibrating motors and

could present 45 basic elements (letters, numbers, short words). Elements were coded by amplitude, duration and location, resulting in reading rates of approximately 38 words per minute [265], which can be considered a good achievement. Studies on deaf children who received multichannel implants demonstrated that the average speech comprehension rate without lip-reading, after 5 years training, was about 44 words per minute [266]. To date, the Vibratese system seems not to be in use any more.

Other researchers who focused on both vibratory [267] and electrical stimulation [268] could improve speech learning performance in deaf children. Vocoders are the most used aids for listening and speech assistance. These devices analyse speech frequencies using a bank of filters to detect spectral data, and convert them into haptic stimuli through a vibro- or electro-tactile display. The speech frequency spectrum is divided into filter channels, each one covering a range of frequencies. When the detected signal energy falls between the minimum and maximum pre-set thresholds for each channel, the filter output activates one of the haptic transducers, which delivers tactile feedback with intensities proportional to the signal energy. Vocoders are developed using a row of stimulators on the skin for each filter band [269]. Among vocoder pioneers, it is worth mentioning the work of Gault and Wiener [270], who in 1928 experimented “Felix”, a haptic glove connected to a vocoder. It displayed different frequencies using vibrating motors placed on each finger. Researches about vocoders used as speech learning devices are presented by Guelke [271], Kringlebotn [272] and Pickett [273]. Their tests did not reach successful results on deaf subjects, especially in the recognition of consonantal sounds. The experiments made in 1974 by Engelmann and his team at the Oregon Research Institute showed good results. They compared the effectiveness of their 32-channels vocoder prototype on hearing and deaf individuals, demonstrating that the performance of subjects was proportional to the amount of training they received. Furthermore, they found out that deaf individuals can be instructed to discriminate speech in a fine way through the tactile sense, thus confirming usefulness of vocoders for speech assistance [267].

Some tactile hearing aids amplify speech sound, transferring it to a single-channel electromechanical transducer (Gault et al. [270, 274], Siemens “Monofonator” [275]), while

other ones convert changes of the speech fundamental frequency in a tactile pattern using an array of transducers (multi-channel tactile aids) [269, 276, 277]. Multi-channel aids can code speech frequency stimulating different areas of the skin while the sound energy is represented with vibrations' amplitude [278]. They can also be bi-dimensional displays where frequency and energy are coded along two perpendicular spatial axes [279, 280]. Stimulation can be delivered discretely, via individual vibrators activated to be perceived separately, or continuously, via arrays of transducers transmitting stimulation patterns on the skin. Single-channel devices are simple, compact, low-weight, and can be easily worn. They only transmit speech rhythm, but information is not as complete as in multi-channels aids [281].

Among multi-channel aids, Tactaid 7 is a haptic amplification system made of seven channels, with seven vibrating motors placed on the user's neck, sternum, forearm and abdomen regions. Vibration parameters like frequency, amplitude, location and duration are proportional to the properties of the detected acoustic signals, and a filtering apparatus allows background noise suppression. The device is equipped with a T-coil so it can be used with audio loop systems and plugged into personal frequency modulation (FM) systems for classroom use. The use of Tactaid 7 by hearing impaired individuals showed an enhancement of speech perception in comparison to the auditory condition only (thus, not-aided). Furthermore, different studies compared the capabilities of Tactaid 7 to those of a previous device having two channels only, the Tactaid II+, as assistive devices in speech production and perception, and in the detection of closed-set contrasts of environmental sounds. In this comparison, both Tactaid II+ and Tactaid 7 enabled subjects to discriminate phonetic contrasts and impaired individuals reported slight subjective preference in the use of the Tactaid 7 [282]. Detection of environmental sounds remains a present challenge for the development of hearing aids, both with haptic hearing aids and with partial audition restitution devices (see Figure 26 for taxonomy). As a related example, initiatives like the "NSF/CISE Hearables Challenge" were established in the last years to support the development of hearing solutions which can overcome the issue of sustaining a clear conversation in noisy environments, *i.e.* to address the so-called "Cocktail Party Problem".

Another category of listening and speech assistance devices are those designed to help the haptic transposition of fricative sounds, reviewed in the work edited by Risberg [283]. Voiceless fricatives are consonantal sounds (*e.g.*, sibilants) present in some languages, as in English. These sounds are generated when the expired breath passes in a frictional way through a narrow point of the vocal tract, and correspond to high-frequency ranges. Some examples of fricatives sounds are the dental "th" in "think", the labio-dental "f" in "fine" or the post-alveolar "ss" in "mission". Risberg analyses four types of systems: modulation systems [284, 285], in which the sound signal is modulated with a carrier frequency of about 4 Hz; distortion systems [285, 286], which distort sounds with low frequencies bypassing the detected sound; frequency-dividing systems [287], in which frequency transposition occurs by dividing the frequencies of a clipped speech signal; and vocoders [288, 289].

A device representative of hand-held speech communication aids is "OSCAR". Thanks to an embedded microphone it detects environmental sounds and supports lip-reading. Transversal stimulation of thumb and perpendicular stimulation of fingers and hand is provided through two vibrators [290].

The use of wearable assistive devices, especially gloves, is quite common among researchers. An example of haptic glove equipped with vibrating motors is the one by Mazzoni and Brian-Kinns [291]. It is specifically designed to help hearing-impaired experiencing mood music when watching movies, which usually are accessible only through visual and hearing senses. The glove communicates emotions through vibro-tactile stimulation delivered by five vibrating motors placed on the back and three on the palm of the hand. Modulation of frequency and intensity of vibro-tactile patterns communicate different moods to the wearer.

Among this category of haptic aids, we also consider some devices in which the actuation is achieved via vibrating motors based on solenoid and voice coil technology.

In 1986, Boothroyd patented a wearable haptic sensory aid transmitting to the users' skin vibrational patterns proportional to sounds and voice intonations that are detected by the device. The haptic interaction occurs by means of an array of eight miniaturized solenoids

placed on the forearm. Intonations are important in speech because they can define beginning and ending of sentences, and identify crucial words, questions and statements. Experiments demonstrated how this device could help deaf individuals to improve their lip-reading and generate intelligible speech [292, 293]. A 23-channel vocoder actuated by small plungers connected to solenoids was used for the stimulation of deaf subjects, delivering vibration on fingers, forearm and legs (in this latter case with the best results). The impaired individuals were able to perform fine speech discrimination via the tactile sense. In the experiment, they were trained for 20–80 h to learn a vocabulary of 60 words and then understand sentences composed of these words. The authors also reported increases in memory and ability to discriminate, as in the number of words mastered [267].

Other solenoid-actuated technologies are the stereophonic devices by Gescheider [294, 295], von Békésy [296] (awarded Nobel prize in 1961 for the characterization of the mechanics of the inner ear) and Richardson et al. [297], which help deaf persons in the localization of environmental sounds through vibrators on arms and index fingers.

Other technologies are actuated via voice coils, like haptic chairs. As an example, the Emoti-chair from the research of Baijal and colleagues [298] allows composing vibro-tactile music and enhancing voice intonation thanks to 16 voice coils distributed on the back and the seat, and it also integrates functions related to communication and interfacing purposes.

Piezoelectric transducers

Among piezo-electrically actuated devices, we report an example of a vocoder based on this actuation principle and developed by Wada and colleagues [299]. They addressed the issue related to conventional vocoders, in which the presentation of sequential tactile stimuli on the same point of the skin made difficult the discrimination of consonants followed, thus masked, by vocals. They developed an 8 x 4 vibrator matrix as an alternative to the conventional array of piezo-electrical actuated pins. This configuration allows the presentation of consecutive stimuli, representative of speech content, from the left to the right of the finger. In this way, the delivery of tactile information on the same point is avoided, and the temporal sequence of speech is transformed in a spatiotemporal sequence

of events displayed on the finger surface. This solution was demonstrated to improve the identification rate of monosyllables. Spatial distribution of pins should be studied to improve skin sensitivity, considering that the range of spatial discrimination on fingertips varies from 0.5 mm [300] to 1.6 mm [7]. In this case, on index fingertip, pins are spaced 1 mm in columns and 3 mm in rows. The frequency value for pins vibration allows a proper sensitivity if it corresponds to the lowest absolute sensation threshold [299]. Another listening and speech-assistance aid conceived for hearing impaired individuals is the "voice pitch control" device. This system converts information from audio to vibro-tactile format by means of a display endowed with 64 piezoelectric-actuated pins [301-304].

Audio speakers

Some audio speakers-actuated devices are described in this section. Haptic chairs prototypes found in literature allow deaf individuals to experience, via the tactile channel, sensations related to the listening of music. The "Haptic Chair" from the University of Singapore is designed to enable the experience of music for the deaf persons. Sounds registered from the environment are translated into vibro-tactile feedback on the feet, back and hands of the subject [305, 306] using audio speakers integrated in the chair. The one by Karam et al. [307] is called "Model Human Cochlea" (MHC) and is a canvas chair the back of which is equipped with a 2 x 8 array of voice coils as vibro-tactile actuators. It is an interface for entertainment, allowing one to listen to music or watch a movie without using hands or arms. Sounzzz is instead a visual and tactile mp3 player that can convert sound into vibrations. The vibration of the audio speakers embedded in the player allows the user to feel the music while hugging the device. It is made of soft urethane, and it is also equipped with LEDs [241].

5.2.2. *Communication and interfacing aids*

A plurality of haptic hearing aids was observed to cover the main needs of a hearing-impaired person living in a community, like communication with other persons and interaction with the surrounding environment. Some of these devices are fully available on the market, while others are only prototypes. In both cases, experimental data show that these technologies are able to enhance, or partially substitute, the hearing sense. In this

paragraph we describe the technologies listed in Figure 26 under “Communication and interfacing”.

Vibrating motors

Some haptic sensory substitution devices integrated vibrating motors as actuators. These haptic technologies integrate rotating mass or hard-disk head-positioning actuators. “Hey yaa” is used to improve deaf persons distance communication through tactile vibrations on the waist. Two waist belts equipped with vibrating motors are activated with a button that, when pressed, induces a vibration in the belt of the receiver catching his/her attention [308].

Another category of devices dedicated to communication purposes and mainly actuated by means of vibrating motors is represented by the so-called “alerting devices” (“Communication and interfacing”, Figure 26). These are the most common haptic systems for deaf individuals on the market which advise the occurrence of a particular event via vibrations or visual signals. A study by Harkins et al. investigates how to optimize the parameters for vibratory alerting signals. The authors underline the importance of the strength, length and patterns of vibration [309]. Other devices are conceived for daily living activities. Clocks and wake-up alarms permit to wake up with a soft vibration. As an example, “Sonic Bomb with Super Shaker” (Sonic Alert) is an alarm clock with a bed shaker to be placed on the mattress [241]. Other technologies will activate at phone ringing, as well as remote receivers situated in different rooms of the house can notify a person when an event occurs in another room. Portable vibrating pagers can alert deaf parents when babies are crying [310, 311]. Other prototyped devices convert sounds, like the ringing of telephones or doorbells, into tactile stimuli [269].

An example of tactile aid actuated via hard-disk head-positioning motors is the two-channel display developed by Yuan et al. [312]. This display acts on the fingertips and is developed in order to give information about consonant voicing during lip-reading. The frequencies of tactile signals employed for the bi-digital stimulation are proportional to the carrier frequencies of the two bands of speech. These frequencies are obtained from the

modulation of the amplitude envelope of each band. The tactile device is actuated by means of three vibrating rods, each one connected to a hard-disk driven head-positioning motor.

Assistive technologies actuated via vibrating motors based on voice coils are also present. A voice coil is a winding of conductive wire in which a permanent magnetic field produces a force which is proportional to the current flowing in the conductor. This force can be used to produce linear or rotational motion, thus for the fabrication of motors.

As an example, the “Emoti-chair” from the research of Baijal et al. [298] is another haptic chair, this time developed to assist deaf persons in communicating and interfacing with other people. It allows composing vibrotactile music and enhancing voice intonation using 16 voice coils distributed on the back and the seat of the chair.

5.3. Haptic technologies for blind individuals

Haptic-assistive systems for blind people convert visual information into mechano-tactile stimulation, which could also involve multisensory feedback for those devices that elicit auditory cues in addition to cutaneous ones. Users require a long training to effectively understand this kind of information and to develop the capability to get oriented and to detect obstacles in the surrounding space. The discussed haptic technologies for blind individuals are focused on the improvement of visually impaired navigation and communication. Although the most widespread devices on the market are smart-canes, hand-held devices and Braille displays, research is oriented towards the improvement and diffusion of ease-handling and wearable aids which can accomplish both these purposes. In the next section, we go through haptic aids dedicated to visual disabilities. We first describe devices specific for in- and out-door navigation, including wearable and non-wearable ones, and then those for communication and interfacing purposes, with aggregation based on actuation technologies as presented in Figure 26. A list of aids for visually impaired people is presented in [241], with specific focus on actuation principles.

5.3.1. Navigation aids

With the expression “navigation aids”, we refer to assistive devices used to help sensory-disabled individuals in the exploration of indoor and outdoor environments. This category comprises ordinary aids like guide dogs and white canes, on which blind people usually rely. However, these aids have some limitations and are not always affordable. White canes give limited information, while guide dogs are expensive, have a work life range between 6 and 8 years and their speed is difficult to manage for some individuals [313].

Assistive devices for navigation also comprehend “smart” devices capable to detect obstacles around the user via different sensing technologies. Recent prototypes include GPS sensors and interact with environmental beacons. Examples of these systems are Electronic Travel Aids (ETAs), Electronic Orientation Aids (EOAs) and Position Locator Devices (PLDs) (“Navigation”, Figure 26). [314]. Among these, only ETAs convert visual information into tactile stimuli, while EOAs and PLDs deliver audio information. ETAs are based on ultrasonic (short range) and/or infrared (long-range) technologies for obstacle detection, and sometimes include video acquisition sensors. Haptic stimulation is achieved with tactile stimuli delivered to different body locations through vibro- or electro-tactile signals. More recently, thanks to widespread use of smartphones, travel aids are interfaced with apps helping the visually impaired user to navigate both out- and in-door.

Vibration motors

Electronic Travel Aids with vibrating motors are probably the widest category of navigation devices for visually impaired due to the high stimulation intensity that such actuators can deliver. We list in the following section some of the implementations that are characteristic of this group, starting with wearables.

The “People Sensor” distinguishes between animate (humans) and inanimate obstacles, and communicates their nature and distance through vibrational cues on the wrist [315]. The “Sunu Band” (Sunu Inc.) is a wristband with sonar sensors and vibrating transducers. It gives vibratory feedback when approaching an obstacle and can also interact with beacon

technology [241]. Kammoun et al. [316] experimented a system composed by two wristbands transmitting information by means of vibrating motors.

Head-mounted systems are equipped with stereo cameras for scene acquisition, vision algorithms and tactile display to represent detected obstacles. The helmet developed by Mann et al. [317] is a head-mounted device equipped with a Kinect camera for object detection and a vibro-tactile array on the forehead, actuated with vibrating motors. The "Tyflos" navigation system by Dakopoulos et al. consists of glasses with cameras and a four by four array of small vibrators attached to the user's chest for haptic stimulation [318].

Based on his study on computer vision systems, Adjouadi formulates an algorithm which identifies "safe" paths in the surroundings to assist navigation. Information acquired by a camera can be used to describe the environment to a visually impaired person, and to identify safe paths, which means paths clear from depressions, obstacles and drop-offs. Directions to take and obstacles are communicated through vocal advices, with the possibility to introduce a tactile module (not yet implemented) specifically dedicated to the representation of the clear route [319].

Haptic vests are commonly actuated by a matrix of vibrating coin motors, allowing the transmission of spatiotemporal vibrational patterns. Arrays of vibrators are usually placed on the torso or on the upper-back region, which is particularly suitable for haptic stimulation since this body area has a relatively high density of mechano-tactile receptors [320]. Tactile vests are commonly interfaced with other navigation technologies for the wireless communication of objects' positions in the surroundings. The vest by Akhter et al. integrates an array of 8 x 8 motors and is actuated with signals coming from smartphones and computer vision systems [321]. Other examples of haptic vests equipped with arrays of vibrating motors are the "Kahru" system by Gemperle et al. [322], the device designed by Jones [323] and the fleece vest by Van Veen et al. which integrates a high-density haptic array with 120 vibrators [324].

Haptic belts are wearables less cumbersome than vests, but in comparison to them they allow the stimulation of a limited body area. These devices are generally equipped with a

host PC, computer vision systems, GPS, sonar and Wi-Fi, like those by McDaniel et al. [325] and VanErp [326]. Other devices interact with smartphones' apps to provide navigation information, like the one from Auburn University [327], or include a buzzer for auditory feedback together with tactile stimulation like in the prototypes by Flores [328] and Gilson et al. [329]. Vibrators embedded in belts can be allocated along different directions and with variable densities. "ActiveBelt" stimulates the skin utilizing eight vibrators around the torso [330], the belt by Nagel et al. [331] gives a continuous stimulation around the waist via 13 vibrators all around its circumference, while the one by Wu transmits information about objects' shape to an array of vibrators on the user's back [332]. The prototype by Johnson is distinguished from the previous ones thanks to the presence of two web cameras for scene acquisition, while actuation is delivered via 14 vibrating motors [333].

Shoe-integrated navigation systems consist in smart insoles or footwear able to detect obstacles and to transmit haptic vibrations to feet or other body locations. "Lechal" (Ducere Technologies) is a commercialized haptic shoe. It is actuated by small vibrating motors, and interacts via Bluetooth with a smartphone app [241]. A similar insole is equipped with a vibrotactile array of sixteen motors (diminished to four in the following versions) [334-336]. Other shoe-mounted devices can send haptic information to arrays on different body areas. An example is a system equipped with infrared sensors interfaced with a vibro-tactile display of two vibrating motors mounted on the arm [337]. The rehabilitative shoe by Abu-Faraj et al. adds to these technologies also a pair of spectacles for the detection of head-level obstacles [338], while Lobo et al. proposed a camera-motion capture system interacting with markers on wearer's feet and lower leg. In this case, haptic feedback is provided through an array of 32 vibro-tactile actuators on the wearer's leg [339].

Another group of wearable navigation aids are haptic gloves, enabling the detection of environmental information with range sensors and delivering haptic vibration over hand's skin. An example is "Tacit" (Grathio Labs), equipped with sonar sensors and actuated through two servo motors [241].

Hand-held devices are another category of haptic aids transmitting navigation information directly on the hand. Despite these devices can limit the use of user's hands because of their

need to be constantly held, some of them are already present on the market, like the "Mowat" sensor (Wormald International Sensory Aids). Others are still prototypes like the "mobile guide", which allows blind individuals to orient in museums between tagged artworks [340]. It comprises a software interface to be integrated with a mobile museum guide, and a two channels haptic module to stimulate index and thumb fingertips via two vibrating rings. It shows success in artworks localization, and is effective with both tactile and auditory cues.

The most common hand-held devices are smart-canes, which are comprised of a sensorized handle that serves as a tactile interface and a cane fixed to that. Several studies were focused on the identification of the best stimulation parameters for the transmission of information regarding obstacles. The studies by Kim [341] pointed out that a four-finger stimulation through tactors, combined with a spatiotemporal variation of stimuli, can lead to a correct identification of information. The smart cane by Gallo et al., together with haptic stimulators, is equipped with a dual-axis gyroscope for orientation detection [342], while the one by Wang et al. [313] interacts with environmental beacons and is actuated by one eccentric mass motor. Fanucci et al. [343] implemented a mobility aid system for visually impaired in outdoor environment, and tested it within Lucca's city walls. The system comprises a smartphone, path detectors and GPS interacting with a smart cane, which conveys vibro-tactile information to the hand guiding the blind person along a safe path. The "interactive cane" (BlindMaps) gives instead real-time information on the surroundings, interesting places and crossroads. It interfaces with user's smartphone and interacts with environmental beacons. "UltraCane" (Sound Foresight Technology Ltd) is already on the market and detects obstacles also at head level [241], while "LaserCane" (Nurion-Raycal Industries) can detect obstacles with light beam emission and gives audio and tactile feedback directly on user's hand [344]. The prototype by Calder can be used in hands-free and stand-alone mode, respectively transmitting tactile feedback on the users' trunk and the cane's handle [345].

Smartphones as well can serve as substitution aids for navigation purposes thanks to GPS, compasses and maps integrated on-board. The haptic feedback is achieved via the

embedded vibrators. An example is the “WalkyTalky” [241], an accessibility application for Android phones which improves the visually impaired navigation. The application, in fact, pronounces the address of nearby locations as the user passes them. It works in combination with spoken walking directions from Google Maps and also provides vibro-tactile feedback. The last device we present for this category is a prototype actuated via a stepper motor. It was designed by Amemiya with the purpose of helping blind persons to escape from dangerous areas. It generates pulling forces in the desired direction using a stepper motor that interacts with a swinging slider-crank mechanism [346]. Regarding haptic displays, it is worthwhile mentioning an array of pins actuated with motors based on solenoid technology [347, 348] and interacting with users’ palm.

Piezoelectric transducers and shape memory alloys

Among piezoelectrically actuated navigation wearables, Zelek et al. [349] developed a navigation glove able to detect environmental information thanks to stereo cameras. It is actuated with piezoelectric buzzers placed one per finger. Some recent applications enable visually impaired persons to interact with the display of smartphones. “BrailleBack” allows connecting different refreshable Braille displays to the smartphone. The displays are piezo-electrically actuated and controlled via Bluetooth technology [241]. “BrailleType” [350] and “MoBraille” frameworks [351] allow instead to write Braille characters on the touchscreen.

Examples of devices actuated through Shape Memory Alloy (SMA) technology are discussed in the following. An example is a haptic vest equipped with a matrix of SMA actuators for the transmission of spatiotemporal patterns [352, 353], while another example is a head-mounted system called “Intelligent Glasses” [354], in which a tactile display actuated through SMA elements delivers visual information from the environment on the user’s skin.

Wired-actuated devices and robotic arms and hands

The “VIDET” wearable robotic system described in the work of Arcara transmits information to a wire-actuated haptic interface that modifies the shape of user’s finger according to the disposition of objects in the scene [355]. “CyARM” is a hand-held device for obstacle detection which is equipped with ultrasonic sensors. Distance from obstacles is

communicated by varying the length of a wire which connects the device to the user's belt. When approaching an obstacle the wire retracts, thus pulling the user's arm back and giving the illusion of an imaginary arm extending from the obstacle [356].

Among the technologies involving a robotic arm, used to support navigation, it is worthy of attention the prototype by Yuan et al. [357]. The robotic arm in this device transmits environmental information to the user. Navigation aids and interfaces also allow blind individuals to explore museums and exposition sites, as reported in the work of Park et al. [358]. This system involves a telepresence robot, an RGB-D sensor and a haptic interface (robotic arm) for feedback. Although this is not the only existing prototype dedicated to the haptic exploration of art works in public expositions, it is the first which makes the user interact with a robot. In this field, it is worthwhile to point out the "Museum of pure form" from the research group led by Bergamasco [359]. In this project, a haptic device mounted on an upper limb exoskeleton allows the visitor of a museum to interact with pieces of art. Pieces of art are scanned and inserted in a virtually reconstructed museum, where the visitors can touch statues while viewing their shape in a virtual reality cave.

5.3.2. Communication and interfacing aids

The most common devices allowing blind people to communicate and interface with the external world are Braille displays ("Communication and interfacing", Figure 26). Refreshable Braille displays (or Braille terminals) are electromechanical devices where Braille characters are represented by means of pins piezo-electrically raised from holes on a flat surface. These systems allow blind users to read text outputs from computers, but they are quite expensive and can display only 40 or 80 Braille cells. A list of available typologies of Braille displays is presented by Russomanno et al. [360], with a focus on refreshable Braille displays which did not achieve a successful commercial diffusion or were developed for research purposes only. Experiments with these devices demonstrated that single-cell displays, that do not allow sliding exploration, decrease the blind person reading performance.

Tactile Vision Substitution Systems (TVSS) ("Communication and interfacing", Figure 26) [320, 361, 362] are a category of haptic devices which acquire visual information with

cameras and deliver vibrotactile stimuli to the skin via a two-dimensional matrix of tactile stimulators. Studies from the 1970s demonstrated the skin's ability to interpret visual information using these systems. The impaired individuals could recognize lines with a vertical, horizontal and diagonal orientation, and the most experienced users could identify common objects and peoples' faces [320]. Recently, studies by Bach-y-Rita confirmed the effectiveness of tactons [363]. The experimentation focused on the conversion of video information in vibrotactile stimuli on the abdomen, the back or the thigh using arrays from 100 to 1032 points.

Tablets and smartphones displays can be used to represent tactile images, thanks to their embedded piezoelectric transducer or vibrating motor. When the finger touches the surface it vibrates in correspondence of a displayed object allowing the detection of edges or the interaction with maps. A drawback of these technologies, arising when the display is too big, is a decrement of vibration strength proportional to the distance from the interaction point.

Representative devices of the aforementioned displays are presented in the following, according to the taxonomy in Figure 26, with aggregation based on actuation technologies.

Piezoelectric transducers, electro-active polymers and shape memory alloy technology

In this paragraph, we present some examples of haptic aids actuated via three technologies, involving materials whose physical deformation, under different circumstances, generates a haptic effect. The first category we review in this paragraph is the one relative to piezoelectric haptic aids. "Optacon" (OPtical to TActile CONverter) (Telesensory Systems Inc.) is one of the first developed communication aids for blind individuals for reading non-Braille text. An embedded camera module is moved across text lines with one hand, while the other hand explores a dynamic Braille tactile array (24 by six metal rods) where the acquired information is displayed. The vibration intensity is regulated through an adjusting knob [364, 365].

Analysing more in general Braille displays, some of them are improved with a speech text functionality which integrates the haptic feedback. An example is the "BrailleNote" (HumanWare) [366]. A particular category is represented by the "lateral skin deformation

displays". These are Braille displays able to communicate a single line of Braille dots through lateral skin deformation instead of normal indentation [367]. Hayward describes a similar display: an array of pins connected to a membrane selectively providing lateral stretch stimulation of the skin [368]. Such technology was also used to perform neuroscientific studies which targeted a more profound understanding of somatosensory system mechanisms [369, 370], that is a major requirement for the development of advanced sensory-substitution devices. Based on the same pinned approach, "STReSS" by Pasquero et al. allows the representation of "tactile movies" with a refreshing rate of tactile images of 700 Hz [371]. The object-detection device by Bliss is a TVSS aid piezo-electrically actuated and equipped with piezo-electric raising pins [372].

Other devices can allow visually impaired users to draw, like the one by Kobayashi and Watanabe. It is equipped with a tactile display and a stylus pen which can be pointed over the image, delivering tactile feedback to the user through pins vibration [373]. Braille displays can also be used for images and graphs visualization, in most cases with the purpose of facilitating interaction with computers. In the research of Wall et al. a graphic tablet for graphs visualization is developed. It is controlled with the user's dominant hand, while the non-dominant one receives tactile feedback through a pin-actuated mouse [255]. Homma developed a tactile display equipped with an array of 16 by two vibratory pins which transmits information about text's formatting to blind computer users. Deaf individuals could also use it for speech communication [374]. The "Graphic Window Professional" (Handy Tech) can represent images from a PC through lines of piezoelectric elements [375]. Similar device is "Dots View DV-2" (KGS Electronics) but characterized by a wider reading aperture, while "HyperBraille" (Metec) [376] is a display that embeds a matrix of a high number of dots (up to 7200) and is actuated with piezoelectric reeds.

The second category we are going to mention here is the one relative to EAP, which were used in some prototypes for the development of haptic aids. The working principle of these devices is based on the EAP property of changing in size or shape when stimulated by an electric field. A relevant example of these systems is the finger-tactile display developed by Koo et al. [377]. Initially designed to stimulate fingertips, its flexibility makes it adaptable

also for different body locations. It is made of a soft polymer which includes a matrix of dielectric elastomer dots. When voltage is applied, dots expand or compress transmitting information to fingertips.

The third technology mentioned here and also exploited for the development of tactile aids is the shape memory alloy. The property of SMA actuators to easily return, after being deformed, to their original shape when heated makes them suitable for the development of haptic devices. An example of a communication and interfacing aid SMA-based is the display by Haga et al. It consists of a line of dynamic Braille characters and is equipped with an array of SMA actuators and a magnetic latch [378].

Pneumatic actuators

Examples of refreshable Braille displays actuated by means of different pneumatic technologies are reported in the following:

The Braille display by Yobas [379] consists of a polysilicon membrane actuated by means of a MEMS pneumatic micro-valve. This membrane inflates when a pressure is applied into the pneumatic cell, thus allowing the user to perceive a deformation like a single Braille dot. The refreshable Braille cell by Lee [380] is instead actuated through melted paraffin wax which increases its volume after a heating process. The wax is placed in containers sealed with a silicon rubber diaphragm, but when it expands the silicon diaphragm undergoes a deformation and raises the Braille dot. “Phorm” (TactusTechnologies) [241] is a commercial bubble display made with a flexible surface that can be shaped in edges and bumps thanks to microfluidics. In the tactile display made by Cunha [381, 382], the mechanical stimulation of the skin occurs instead through CO2 jets spilled by an injection needle. The needle is moved by a tactile plotter that can draw characters on the user’s skin, and can be used for both blind and deaf–blind persons. A drawback of this system, with respect to the other ones previously described in this paragraph, is its size which precludes its wearable application. Portability is, in fact, an essential feature that can enlarge the application field of assistive devices.

Vibrating motors

The experiments carried out by Bach-y-Rita on TVSS led to the commercialization of "VideoTact" [383], a device which allows blind users to recognize the shape of simple objects and line orientations thanks to array of vibrators acting on different areas of the skin. Other two devices enabling vision substitution are the "Visotoner", which converts video inputs in haptic signals through vibrators placed on fingers, and a camera system electronically interfaced with a flexible pad of vibrators placed on stomach's or back's skin [384]. Minagawa et al. proposed instead a device which represents visual diagrams on a tactile display, combined with auditory information [385]. "PhanToM", already common on the market, is a force display equipped with an end-effector which gives haptic feedback to the user's fingers and hands [386, 387]. It is mainly used by non-impaired persons, but it can also be used in virtual reality both for visually impaired and deaf users [388].

Researches on haptic substitution aids addressed the problem of colour representation as well. Some examples of devices enabling blind persons to appreciate colours are haptic gloves. The "Color detection glove" by Schwerdt et al. [389] is equipped with colour sensors on thumb and index fingers, and interacts with electromagnetic vibrotactile motors (tactors) placed on armbands. A similar device is the "VIDET Glove" developed by Cappelletti et al. [390], but in this case, the actuation is performed using tiny headset loudspeaker stimulators, placed on three fore-fingers. They refer to red, green and blue dimensions that code colours by vibrotactile frequency modulation. Despite experimental results are satisfying, these devices require a high cognitive load and a long training.

We mention here some devices actuated via vibrating motors based on solenoid technology. The dental chair in the research of Collins [391] is a TVSS developed in the shape of a haptic chair. Here, polarized solenoid actuators stimulate the skin depicting bi-dimensional silhouettes of detected images. This actuation technology is also used for the development of displays which enable blind individuals to appreciate graphic elements and figures. Subjects can try to follow tactile images' contours with hand exploration and lateral motion of the fingers. "Moose" is a bidirectional haptic computer interface which represents windows, menus and buttons as patches and lines. Basically a powered mouse, it gives

haptic representation of icons. The actuation is obtained with a manipulandum coupled with two linear voice coil motors through two perpendicular flexures [376].

Electro-rheological fluids and electro-vibration-based actuators

Two actuation technologies based on the variation of the properties of a system, induced by an electric field, are Electro-Rheological Fluids and Electro-Vibration-based assistive devices.

ERF are suspensions of non-conducting but electrically active particles in an electrically insulating fluid which viscosity changes reversibly in response to an electric field. In the last years, this technology was also integrated in tactile displays. As an example, we mention "Tactel", a display shown in the work of Klein et al. [392]. It is a cylindrical tactual element made of a piston that can move vertically in a gap filled with a ERF. Metal electrodes on the walls of the cell generate an electric field activating the fluid. These tactual elements can also be organized in arrays, which dimensions can vary according to the body area on which they are required, and can be used for the development of Braille displays or the transmission of tactile sensations in virtual reality applications [393].

Other devices allow the representation of images thanks to the electro-vibration principle. Haptic displays based on this technology transmit vibration on the user's finger through the modulation of the friction created between this and the surface of a display. Here, a time varying voltage is applied between an electrode and an insulated ground plate, generating an electrostatic force between the plane and the finger. An example worth to mention is "TeslaTouch" [394] that, for this reason, is considered a "surface haptic display".

5.4. Haptic technologies for deaf-blind individuals

"Communication and interfacing" technologies as well as alerting aids designed for deaf individuals can also address deaf–blind population. This is true for "navigation" technologies

and “communication and interfacing” aids designed for blind as well. Examples are haptic Braille displays for computer interaction or haptic ETAs.

In the following paragraphs, we report some devices and prototypes specifically developed for deaf–blind people, according to the taxonomy presented in Figure 26. Their working principles are mostly inspired by the communication languages previously discussed. The dissertation starts from navigation aids, some of those being also suitable for blind users. Then the section is concluded with communication and interfacing technologies and listening and speech assistance aids, which can also address deaf communities. In [241], haptic technologies for deaf–blind individuals are summarized and listed according to actuation principles.

5.4.1. Navigation aids

Navigation devices for deaf–blind individuals are based on various actuation principles and may stimulate several body locations (“Navigation”, Figure 26, listed with aggregation based on actuation technologies).

In this section, we focus on the devices specifically conceived for deaf–blind individuals. The present section does not discuss assistive aids that have already been presented for blind and that are also used by deaf–blind persons.

Vibrating motors

Here we treat tactile ETAs for deaf–blind persons, actuated by means of vibrating motors. In order to communicate to the impaired user his proximity to a street or a crossroad, Schmitz and Ertl designed a map display with a rumble gamepad [395]. It guides a cursor over the map giving a vibration to communicate users’ position. The “Tactile Handle” [396, 397] consists in a 4 x 4 array of actuators placed on fingers’ phalanxes and interfaced with proximity sensors and micro-controllers. A commercial hand-held device is the “Miniguide”. It is equipped with ultrasonic sensors to detect information about the environment. The experimental evaluation provided evidences that this device is reliable for obstacle detection and to increase users’ functional mobility, free-time activities, community life and social

interactions. Anyway, the device can be non-efficient in crowded or snowy environments [398]. “Polaron” (Nurion Industries) [399] is another commercial device which can be mounted on a wheelchair, held in hand or worn around the neck. It detects obstacles with laser and ultrasound sensors and gives haptic feedback through vibrating motors. Concerning environmental systems, Max et al. developed a virtual interface consisting of beacons which interact with echo-sensors [400]. This system allows the exploration of a three-dimensional map and permits the appreciation of complex textures. It provides feedback in the form of audio cues and vibrations. The field of wearables comprises the haptic system by Ogrinc et al. [401]. It is conceived to help blind and deaf–blind individuals in riding horses. The rider is informed about the directions that the horse must take through the haptic signals originating from two vibrating motors installed on his upper arms. These are wirelessly controlled by a smartphone held by the instructor, who can remotely drive the impaired rider. In this way, the rider can pull the reins according to vibration received on the left or right arm. An example of shoulder-mounted systems is instead the one developed by Cardin et al. [402]. It is interfaced with sonar sensors and actuated by means of eight vibrators mounted along the shoulders line. “Anotimous”, developed by Spiers and Dollar [403], is a cubic hand-held device composed of two halves. It is conceived to help sensory impaired users in navigation, especially deaf–blind, but can also be addressed to blind and deaf persons. Information about direction and distance of navigational targets is delivered to the users’ fingers via translation and rotations of the upper half. It is actuated via one servo motor and can be optionally equipped with a vibrating motor. An example of a haptic device in which the embedded vibrating motors are based on solenoid technology is the “Finger-Braille” [404, 405]. It is a wearable ring-shaped device equipped with a vibrating motor or a solenoid motor on each ring. It is based on Finger-Braille method and interacts with radio-frequency identification (RFID) tags. Worth to mention among wearable haptic aids is the shoulder-tapping interface by Ross et al. [406]. This is a backpack where a 3 x 3 array of audio-speakers actuated by solenoids performs the same function of an array of vibrating motors, in order to prove spatiotemporal vibrational patterns to the user.

5.4.2. Communication and interfacing aids and listening and speech assistance aids

The devices for deaf–blind individuals that we discuss in this paragraph are those specified in Figure 26 under “Communication and interfacing aids” and “Listening and speech assistance aids”, and are listed with aggregation based on actuation technologies. These devices deliver information through haptic stimulation of the hand, mainly following the codification of manual sign languages. In this section, we focus on the devices specifically conceived for deaf–blind persons. This section does not discuss assistive aids that have already been presented for blind and deaf and that are also used by deaf–blind persons.

Robotic arms and hands

Based on a haptic robotic arm is the device developed by Murphy et al. [407], a PC-based application to improve math and science learning for students. They integrated the low-cost haptic interface “Novint Falcon” into the learning system. The interface is a commercial controller with three degrees of freedom. The student, holding the grip at the end of the controller, can interact with a virtual environment and receive haptic feedback when the cursor intercepts a virtual object on the screen. Results showed an improvement in math learning for students who used these applications in classrooms, confirming the effectiveness of haptic-based applications for education purposes. “Parloma” is a system for remote communication between deaf–blind individuals using hand shapes. It consists of a low-cost depth sensor as an input device, and a robotic hand to provide output to the receiver. The communication is achieved through the web, similarly to instant messaging technologies [408, 409].

Vibrating motors

Among vibrating motors displays, we collected examples of devices characterized by various working principles. An example of wearable device is the “Body-Braille” by Sarkar et al. [410]. This system can allow long distance communication of deaf–blind and blind with

disabled and non-disabled persons. It consists of six armbands and allows the conversion of Braille text into vibrations on the body.

“V-Braille” [411] allows us to use the smartphone touch-screen for the representation of Braille characters, while smartphones haptic vibrations deliver haptic cues. “MyVox” comprises a Braille display, a keyboard, a visual display, a speaker and is actuated by a vibration motor [412]. “Autosem” is a bimanual communication aid. A set of semaphores is used to represent an alphabet, which is defined by different orientations of both hands. The hand orientation is detected by means of low-cost game controllers with integrated accelerometers. Users can detect outputs by scanning series of available orientations, where the correct one is communicated with a vibrotactile feedback [413].

Since deaf–blind persons are used to receive haptic speech information mainly on hands, gloves are a good solution for wearable assistive devices dedicated to these persons. The “Mobile Lorm Glove” translates the “Lorm” alphabet into text. Textile pressure sensors on the palm enable the user to compose messages that are then sent via Bluetooth in the form of SMS. The message received from the user is conveyed to the back of the glove following tactile patterns, according to the “Lorm” alphabet. Actuation is achieved by small vibrating motors [258]. The “DB-Glove” by Caporusso is based on “Malossi” language. Pressure sensors and vibrotactile actuators are located at the 16 locations assigned to “Malossi” alphabet [259]. The glove by the Birla Institute of Technology & Science is instead based on Braille code [414]. Capacitive touch sensors on the palm receive input information, while miniaturized vibrational motors on the dorsal side deliver information to the receiver in the form of vibrotactile messages. A PC or mobile phone manages the information conversion and transmission. The device developed by Nicolau et al. [415] is instead based on Finger-Braille. Six rings, each one of those equipped with a coin motor, are placed on both users’ hands. Experiments showed that the subjects could recognize characters between 40% and 100% of trials, although the recognition is very character- and user-dependent. Also, haptic vests were developed, like the one by Ohtsuka et al. [416] equipped with micro vibrators. It can transmit Body-Braille characters sent from a hand-held device via infrared technology. In the end, we mention “Omar”,a haptic device mainly conceived for listening and speech

assistance based on “Tadoma” method. It stimulates kinesthetic and tactile receptors in one or two dimensions using head-positioning DC motors actuators [417].

Piezoelectric and pneumatic displays

Kramer et al. [418] developed a communication glove equipped with strain gauge sensors that flex with hands movements. An algorithm detects characters in the sign language, and the information is sent to a piezoelectrically actuated Braille display, a voice synthesizer or an LCD monitor, depending on the visual and hearing capabilities of the interlocutor. Another device involving piezo-actuated raising pins is “SPARSHA” [419]. It is a haptic display interacting with a computer that allows the conversion of text printed on a PC in haptic Braille. The actuation occurs via 6 piezo-electrically actuated pins. Among piezo-electrically actuated devices, worth to mention is a vibrotactile glove equipped with piezoelectric transducers encapsulated in a soft polymeric matrix [420]. The haptic glove can be equipped with a variable number of actuators, addressing different areas of the hand from the fingertips to the hand palm. It delivers tactile information in a reliable manner and can be used for sensory substitution purposes like communication and navigation.

Haptic displays for deaf–blind individuals can also be pneumatically actuated. The example we mention here is the one developed by Caporusso et al. [421]. It is a tactile interface equipped with a pneumatic Braille display through which a blind or deaf–blind user can access computer games.

5.5. Discussion

Haptic sensory substitution systems allows redirecting missed information from the impaired sense/s to touch, as it is already in use, especially in the blind community with the use of tactile-based languages and tools such as white canes or guide dogs. This is also supported by the common belief that visually impaired people have higher tactile acuity compared to non-impaired ones. Recent studies showed, indeed, that visually impaired have a 15% higher tactile acuity in two-point discrimination. According to these studies, this is reflected at the

cortical level, where the representation of reading fingers in blinded results greater than in sighted. Anyhow, at the moment the phenomenon has no scientific explanation. Hypotheses are that it can be related to a neural network remodelling experienced by blind Braille readers, as an adaptive mechanism [422]. However, other experiments demonstrated that performances of the two groups in Braille reading could equalize with practice. The superior performance of blind individuals was not found even with different tactile stimuli [423-426]. So, there are no consolidated evidences about whether blinded tactile acuity is better than the sighted one in an absolute way, whether blind persons outperforming occurs only in comparison with untrained sighted subjects and whether this superior tactile acuity is related to neural adaptation consequent to the blind individuals tactile reading experience.

In any case, haptic sensory substitution technologies can help disabled persons **overcoming a condition of isolation** from the external world and improving interaction with not-disabled people. Disability is a physical, mental, cognitive or developmental condition which impairs, interferes with or limits a person's ability to accomplish certain tasks or actions, or to participate in typical daily activities and interactions. Thanks to technology, the sensory disabled can benefit from a better **integration into society**, without the feeling of alienation and inadequacy. Haptic sensory aids improve users' independence in navigating unknown environments and their communication abilities. The role of these assistive devices becomes **important also in the workplace**, where sensory disabled users can use technologies such as computers, otherwise accessible only to non-impaired. Deaf individuals can benefit from haptic technologies mainly in the language-learning phase. Tactile aids can facilitate the understanding of lip-reading, and improve vocal production when used on pre-lingually deaf children [281, 427, 428]. **Early interventions** with haptic sensory aids during childhood would improve speech learning, spatial awareness, orientation and interactions with other people, especially with non-disabled. This is true primarily for deaf–blind individuals. Their quite-complete sensorial isolation is a condition much more compromising compared with the possession of a single sensory disability. Anyway, individuals affected by a single sensory disability can also take advantage of haptic aids, which have a big potential in improving the disabled quality of life.

Implanted sensory neuro-prostheses are a promising technology for restoring vision [429, 430]. However, in some cases, major and minor complications were reported, including infections, facial paralysis, bacterial meningitis and postoperative vestibular symptoms [431]. They can provoke damages in the electrode-nerve tissue interface, can cause acute and chronic astrocytic and microglial encapsulation of electrodes [432, 433], together with chronic inflammation leading to localized neuro-degeneration [434, 435]. Moreover, electrical stimulation can lead to neural degeneration [436]. They are also suspected to damage the peripheral vision in patients with macular degeneration [437]. On the other hand, haptic assistive devices represent a less invasive option to visual neuro-prostheses, avoiding possible drawbacks linked to surgery, even though providing sensory substitution in a non-homologous manner (involving another sense). Furthermore, in those cases where surgical intervention is not possible, they represent the sole viable option. With the increasing diffusion of high-performance-implanted sensory neuro-prostheses and a high variability of haptic sensory substitution aids, researchers focused on the comparison between results achieved with the use of tactile aids and those obtained with implants. An old study reported that, after a consistent training, subjects using tactile aids showed abilities comparable to that of implanted subjects with the technology available at the time [438, 439].

The revised technologies refer to vibro-tactile stimulation, with some reference to electro-tactile. Researches were carried out to investigate which one of these stimulation protocols was more effective. Results showed that sending **vibro-tactile cues is preferred to electro-tactile**, especially for stimulation of fingertips, whose high electrical resistance makes them less sensitive to electro-tactile stimuli [440]. In order to transmit vibro-tactile information in a reliable manner, the definition of proper geometries of actuators and their vibrating parameters become crucial. **Low noise**, **low energy** requirements and an **adequate dynamic range are key features**. A fine tuning of frequency, intensity and duration of the vibration is required, as well as the timing between stimuli and the selection of the stimulation area. Identification of minimum and maximum levels of stimulation is important to match the individual sensitivity thresholds and is strictly related to the involved area on the skin.

Studies [441] show that the vibration frequency corresponding to the maximal perception for the receptors in our hand is around 250 Hz, and that tactile stimulation at frequencies under 100 Hz improves spatial discrimination [4]. The duration of the vibro-tactile stimulus shall be chosen according to the purpose of the transmitted information. The identification of a tactile pattern is easier when stimuli are between 80 and 320 ms, while for alerting purposes, a stimulation between 50 and 200 ms is preferred to avoid annoyance [262]. The positioning of the actuators must respect the criteria for two-point discrimination, *i.e.*, thresholds and size of the region of stimulation. The static **two-point discrimination** distance varies case by case, increasing from 0.5 mm [300] to 1.6 mm [7] on fingertips to 4–5 mm on the hairy skin [442]. To design arrays of actuators respecting the two-point discrimination minimum distance is difficult especially in children, whose small skin areas limit the dimensions of transducers [269]. This is one of the reasons making the **actuators miniaturization** mandatory. At present, most diffused aids are based on piezoelectric transducers, whereas in the near future the integration of components based on other actuation principles would be a key point in scaling devices dimensions. Promising technologies are **EAP displays**. They can easily be encapsulated in polymers for the development of miniaturized soft displays, and the manufacturing process is highly automatable. The characteristics of such displays make them suitable for the stimulation of different body areas, especially if integrated in clothes. However, one of their main limitations is the need of very high driving voltages. Together with the definition of optimal geometrical specifications for actuators, researchers identified that a desirable weight for transducers to be inserted in arrays is around 15–20 g, especially for children applications. The investigation of the proper stimulation parameters is important in order to match the sensory disabled perception acuity.

Among the **drawbacks shown by haptic sensory substitution aids**, one is the high **cognitive load** they require [316], particularly true in an outdoor environment where the interpretation of stimuli becomes challenging and may limit the usability of such devices [443]. Another critical point is the scarce success on the market, even though the current availability of a variety of sensory substitution technologies at a good readiness level.

Reasons of the scarce diffusion of sensory substitution aids are different and related to the disability they are addressed to. Concerning the blind community, many of them prefer to move around without electronic aids, choosing the assistance of care-givers instead. **Affordability** of sensory aids is another factor limiting their diffusion. Most of the impaired population comes from underdeveloped countries, while the wealthy in many cases do not have propensity for new technologies. Elderly encounter instead problems in learning how to use the devices. Moreover, sensory aids for blind persons are mainly conceived for adults and they are not easily adaptable to be worn by children. In many cases, they are bulky devices which require a high cognitive load or a long training, and children find difficult to reach a proper level of attention to properly learn how to use these devices. This is an obstacle for early interventions, which are instead important since blindness affects the development of social relationships, emotions and psychomotricity, and can lead to spatial and social deficits at the cognitive level [444].

Acceptability and diffusion of sensory aids in the deaf community is an issue for both children and elderly individuals. The former group is divided in those who accept suddenly hearing aids, and those who do not accept them at all. Clinicians must try to find ways, through gaming and long training, to make them more confident about the technology. People in the latter group often associate hearing impairment with a disability condition related to getting older and find the adaptation to new technologies challenging. Impairment misperception is another important cause of non-acceptance of hearing aids since some individuals do not realize the increasing of their impairment because it appears gradually. Anyway, experimental studies comparing behaviours of the two age groups showed that the acceptance of hearing impairment is higher for older individuals than for young ones. Elderly report fewer difficulties in daily living activities compared with younger subjects [445], and they are more prone to accept this disabling condition which is considered a natural consequence of the ageing process. **Cosmetics** aspects are also relevant. The importance of social factors is a key component for the acceptability of sensory aids. This fact was already discussed for blind individuals, but keeps valid for all kind of disabilities. A different attitude of non-impaired persons is common during the comparison

with impaired ones. More in general, making use of an assistive device implies to wear something that underlines a disabling condition, and can marginalize the disabled person in the society. This occurs even if assistive devices were proven useful [446].

Future research in haptic assistive technologies should aim at improving diffusion among sensory disabled population, through the development of low-cost and more efficient systems conceived ad-hoc for patients' needs. Portability and ease of handling are important characteristics for sensory aids [269]. Intuitiveness and low invasiveness are two other key features for the development of a new generation of sensory substitution aids, in order to improve their diffusion on the market and exploit their potentialities for a better living.

In addition to rehabilitation purposes, haptic sensory substitution technologies have a potential that can be exploited for sensorial augmentation of non-disabled. A synergy between all these technologies can lead to the development of multisensorial interactive environments with applications in virtual reality, gaming, long distance communication, manufacturing and rehabilitation. Video and audio acquisition devices, robots and controllers could interact, sending information via haptic feedback to the end users, thus enhancing their sensorial awareness. If integrated into work-wear, haptic sensory aids can also be used for security and rescue purposes, allowing the exchange of information in dangerous situations (*i.e.*, firefighters, police forces), or to communicate safety information to workers like the proximity to robotic arms in manufacturing environments.

Chapter

6. Encapsulation of piezoelectric transducers for wearable devices[5]

In recent years, the development of haptic devices for different application purposes has increased. The growing spread of tactile displays is due to the high potential of the tactile sense as a communication channel for the remote transmission of information in a variety of situations. Due to the high number of tactile receptors located on our skin, particularly on the hands, the sense of touch represents a means to deliver information, which can also come from other sensory modalities such as vision and audition in sensory-disabled subjects. In this case, the information coming from one sensory channel is conveyed to the tactile sense in an understandable way.

In this chapter, we report the development and evaluation of a piezoelectric transducer encapsulated in a polymeric matrix, and its integration in wearable haptic displays to deliver information via the tactile sense, starting from the hypothesis that the introduction of a compliant interface between the stiff piezoelectric element and the soft human skin can have an influence at a perceptual level. In previous studies a polymeric layer has usually been introduced to cover an array of active elements, or a tactile sensor. Our customized fabrication procedure allows to obtain an encapsulated element that enables the development of a single encapsulated actuator, scalable in size, with a very good match between modelled transduction and the actual prototype, and which can be integrated in a straightforward manner in wearable haptic devices for the stimulation of different body

[5] The contents of this chapter are adapted from the journal paper "Sorgini, F., Mazzoni, A., Massari, L., Caliò, R., Galassi, C., Kukreja, S. L., Sinibaldi, E., Carrozza, M. C. & Oddo, C. M. (2017). Encapsulation of piezoelectric transducers for sensory augmentation and substitution with wearable haptic devices. Micromachines, 8(9), 270."

areas on single or multiple contact points. We found that the geometry and the material selected for the encapsulation of the transducer resulted in a system capable of reliably delivering vibro-tactile information, where this was confirmed both on the side of electro-mechano-transduction behaviour and on the human somatosensory perception.

6.1. Materials and methods

6.1.1. Piezoelectric encapsulated transducer

The implemented solution consists in the integration of a piezoelectric disk (7BB-12-9, MuRata, Kyoto, Japan), 12 mm in diameter and 220 µm in thickness, in a polymeric matrix (polydimethylsiloxane, PDMS, Dow Corning (Midland, MI, USA) 184-Silicone Elastomer). The PDMS encapsulation serves both the mechanical and electrical roles. It allows electric contacts to be encapsulated, providing electrical insulation of the element. In addition, it allows obtaining a system that can be easily inserted in wearable haptic devices, such as gloves and wristbands for upper-limb stimulation, or ankle bands and insoles for lower-limb

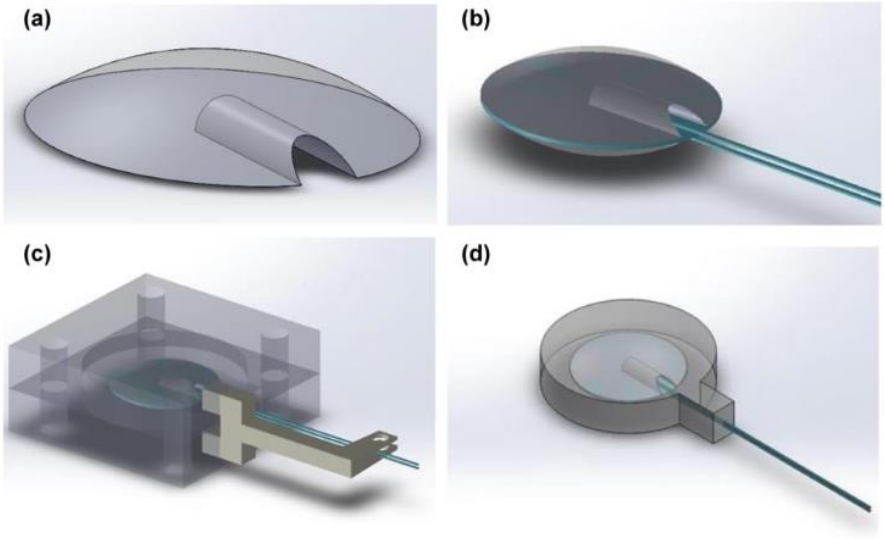

Figure 27 – Encapsulated transducer for haptic applications. a) Upper view of one of the spherical cups; b) Encapsulated transducer with the two spherical cups on the opposite sides and the embedded electrical contacts; c) 3D-printed customized mold for the development of the geometry of the transducer with PDMS polymer. The piezoelectric element with the spherical cups and the electrical connections are located at the center of the molding stucture; and d) an upper view of the transducer, with evidence of the internal structure where two spherical cups enclose the piezoelectric disk and the electrical wires.

stimulation. The compliance of the polymeric encapsulation constitutes also an adaptation interface between the stiffness of the transducer (piezo devices made of lead zirconate titanate (PZT) on a brass mass) and the softness of the human skin.

The development of the encapsulated transducer is articulated in different steps. The first step is the development of two polymeric (PDMS) elements in the shape of spherical cups with the same diameter of the piezoelectric disk (2 mm in height – see Figure 27a). These elements are obtained by a casting process in customized 3D-printed moulds. Elements are designed with a housing on the flat side, to contain the electrical wires connected to the piezoelectric disk. In order to fix the wires on the transducer, the spherical cups are placed on the opposite sides of the piezoelectric disk after the application of a conductive epoxy (CircuitWorks conductive epoxy—Chemtronics (Kennesaw, GA, USA)) (Figure 27b), and the whole resulting system is closed in a 3D printed customized mould for the final polymeric encapsulation (Figure 27c).

The role of the polymeric spherical cups protruding from each side of the external surface is to keep the piezoelectric element centred in the encapsulating polymer (Figure 27d). At the same time, they create two bumps on the external sides of the element in order to focus the transducer deformation, the vibro-tactile stimulus, in a specific contact area on the skin.

The choice of a spherical cup as a contact region on the skin is due to heuristic design criteria. On one side, a spherical protrusion simplifies the implementation of some steps of the encapsulation process. Furthermore, protruding edges [447] or bumps [377, 448, 449] showed proper functionality in the design of matrices of tactile actuators, and bumps are the most used in Braille displays. We opted for a spherical-like shape to avoid sharp edges on the actuator surface and to increase the comfort of the wearer. The dimensions were chosen in order to have a perceptible protrusion which could help position the actuator on a specific contact point on the skin, but also to avoid a very large difference in height from the actuator surface. The resulting contact area was about 18.2 mm^2 which, in case of multiple transducers, results in a spatial distribution just higher than the minimal range guaranteeing reliable two-point discrimination on fingertips (0.5 mm [300]–1.6 mm [7]).

6.1.2. FEM Model of transducer's electro-mechanical behaviour

A finite element method (FEM) simulation of the piezoelectric transducer was performed using COMSOL Multiphysics (COMSOL Inc., Palo Alto, CA, USA). We considered the geometry introduced in the previous section. The mechanical properties of PDMS necessary to run the simulations are the Young's modulus, Poisson's ratio, and density. The acoustic properties are not explicitly needed as inputs for the simulation. They were consistently derived by the numerical solver so that no additional characterization was required. The density was verified from the mass/volume ratio of auxiliary samples. The derived value was in agreement with the one available in the adopted library (970 kg/m^3). Regarding the PDMS Poisson's ratio, we adopted 0.5 from the literature [450, 451] (its dispersion is low, and the same value was provided as the reference PDMS Poisson's ratio in the material library of the chosen solver). Differently, the PDMS Young's modulus sensibly depends on the actual material composition and therefore we assessed the reference value provided in the material library through a complementary calibration experiment described in the next section. Finally, as for the PZT material properties, we adopted the elastic and piezoelectric coefficients and electric permittivity provided by the material library of the chosen solver (an extensive characterization of this commercial material was beyond the present scope).

The purpose of the numerical simulations was to estimate the normal force exerted by the piezoelectric transducer at different frequencies and driving voltages. In particular, we chose 50 V, 100 V, and 150 V as the driving peak-to-peak voltages for the sake of definiteness, and we selected a frequency range between 200 Hz and 700 Hz. The choice of such a frequency interval allows the activation of the transducer within the Pacinian frequency range, centred around 300 Hz [7, 263, 452, 453], for which the maximum sensitivity for vibro-tactile stimulation is expected. Furthermore, previous studies [441] showed that the subjective amplitude perception of the vibro-tactile stimulus is not influenced by the frequency in this specific interval (200–700 Hz).

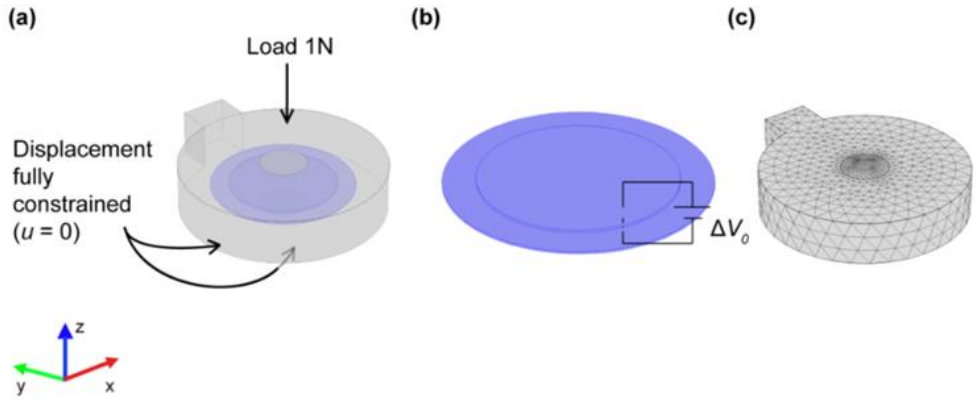

Figure 28 – Finite element method (FEM) model of the encapsulated transducer. a) Schematic of the actuator showing the boundary conditions on the PDMS structure; b) detail of the piezoelectric disk showing the driving voltage imposed on the element; and c) a view of the meshed geometry of the whole encapsulated transducer.

Based on the experimental conditions described in the next sections, we imposed a null displacement (u = 0) on the bottom and lateral surface of the PDMS encapsulation material, whereas we imposed a compression load of 1 N on the PDMS upper surface (see Figure 28a). We imposed the driving voltage on the piezoelectric disk (ΔV_0), and we gathered via a load cell (Nano 43, ATI Industrial Automation, Apex, NC, USA), the resulting force normal to the PDMS bottom surface. In addition, we preliminarily set up the numerical discretization so as to obtain grid-independent results, which led to a mesh composed of 675,062 tetrahedral elements (160,731 volume elements, 23,068 surface elements, and 843 edge elements). We also considered an axisymmetric model, derived from the three-dimensional one through minor geometrical simplifications, to assess the adopted numerical technology. For all the runs, we considered the fully-coupled (*i.e.*, electro-mechanical) problem by exploiting the corresponding modules natively provided with the FEM simulation environment.

6.1.3. Preliminary mechanical characterization of PDMS

A mechanical characterization of the PDMS was performed in order to assess the Young's modulus. A cylindrical probe (ϕ 6 mm) moving along the Z-axis through a motorized translational stage was used to indent a PDMS sample (30 mm × 30 mm × 3 mm). The probe was mechanically linked with a load cell (Nano 43, ATI Industrial Automation) in order to

apply a predefined value of force and, thus, establish a relationship between the applied force and the corresponding polymer displacement (indentation; set to be null when contact was first established). The resulting experimental trend was then compared to the one obtained from a numerical simulation of the considered indentation test, exploiting, in particular, the Young's modulus provided by default by the adopted numerical solver.

6.1.4. Electro-mechanical characterization of the encapsulated transducer

In order to perform the mechanical characterization, the transducers were actuated by means of a piezo haptic driver (DRV2667 Evaluation module, Texas Instruments, Dallas, TX, USA) using a graphical user interface (GUI) (LabVIEW, National Instruments, Austin, TX, USA) that activated the driver through an electronic board (sbRIO 9636, National Instruments). Before human evaluation of the system, we assessed the ability of the haptic interface to deliver perceptible and discriminable stimuli using a load cell (Nano 43, ATI Industrial Automation), in order to provide input stimuli and record the resultant vibrations (Figure 29b) [45]. Such measurements were then compared with the FEM simulations described in above.

The experimental mechanical characterization of the encapsulated transducer was performed in order to evaluate the element behaviour with the variation of the driving voltage (measured in peak-to-peak voltage - V_{pp}) and the frequency. In order to do so, we measured the amplitude of the normal force (F_z) exerted by the piezoelectric element on a load cell. To stabilize the transducer during the experimental tests, a 3D-printed housing was fixed on the load cell (Figure 29b). Furthermore, a load of 1 N was placed on the upper surface of the encapsulated transducer in order to keep it stable during the measurements and to emulate a typical pre-load that can be exerted on the device during its use. Such an offset load was then subtracted from the dynamic measurements of the load cell.

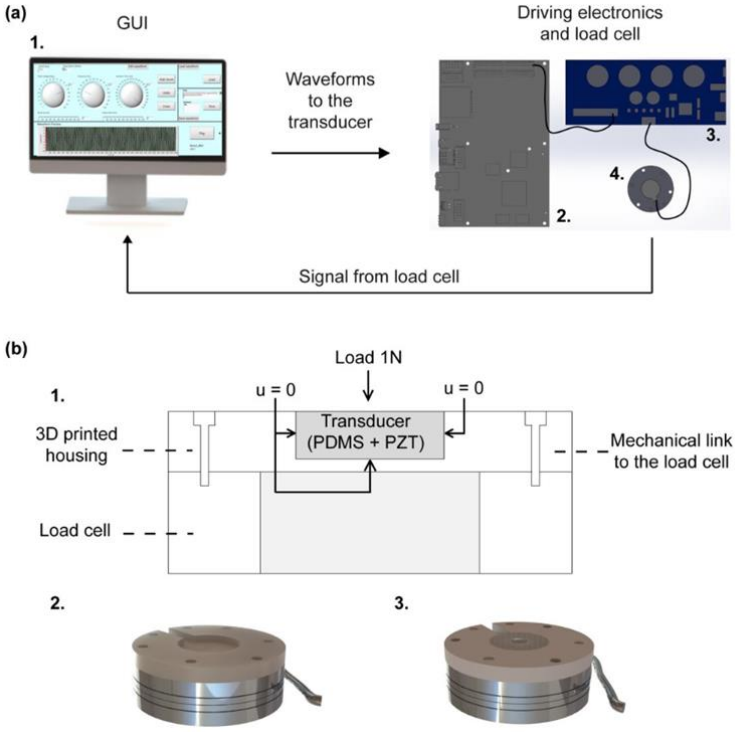

Figure 29 – Experimental setup for the evaluation of the normal force exerted by the encapsulated transducer. a) Schematic drawing of the experimental setup: 1.) PC running a GUI to send selected waveforms to the piezoelectric transducer via a driving electronics; 2.) electronic board for the communication between the GUI and the piezo haptic driver; 3.) piezo haptic driver for the activation of the piezoelectric transducer; and 4.) load cell for force measurement: the measured forces are saved for post-processing. b) Detail of the mounting for the electromechanical characterization of the transducer, where the encapsulated transducer is fixed on the load cell: 1.) Section of the measurement system, in which the encapsulated transducer in fixed in a 3D printed housing linked to the load cell, with detail of the experimental boundary conditions; 2.) 3D view of the experimental setup for the electromechanical characterization of the transducer, with a 3D printed housing linked to the upper part of the load cell; and 3.) 3D view of the whole measurement system, in which the encapsulated transducer is inserted.

The piezoelectric element was driven with stimuli lasting 1 s. The stimulation signals were characterized by three values of amplitude (50, 100, and 150 V_{pp}), kept constant across each stimulation, and 21 values of frequency varying between 200 Hz and 700 Hz, with 25 Hz steps. These settings were consistent with those adopted for the aforementioned FEM model. The values of the normal force (F_z) exerted on the load cell during the excitation were acquired across 10 repetitions for each vibration frequency and each peak-to-peak voltage. The waveforms obtained from the measurements of the load cell were then analysed with the calculation of the signal power (standard deviation of the amplitude of F_z). The data analysis was performed across 750 samples for each frequency value, where the sampling window was selected in the central part of the signal to focus on the steady state of the dynamic activation of the piezoelectric transducer. Spectral analysis was performed

on F_z using the MATLAB (R2016b, MathWorks, Natick, MA, USA) wavelet coherence package [454], for each peak-to-peak voltage and each frequency value in the range between 200 Hz and 700 Hz, with 25 Hz steps and 50 Hz steps.

6.1.5. System integration for psychophysical evaluation

The described encapsulated transducer was used in a wearable vibro-tactile device for hand stimulation, *i.e.*, a haptic glove (Figure 30). For the psychophysical evaluation of the tactile display, we designed three experimental configurations: two single-finger, with the stimulation of the index (SF-I) or thumb (SF-T) fingertip; and one bi-finger (BF-S), with the simultaneous stimulation of the index and thumb fingertips. In the SF-I and SF-T configurations, one transducer was integrated, respectively, on the tip of the index finger (Figure 30b) or thumb (Figure 30c) of a spandex glove; for the BF-S configuration two transducers were integrated on the tips of the index finger and thumb of the same spandex glove (Figure 30a). In all configurations, the glove allowed a secure positioning of the vibrating element on the participant's fingers. The transducers provided a contact area with the finger pad of approximately 250 mm^2. The electrical actuation was delivered to the

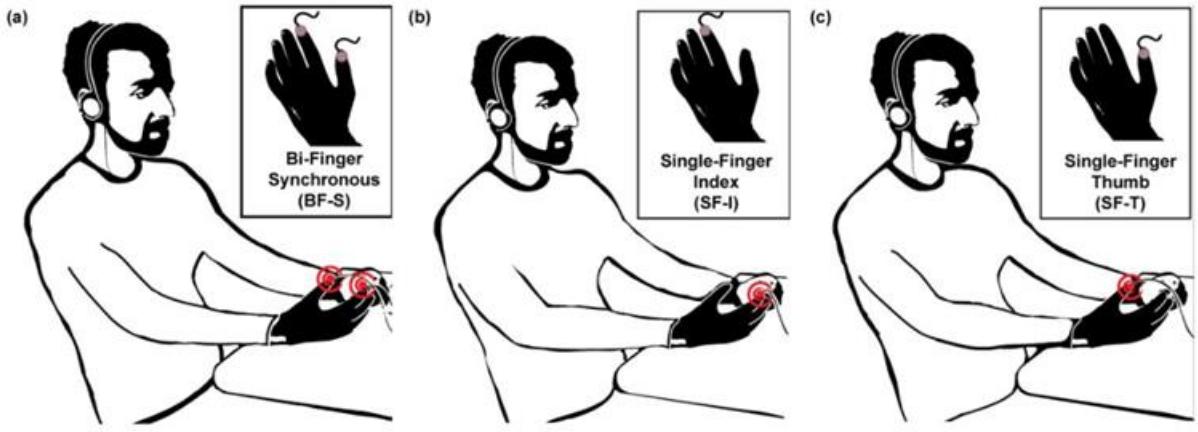

Figure 30 – Experimental setup with the three experimental configurations. a) Bi-finger synchronous (BF-S) configuration: two piezoelectric transducers, embedded in a spandex glove, synchronously stimulate the tips of the index and thumb finger; b) single-finger index (SF-I) configuration: single-finger stimulation on the index fingertip with one piezoelectric transducer embedded in a spandex glove; and c) the single-finger thumb (SF-T) configuration: stimulation on the thumb fingertip with one piezoelectric transducer embedded in a spandex glove.

transducers via the electronics already described in previous sections, *i.e.*, a piezo haptic driver controlled using a GUI and interfaced with the driver through an electronic board [455].

6.1.6. Psychophysical evaluation

We evaluated the ability of the integrated wearable haptic system to deliver accurate tactile feedback using a two-alternative forced choice (2-AFC) psychophysical protocol. According to previous studies, we chose to use frequency modulation as a mean to deliver haptic information. Even if the exact number of discriminated levels is not clear yet, it can increase when stimuli differing in frequency are relatively compared [263]. Studies regarding the amplitude modulation showed instead that, for constant frequencies, when the vibration amplitude increases, the perceived frequency also increases [262].

According to these studies, and to the experimental data from our measurements, we decided to select a fixed driving voltage of 150 V_{pp} for the psychophysical experiments. This value corresponds to the higher value of normal force exerted on the actuators' sides and, according to preliminary psychophysical tests, was the one which showed the best performance across 10 participants [455]. The frequency modulation was then performed in the range between 200 Hz and 700 Hz, which guarantees a proper functioning of the transducer according to the FEM analyses.

6.1.7. Participants

Thirty-three healthy participants (15 females and 18 males), aged between 25 and 37, participated in psychophysical experiments. Haptic stimulation was performed on the dominant hand which, for 31 participants, was the right hand. No participant had previously performed any activity presumably compromising finger tactile sensitivity. All participants provided written informed consent for inclusion before they took part in the study. The study was conducted in accordance with the Declaration of Helsinki, and the protocol was approved by the Ethics Committee for non-clinical experimentation of Scuola Superiore Sant'Anna of Pisa.

6.1.8. *Experimental procedure*

A tactile discrimination task with the two-alternative forced choice (2-AFC) procedure [456] was submitted to each participant. Periodic vibro-tactile stimulation was delivered using the haptic glove described in the previous sections. The experimental session consisted of the presentation of 150 pairs of stimuli divided into 15 sequences, as described in the following.

Each participant was presented with paired vibro-tactile stimuli (Figure 31a,b) and was asked to identify which stimulus of the pair had the higher frequency content (Figure 31c). A stimulation sequence included a single presentation of each of the 10 pairs of stimuli described in TABLE V in random order. An 8 s interval was introduced to separate each subsequent stimuli pair, leading to a sequence duration of about 2 min. A rest period of about 1 min spaced the 15 sequences, for a total average duration of 45 min. Two randomized sequences were used for training purposes. These sequences were not included in the statistical analyses and were sufficient for the participants to familiarize with the stimuli.

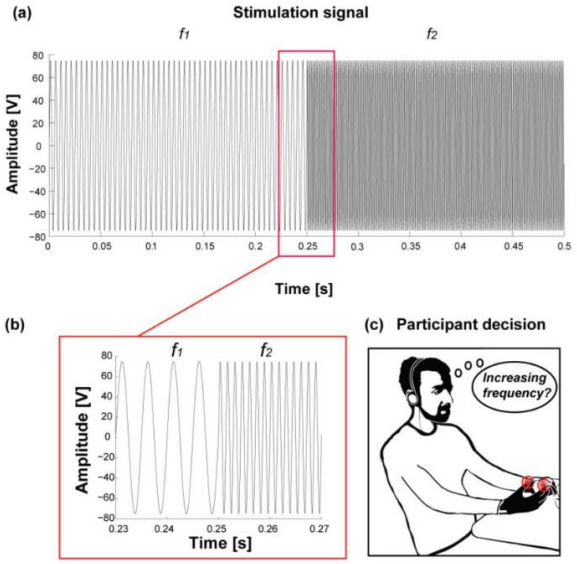

Figure 31 – Stimulation and task. a) An example of a pair of stimuli: 250 ms of sinusoidal oscillations with a frequency of 200 Hz followed by 250 ms sinusoidal oscillation with a frequency of 700 Hz. The peak-to-peak amplitude activating the transducer was fixed at 150 V; b) a 0.04 s close-up showing the frequency transition at 0.25 s; and c) the participant decision phase: after perceiving the vibro-tactile stimuli pair, the participant was asked to determine whether the first or the second had the higher frequency content.

As briefly explained in the introduction, we delivered vibro-tactile stimuli following three experimental configurations. In this way, we were allowed to test the human hand tactile sensitivity to frequency variations under different perceptual conditions. Each configuration was tested with 11 participants. Each participant was comfortably seated on a chair for the duration of the experiment for all tested configurations, and he/she was acoustically isolated from the environment with white noise provided by headphones.

6.1.9. Data analysis

Data analysis was performed using the Statistics Toolbox in MATLAB. To compare the performances of different configurations, the Kruskal-Wallis test was used. For each configuration and frequency variation, the vibro-tactile perception of a population of participants was evaluated by the median and the 95% confidence interval of the rates of identification of stimuli having an increasing frequency ($\Delta f > 0$), calculated with binofit test. A logistic fit of the resulting psychometric curves was computed for each configuration across presented frequency variations. To analyse the significance of participants responses for each frequency variation Δf and experimental configuration, the binofit test was used.

6.2. Results

We developed an encapsulated transducer, 18 mm in diameter and 4 mm in thickness (Figure 32) (see section 6.1 for details). Its shape is characterized by two spherical cups which protrude out 250 µm from the upper and lower levels of the polymeric matrix (upper

TABLE V
EXPERIMENTAL STIMULATION PARAMETERS. TEN PAIRS OF VIBRO-TACTILE STIMULI.

	Vibro-tactile stimuli pairs									
f_1 (Hz)	700	650	600	550	500	400	350	300	250	200
f_2 (Hz)	200	250	300	350	400	500	550	600	650	700
Δf (Hz)*	-500	-400	-300	-200	-100	100	200	300	400	500

* $\Delta f = f_2 - f_1$

part of Figure 32a,b). These elements allow skin stimulation at a specific contact point. The presence of the spherical cups allows centring the piezoelectric element in the polymeric shell, as shown in the lower part of Figure 32b.

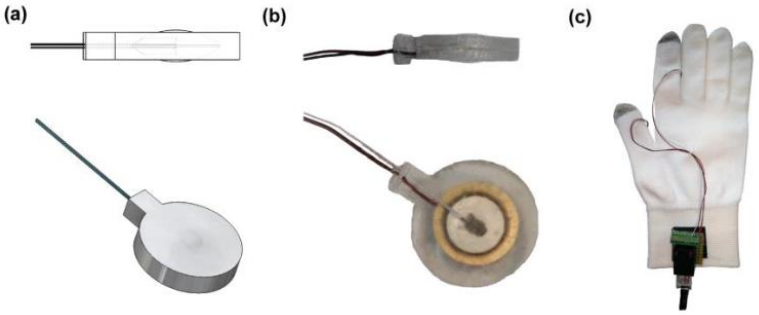

Figure 32 – Embedded piezoelectric transducer. (a, upper part) Drawing of the lateral view of the piezoelectric transducer embedded in the polymeric matrix, with evidence of the two protrusions on the external opposite faces of the geometry; (a, lower part) drawing of the upper view of the piezoelectric transducer embedded in the polymeric matrix; (b, upper part) lateral picture of the developed prototype showing the side of the actuator; (b, lower part) upper picture of the developed prototype showing the whole surface of the actuator; and c) a picture of the integrated system used for the psychophysical evaluation: a textile glove equipped with two encapsulated transducers on the thumb and index fingertips.

6.2.1. Results of the preliminary experimental mechanical characterization of PDMS

Results from the experimental characterization of PDMS validated the stiffness of PDMS test blocks, maintaining the mechanical parameters of the material as available in the software library. In particular, the trend of the obtained force vs. displacement was compared with the one obtained from the model of the considered indentation test.

The simulation outcomes appear to match the experimental data, to consider the library parameters of the material accurate enough to describe the PDMS used in our study (Figure 33). As a consequence, we could safely exploit the parameters available in the COMSOL material library to run the FEM dynamic simulations.

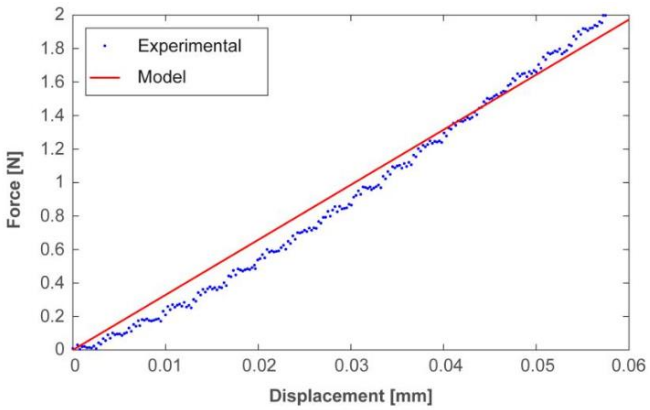

Figure 33 – Characterization of the stiffness of the fabricated PDMS test samples and corresponding model calibration. The agreement between experimental (blue dots) and simulated data (red line) confirmed the suitability of the chosen model parameters.

6.2.2. Transducer FEM model and experimental characterization

The results of the FEM model are shown in Figure 34 (solid lines with circles), together with the corresponding experimental measures (dots). The model was able to accurately predict the observed experimental response. For each driving voltage and each frequency, the mean value and the standard deviation of the normal force (over the 10 repetitions) are represented in Figure 34.

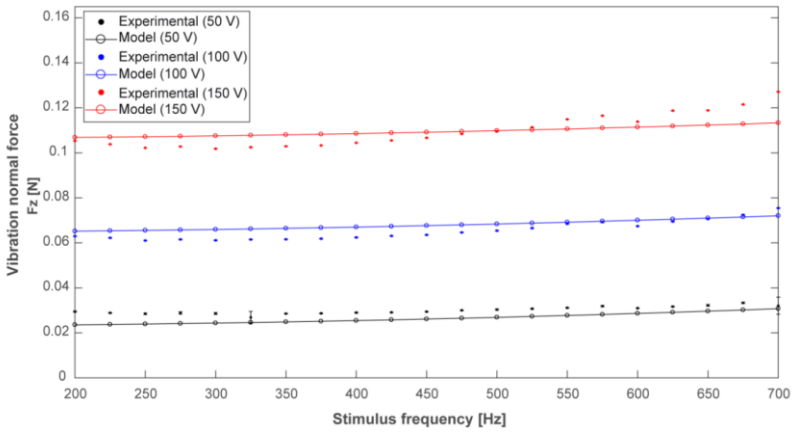

Figure 34 – Vibrational component of the normal force exerted during transducers actuation. Predicted trend (solid lines with circles) and experimental measures (dots) of the normal force for the considered driving voltages. For each experimental point, the standard deviation is represented by vertical bars.

In most cases, the vertical bars representative of the standard deviation are hardly visible thanks to the high repeatability of the experimental conditions.

From Figure 34 we can conclude that, as expected, the amplitude of the vibrational component of the normal force increases with the increase of the transducer driving voltage. Figure 34 also shows how the vibration amplitude is weakly varying over the analysed frequency range for each driving voltage (for 150 V_{pp} driving voltage, the variation of the normal force amplitude is about 0.025 N across the selected frequency range). These results demonstrated that the variation of the normal force is mainly related to the driving voltage

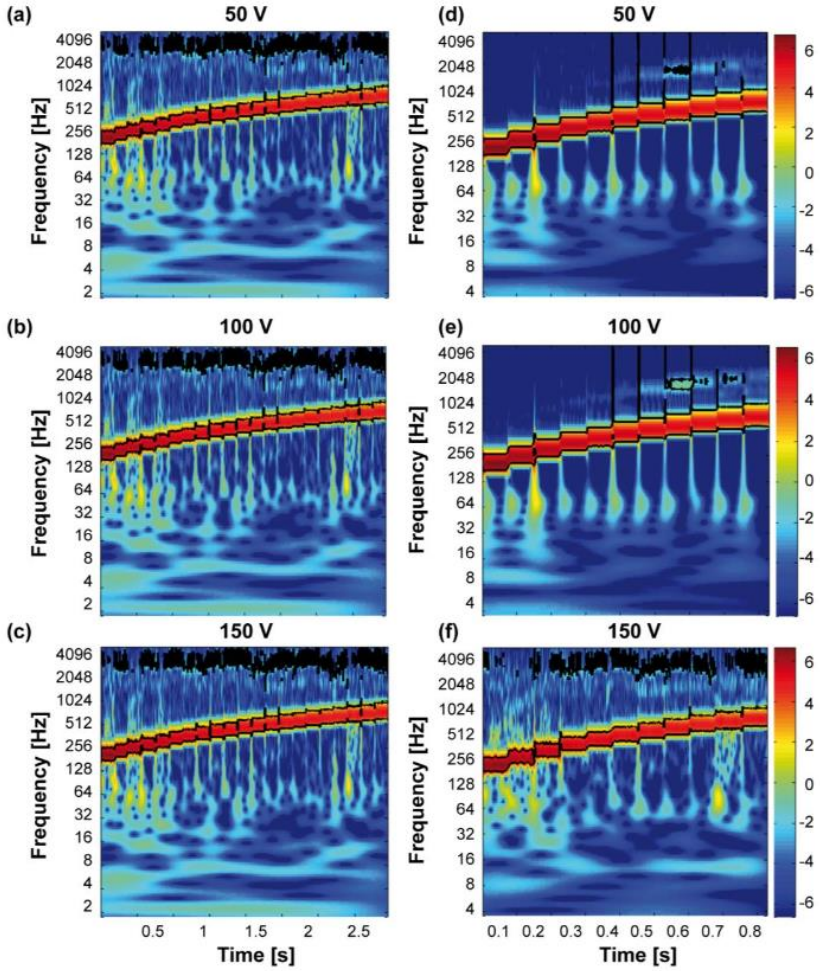

Figure 35 – Frequency power spectrum of the normal force. Spectral analysis of the normal force recorded by the load cell while activating the piezoelectric actuator/polymer system. a) Results for 50 Vpp and 200–700 Hz, with 25 Hz steps (electromechanical characterization); b) results for 100 Vpp and 200–700 Hz, with 25 Hz steps (electromechanical characterization); c) results for 150 Vpp and 200–700 Hz, with 25 Hz steps (electromechanical characterization); d) results for 50 Vpp and 200–700 Hz, with 50 Hz steps (pilot psychophysical experiments); e) results for 100 Vpp and 200–700 Hz, with 50 Hz steps (pilot psychophysical experiments); and f) results for 150 Vpp and 200–700 Hz, with 50 Hz steps (psychophysical experiments).

amplitude. Increasing the voltage value (from 50 V to 150 V) three times leads to a fractional variation of the recorded force of about 300% ± 25% over the whole range of frequencies. Increasing the frequency value three times (from 200 Hz to 600 Hz) leads, instead, to a force variation always lower than 10% for all of the driving voltage conditions (50 V, 100 V, and 150 V). The weak relationship from the value of frequency within the selected range allows a straightforward application of the transducer in haptic displays for the stimulation of the human hand.

Spectral analysis showed coherence with the nominal stimulation parameters. For each stimulation amplitude (50, 100, and 150 V_{pp}, see Figure 35a–c) the encapsulated transducer showed coherency in the stimulus presentation within the whole examined frequency range, with evident vibratory changes across the analysed peak-to-peak amplitudes and frequencies. The same is visible in Figure 35d–f showing the frequency values selected for the psychophysical testing (range 200 Hz–700 Hz, with 50 Hz steps). These experimental results allow concluding that the vibro-tactile stimuli delivered to the participants were

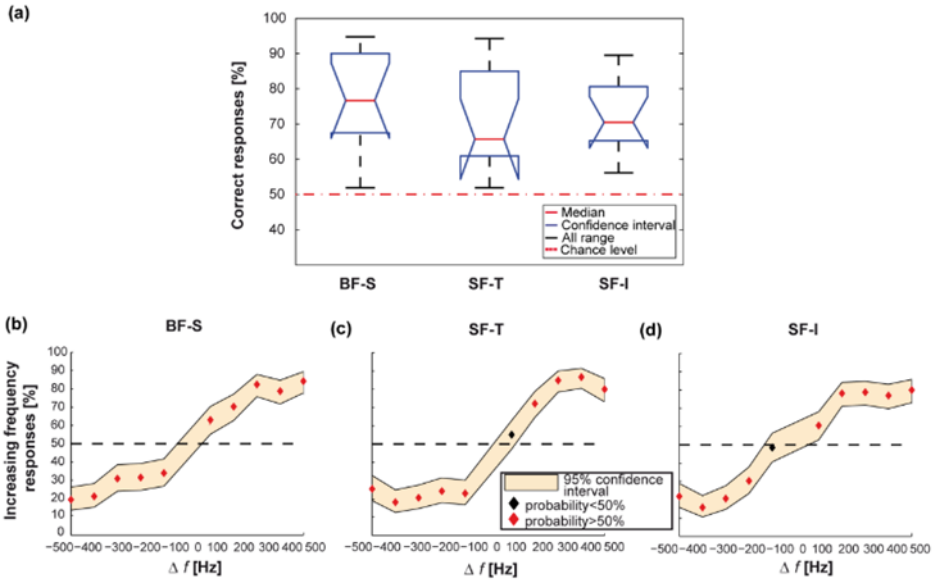

Figure 36 – Stimuli perception with both bi- and single-finger configurations. a) Comparison between the fraction of correct responses (i.e., increasing frequency variations identified as increasing or decreasing frequency variations identified as decreasing) in all three configurations. Boxes represent the interquartile range and black dashed lines show the complete range across participants; b) psychometric curve for the BF-S stimulation configuration. Each dot represents the fraction of times each stimulus was classified as having an increasing frequency (median across participants). If the identification rate is significantly different (average > 50%, binofit test) from chance the dot is red, otherwise, it is black. The filled area indicates the 95% confidence interval (binofit test) across participants and the black horizontal dashed line represents chance; c) the same as b) for the SF-T stimulation configuration; and d) the same as b) for the SF-I stimulation configuration.

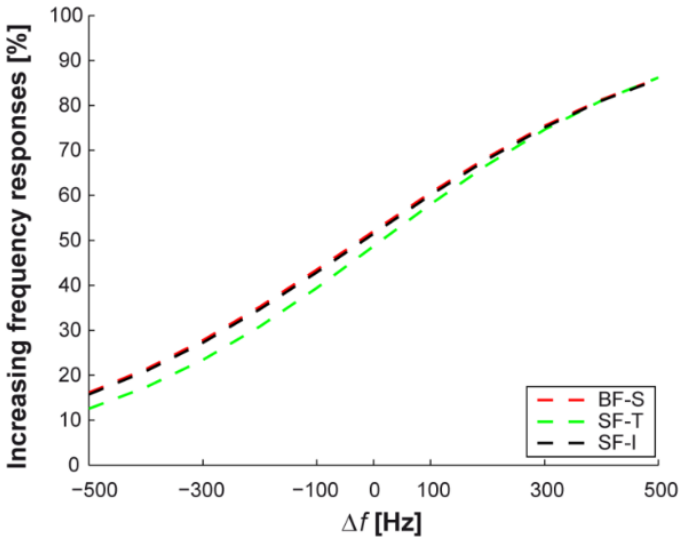

Figure 37 – Comparison of the logistic fit of psychometric curves for all configurations. Comparison of logistic fit curves over the whole range of frequency variation. The curves are similar for all three experimented configurations.

coherent with the frequency values selected for the experimental testing and, thus, the transducers embedded in the polymeric matrix can deliver vibro-tactile information in a reliable manner.

6.2.3. Psychophysics results

Results from psychophysical testing for all the experimental configurations, shown in Figure 30, are reported hereafter. The average performance over all the 10 frequency variations was significantly above chance for both bi- and single-finger configurations, with non-significant differences between the mean discrimination performances achieved under different stimulation configurations (as shown in Figure 36a: n = 11 for every group; 77 ± 11% for BF-S vs. 70 ± 8% for SF-I vs. 66 ± 12% for SF-T; p = 0.51, Kruskal-Wallis test). In particular, frequency differences larger than 100 Hz were reliably identified in all configurations (Figure 36b–d).

The developed integrated haptic system was thus effective in delivering vibro-tactile information for both single-finger and bi-finger configurations when the frequency delivered to the skin was within the 200–700 Hz range and the stimulus variation was larger than 100 Hz.

Furthermore, in the explored frequency variation range (Δf = −500 ÷ 500 Hz) the psychometric curves obtained from experimental data for single-finger configurations, as well as the one for bi-finger configuration, were accurately fitted by logistic curves over the whole range of frequency variations (Figure 36b–d), χ^2=0.43 for BF-S, χ^2=0.68 for SF-I and χ^2=1.02 for SF-T).

When calculating the psychometric curves to evaluate performance as a function of frequency variation, the differences between bi-finger and single-finger configurations showed that two-digit perception has a frequency sensitivity to vibro-tactile stimulation comparable to the one relative to single-finger perception (compare Figure 36b with Figure 36c,d).

For all configurations, Figure 37 shows the comparison between logistic fits of frequency variations identified as increasing. Over the full range of frequency variation, the two single-finger configurations and the bi-finger configuration had similar logistic fit curves.

6.3. Discussion

In this work we *i)* described the mechanical behaviour of a piezoelectric disk encapsulated in a polymeric matrix, specifically designed for the integration in wearable haptic displays, and *ii)* characterized the behavioural performance in sensory discrimination of healthy human subjects wearing such displays.

The FEM modelling showed that the normal force exerted by the encapsulated element presents a constrained variation across the experimented frequency range for the three selected driving voltages. This modelled behaviour was confirmed by the experimental testing.

The psychophysical testing of an integrated haptic system, a vibro-tactile glove for the stimulation of the index and/or thumb fingertips of the human hand, demonstrated that the developed haptic transducer is effective in delivering vibro-tactile information.

The transducer described herein presents some advantages with respect to the recent technological solutions for wearable tactile displays. The piezoelectric actuator enables the selection of a wide range of stimulation frequencies in the perceptual frequency range with a fine selection of frequency steps. This is true especially when piezoelectric elements are compared to polymeric actuators, like dielectric elastomers. The former allows selecting frequencies in both low and high frequency ranges. They can be used for the stimulation of both slowly-adapting and fast-adapting tactile receptors, in particular Pacinian corpuscles more sensitive to vibro-tactile stimuli. Piezoelectric disks also limit the space required by the actuator, enabling a straightforward integration in wearable systems like gloves, and provide appropriate spatial resolution for being placed on different areas of the skin. These advantages are evident when our solution is compared to tactile actuators like pneumatics, vibrating motors, solenoids and to exoskeletons. In fact, a wearable device should fit the wearer's body and allow the natural movements of the body part on which it is applied. When worn on the hands, tactile actuators must be lightweight and have limited dimensions [457]. The introduction of a polymeric shell to encapsulate the active element allows obtaining an integrated actuator which can easily fit in a wearable system for the stimulation of different body areas. The polymeric encapsulation also behaves as an interfacing layer between the piezoelectric element and the user's skin, and our particular geometry allows the selection of a precise contact site to stimulate the insulation of the electrical connections increasing the actuator safety, and obtain an easy-fitting element.

The transducer presented herein, thanks to its particularly shaped polymeric encapsulation and its broad range of actuation frequencies, can be effectively employed for the development of tactile displays suitable to different application scenarios. This encapsulated piezoelectric transducer can be integrated within tactile displays for sensory substitution to assist the blind or visually-impaired, deaf or hearing-impaired, and combined sensory impaired (deaf-blind) individuals. Several examples can be found in the literature about tactile aids used to convey the information coming from one sensory channel to the tactile sense in a perceptible manner [452, 458-460].

Other applications can involve the integration of our encapsulated actuator in devices providing non-invasive tactile feedback to amputees. It can be also integrated in sensory augmentation technologies for healthy subjects in applications such as virtual reality, gaming, rehabilitation, navigation, rescuing, and remote control of robots, where vibro-tactile stimulation is already widely used [461-465]. Haptic feedback also has significant advantages in robotic surgery and industrial environments for human-robot co-working activities. We are also considering the possibility to integrate this encapsulated actuator in haptic wearable systems for alerting purposes, in environments where the interaction with automated machinery can be dangerous for operators. This solution may improve safety in dangerous workplaces and the adoption of collaborative robotics in common applications.

Chapter

7. Upper Limb Stimulation in a Virtual Reality Cave[6]

The transmission of force perception from a physical or virtual object to an operator who may be in a remote location has significance in virtual reality and tele-robotic operation [466]. Immersive virtual reality (VR) has the ability to envelope an operator into a simulated world with the effect of altering the user's perception of reality [467]. The Oculus Rift and Google Glass (Google Cardboard) have the advantage of relative low cost but with limited functionality [468]. The immersive capability of these devices is encompassing but they have limitations. The restrictions are due to safety concerns since the user cannot see outside the goggles, creating trip and fall hazards.

A cave automatic virtual environment (CAVE) is an alternative immersive environment [469]. The CAVE uses projectors to create a virtual world on three to six walls of a room-sized cube. This approach avoids safety issues related to wearing goggles.

Figure 38 shows our CAVE system. A user is able to step into this space to experience a virtual environment. Optical tracking cameras are used to track and understand the operator's movements or gestures. The gesture kinematics is transmitted to a real world robot for tasks such as advanced control and manipulation.

[6] The contents of this chapter are adapted from the conference paper "Sorgini, F., Ghosh, R., Huebotter, J. F., Caliò, R., Galassi, C., Oddo, C. M., & Kukreja, S. L. (2016, June). Design and preliminary evaluation of haptic devices for upper limb stimulation and integration within a virtual reality cave. In Biomedical Robotics and Biomechatronics (BioRob), 2016 6th IEEE International Conference on (pp. 464-469). IEEE."

Figure 38 – Four-wall CAVE system with optical tracking cameras.

Touch augmentation

Tactile augmentation combines touch of the real environment with synthetic touch stimuli, which serves to enhance haptic perception of an object [470]. This fused approach has the promise to provide a more realistic tactile perception of an object with the ability to alter its characteristics. Traditionally, haptic augmentation and feedback have been used for training and rehabilitation purposes, *e.g.* surgical training [471, 472] and impairments following stroke [473, 474]. Inspiration from these approaches has led to the development of augmented haptic methods to palpate tissue for tumour exploration during surgery [475] and object shape representation and determining its pose [476].

Visual augmentation

Visual search is an important task for target pursuit in many applications. In an augmented reality (AR) environment a user's ability to search a scene can be augmented to help him/her rapidly assess the setting through the use of virtual cues [477].

Integrated platform

The state-of-the-art in augmented reality is primarily limited to visual augmentation and basic haptic feedback. To the best of our knowledge, the integration and development of technologies to enable a virtual reality CAVE platform to be used as a master-slave system

with augmented tools such as vision, touch and gesture recognition has not been implemented yet. In this chapter, we describe our design principles, which include haptic and visual feedback and gesture identification within a virtual field. This study is concerned with broad design principles and philosophy of a master-slave system for performing advanced human augmentation with a virtual environment for applications such as tele-robotics. We also describe our conceptual system and present results for two subcomponents; namely, haptic feedback for hand and wrist augmentation.

7.1. System overview

Human-machine interface (HMI) is the integration of a human controller with a machine. Typically, switches, keypads and touch screens are used as the physical part of a HMI. However, the availability of virtual reality systems such as the CAVE integrated with haptic and visual feedback and gesture recognition has made robust and intuitive HMI a possibility [478].

Figure 39 shows a conceptual sketch of the system. The goal of this project is to develop an

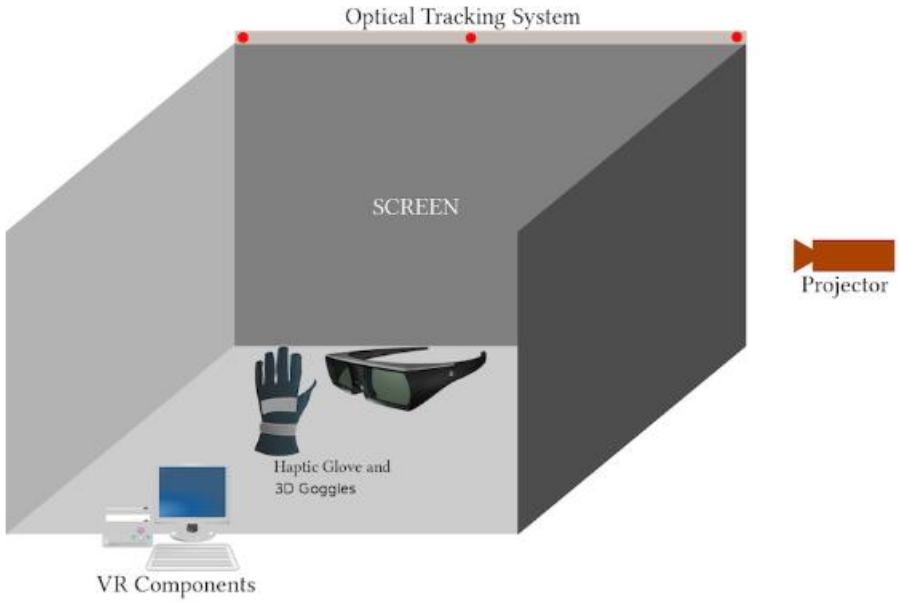

Figure 39 – General schematic overview of our advanced HMI system. General components are: a) CAVE, b) haptic gloves, (c) optical tracking cameras and d) computer hardware and software for visual and haptic feedback and gesture recognition.

AR/VR room for experimenting advanced object recognition and manipulation algorithms suitable for extreme surroundings to control remote robots or vehicles for search-rescue and rehabilitation. This platform will allow a user to remotely operate a robot/vehicle using natural and intuitive body motions (*e.g.* movement of upper limbs, natural hand gestures, etc.) with high flexibility, accuracy, and low latency. We are in the preliminary stages of developing haptic feedback technology to be used with this platform.

Assuming robots or other devices are equipped with advanced high-density e-skin, tactile information generated from the interaction between robot/vehicle and physical objects will be transmitted to the operator inside the VR room through wireless communication channels. Similarly, we will enable haptic capabilities for interactions with avatars within this environment.

7.2. Haptic and visual feedback

Force is one of the first sensory events felt by humans. However, it is challenging to replicate and render force feedback accurately, particularly in confined spaces such as surgery. In addition, force feedback is faced with robustness and control issues leading to high costs [479]. For haptic rendering, we use a sensory substitution approach, which transforms pressure characteristics to vibratory stimuli. This design approach reduces size and bulkiness of a haptic device [480]. However, a vibro-tactile feedback strategy is limited by actuator size and a desire for flexibility, which restricts the number of actuation (sensing) points. This reduces spatial precision and range of stimulus presentation. Therefore, we aspire to develop an advanced high-density vibro-tactile glove that is exceptionally compact and form fitting, permitting more precise localization, possibly leading to a wide range of stimuli rendering. The tactile sensing glove will be used to remotely assess an object's properties, possibly leading to recognition in some applications. We will also investigate whether the current level of precision allows the representation of complex tactile perception in an intuitive manner.

Typically, virtual cues are presented in an overt manner and result in excessive visual clutter [481]. The clutter leads to degradation in search ability [482]. In addition, explicit visual cueing may have the unintended consequence of reducing a user's concentration on a specific task that may supersede the cued task. For this reason, alternatives to explicit cueing are being explored. The use of subtle (lightweight) cues is an emerging area that often relies on heuristic approaches for stimulus presentation and remains largely unexplored [483].

7.3. Gesture recognition

Gesture recognition is concerned with the identification of a pattern from data. It is often characterized by short spurts of activity with an underlying meaning and intention. Algorithms developed to recognize gestures need to be capable of processing large amounts of data in real-time and be precise [408, 484]. The patterns identified need to be mapped

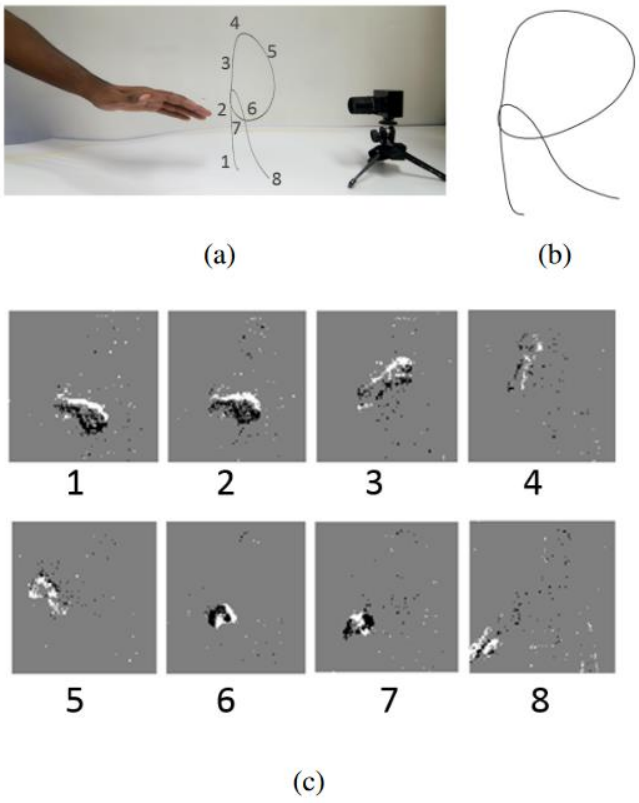

Figure 40 – a) DVS setup with super-imposed hand motion trajectory for the letter R in the order of occurrence. b) Output of the tracking algorithm. c) Sensor output from the DVS at each point of the recording.

from the user coordinates to a robot operating outside the master environment. The mapping needs to be highly accurate and transmitted with minimal latency.

To accomplish the task of mapping, an optical-tracking human motion capture method is under development. Optical markers are attached on a user's hands, upper-limbs and head to track motion and enable control of a remote robot. A marker-based system alleviates the significant computational burden of marker-less methods. In addition, a platform with multiple cameras minimizes occlusion and permits marker detection robustly. The proposed method will solve problems related to unnatural hand and arm motions required by mechanical device (*e.g.* joysticks) based motion capture techniques and concerns related to human body part occlusion.

However, a consequence of using multiple optical trackers is the high computational load due to continuous processing of marker locations, even when they are static. Neuromorphic asynchronous marker-less sensors may offer a solution to this issue because they only respond to dynamic changes in the visual scene. This approach consumes significantly less power than conventional cameras. In addition, they operate at a microsecond temporal resolution, providing appreciably faster responses to changes in tracker position without the need for Kalman-smoothing and prediction. Figure 40 shows an example of a marker-less hand tracking application with a dynamic vision sensor (DVS) [485]. The figure shows that a DVS is able to generate smooth trajectories using its high temporal resolution in the presence of noisy distractors and, hence, it may be useful for gesture recognition.

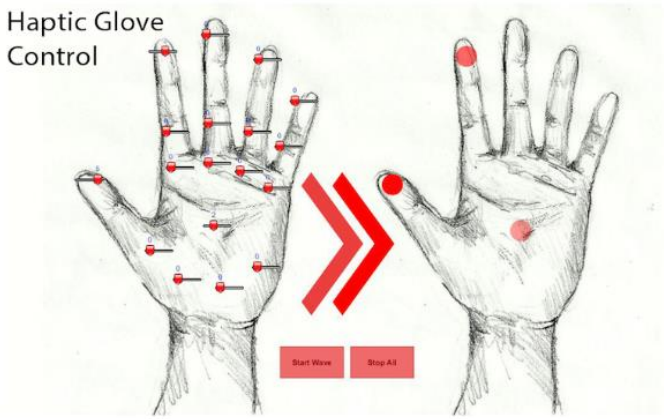

Figure 41 – GUI to control individual actuators during evaluation.

7.4. Materials and methods

7.4.1. Glove

We designed and fabricated a first generation haptic glove that is lightweight, flexible and capable of delivering haptic information with high spatial precision and intensity. A prototype of the haptic glove is shown in Figure 42. The glove had 18 vibratory eccentric rotating mass actuators. It was controlled by an Arduino microcontroller and two pulse width modulation drivers encased in a 3D-printed box on the back of the glove.

A custom made graphical user interface (GUI) (see Figure 41) was used to assess the ability to render precise vibratory touch perception in two different ways: *i)* intensity and *ii)* spatial locality.

Forty untrained subjects were asked to distinguish stimulation region and intensities. Specifically, each subject was asked to identify the location of a single active actuator while vibration intensity was kept constant or varied as ±20% and ±40% of the actuators maximum. In addition the subjects were asked to identify the quantity and location of 2 to 5 simultaneously active actuators with varying area of stimulation.

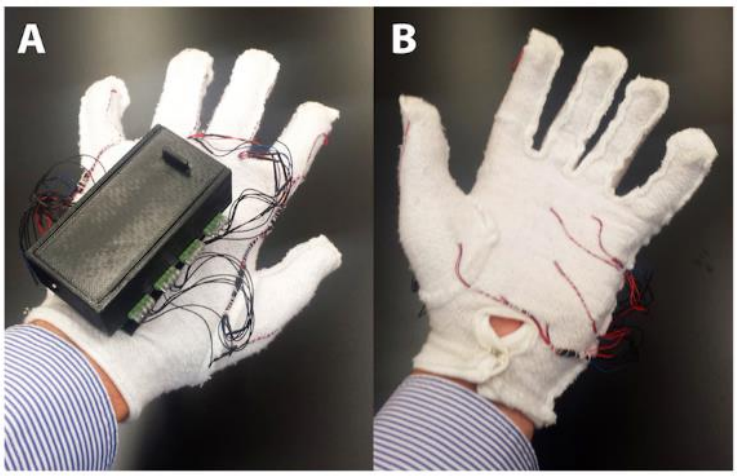

Figure 42 – Haptic glove: a) back, b) front.

7.4.2. Wristband

Piezoelectric transducers are integrated in a wearable device to be used in a virtual reality environment with the purpose of providing haptic feedback (see Figure 43a-b). The signals of the haptic wristband can be coupled with those of the haptic glove's to enhance user experience.

The transducers used in this device are piezoelectric disks (7BB-12-9, MuRata) with 12 mm diameter and 220 µm thickness. The piezoelectric element is integrated in a polymeric matrix (PDMS, Dow Corning 184 - Silicone Elastomer), as discussed in section 6.1.1. The PDMS encapsulation serves both for mechanical and electrical purposes. It allows electric contacts to be encapsulated, providing electrical insulation of the element. In addition, such encapsulated system is easily embeddable in a wearable haptic device, as the wristband. After customization the transducer is 18 mm in diameter and 4 mm in thickness. The shape of the embedded system is characterized by two spherical cups protruding out 250 µm from the upper and lower levels of the polymeric matrix (Figure 43c-d). These elements allow skin

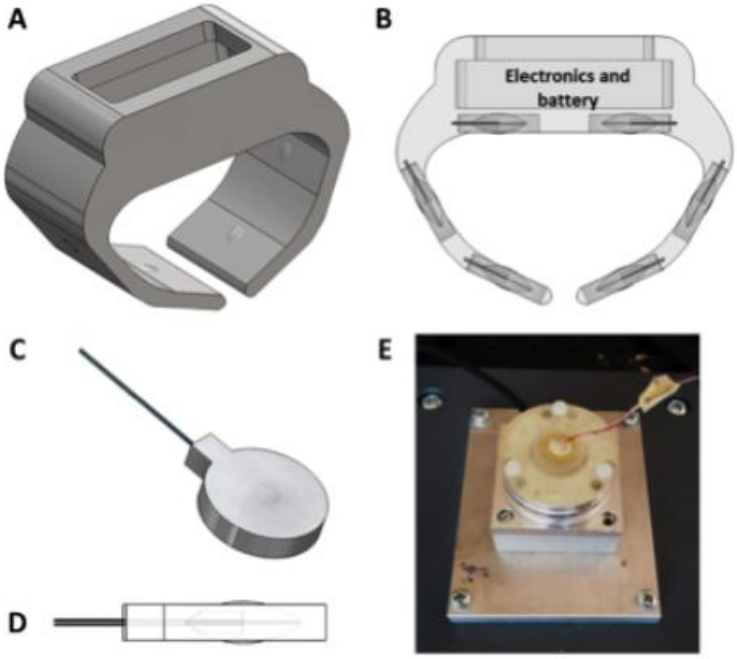

Figure 43 – Piezoelectric transducer integration and experimental measurement system. (a-b) Haptic wristband with embedded transducers. c) Piezo-electric transducer embedded in a PDMS matrix. d) Lateral view of piezoelectric transducer. e) Measurement system setup with load cell and 3D printed holder for transducer placement.

TABLE VI
EXPERIMENTAL STIMULATION PARAMETERS.

Stimulation amplitude [V_{pp}]														
	100							150						200
Frequency variation $\Delta f = f_2 - f_1$ [Hz]														
Δf	-700	-600	-500	-400	-300	-200	-100	100	200	300	400	500	600	700
f_1	800	750	700	650	600	550	500	400	350	300	250	200	150	100
f_2	100	150	200	250	300	350	400	500	550	600	650	700	750	800

stimulation at a specific contact point. The transducers are controlled with a custom designed GUI (LabVIEW, National Instruments) activating the digital outputs of a FPGA on an electronic board (SB-RIO 9636, National Instruments). These in turn serve to control a piezo-driver (DRV2667 Evaluation module, Texas Instruments) that provides power to the transducers.

Before human evaluation of the system, we assessed the capability of the haptic interface to deliver perceptible and distinguishable stimuli using a load cell (Nano 43, ATI Industrial Automation) to record the resultant vibrations (Figure 43e). The selection of stimulation parameters included amplitude and frequency values that resulted in significant vibrations of the transducer. Previous works showed skin sensitivity to vibro-tactile frequencies up to several hundred Hertz [7, 263, 452, 453]. Specifically, our experimental protocol consists in 500 ms lasting stimulation. Each stimulus has constant amplitude (chosen among three different peak-to-peak amplitudes, as shown in TABLE VI) and two frequency levels, each one lasting 250 ms. We chose 450 Hz as central frequency, and 100 Hz and 800 Hz as lower and upper limits (see TABLE VI for frequency combinations). Two series of stimuli were generated to test increasing and decreasing frequencies.

Psychophysical experiments with subjects were structured according to the protocol described below, which is a 2AFC paradigm. One of the main methods used in psychophysical literature to describe the correlation between a quality of a stimulus and its perceptual effect [456]. The complete sequence of 42 stimuli (TABLE VI) was delivered to the

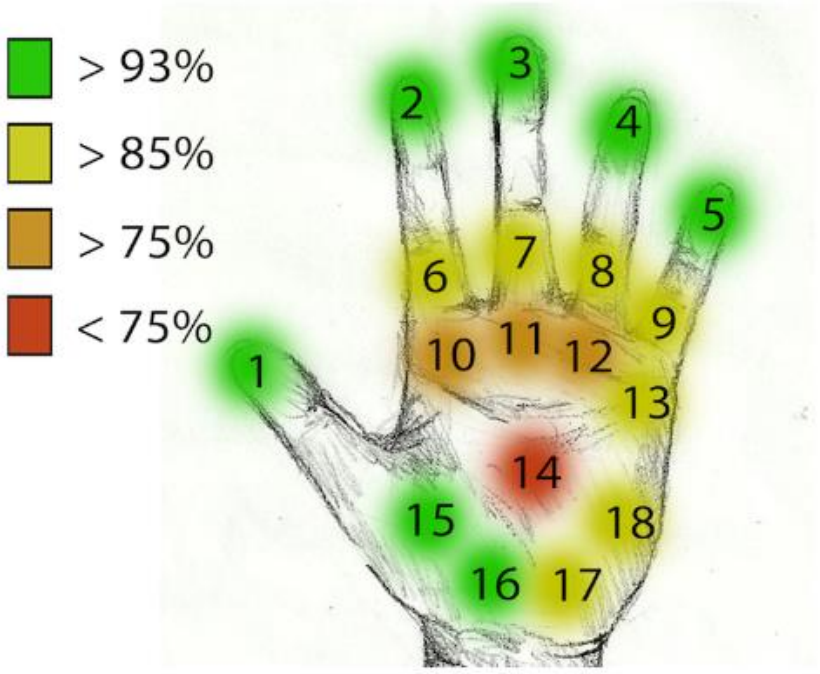

Figure 44 – Precise actuator localization.

piezoelectric element while it was held between the thumb and index finger of the subject. Each sequence was randomized and repeated in 5 sessions with a pause of approximately two minutes between sessions, for a total duration of about 40 minutes for the whole protocol. Within each sequence, the stimuli were spaced in time with 8 s intervals, during which the subject was asked to judge whether the frequency variation Δf of the preceding vibro-tactile trial was increasing ($\Delta f > 0$) or decreasing ($\Delta f < 0$). The subjects were wearing a headset with white noise for being acoustically shielded from the environment.

7.5. Results

7.5.1. Glove

The results show that we had a 64-93% rate of success to identify an active actuator location (see Figure 44). Actuators at the fingertips were more accurately identified than at the palm.

The findings in Figure 45 illustrate that the intensity variation was easily identified with a 78-93% rate of accurate association.

The region of active stimulation had a 60-100% rate of correct identification (see Figure 47). The results indicate that a higher quantity of localized stimulation reduces precise actuator identification accuracy. However, the region of activation was well recognizable.

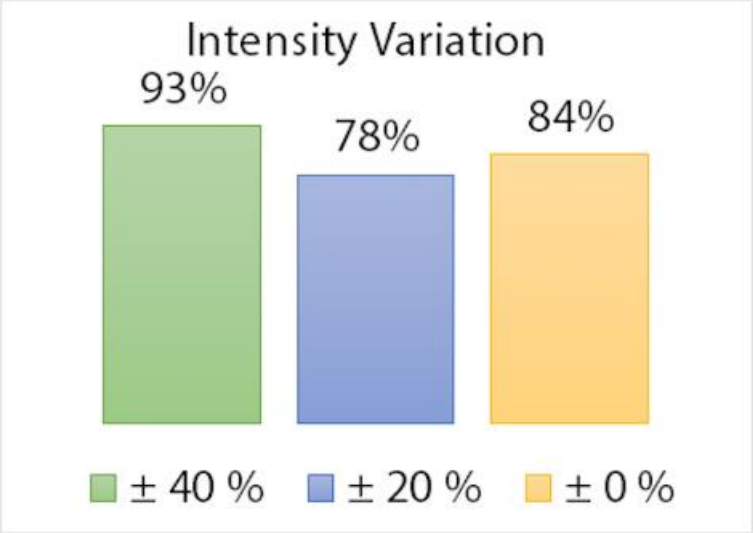

Figure 45 – Stimulus magnitude perception.

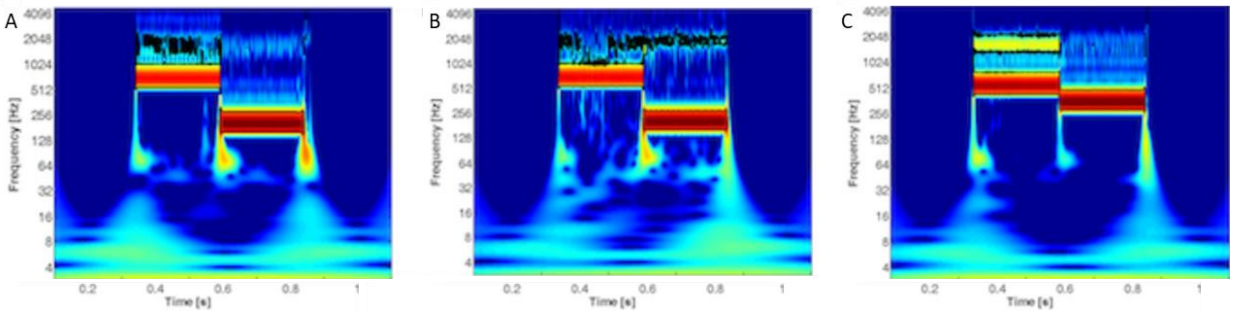

Figure 46 – Spectral analysis on the normal force recorded by the load cell while activating a piezoelectric actuator. The red regions show the spectral frequencies bringing highest signal power and point out their occurrence with time as the stimulation starts. a) Results for 200 Vpp and 700-200 Hz frequency change (-500 Hz Δf). b) Results for 100 Vpp and 700-200 Hz frequency change (-500 Hz Δf); c) Results for 200 Vpp and 550-350 Hz frequency change (-200 Hz Δf).

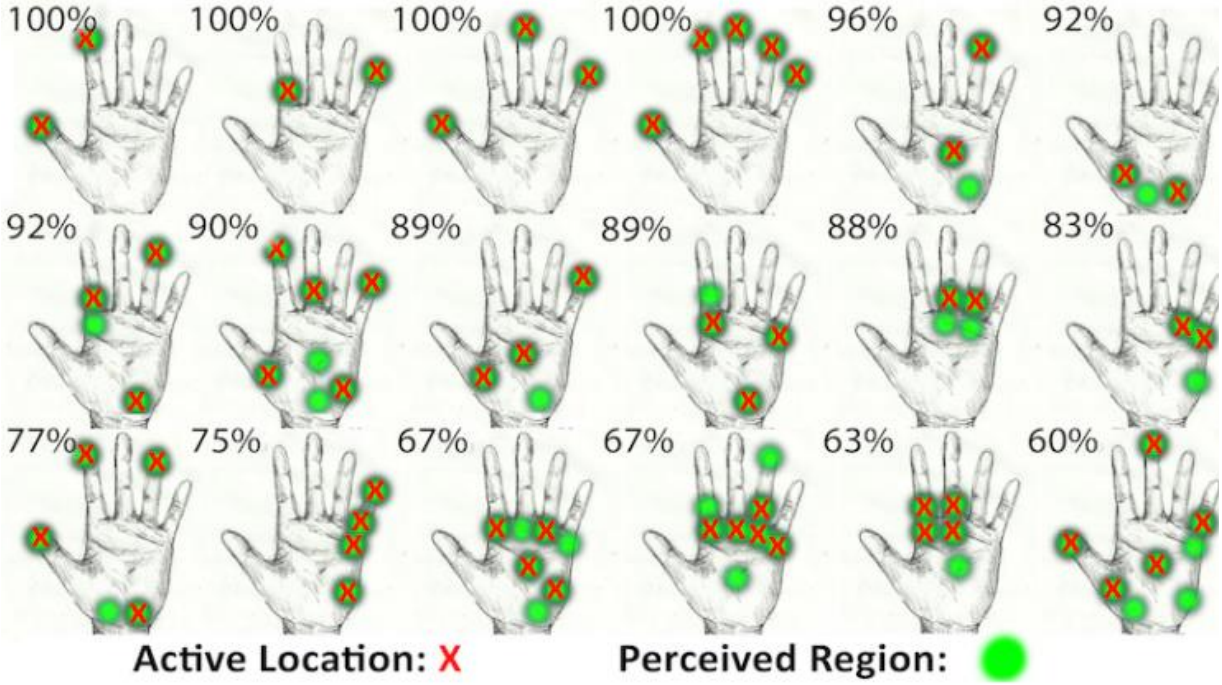

Figure 47 – Perception of active region.

7.5.2. Wristband

Spectral analysis was performed using a wavelet coherence package [454] on normal forces (F_z) recorded by the load cell during actuation. This analysis showed coherence with nominal stimulation parameters. Vibratory changes were substantial for different peak-to-peak amplitudes and frequency differences (see example analyses in Figure 46). Hence, the device delivered vibro-tactile stimuli in a reliable manner. In addition, we evaluated the efficacy of the system to deliver accurate tactile feedback using a 2AFC psychophysical protocol.

Results of the psychophysical tests show that the detection rate increased almost monotonically with frequency variation, Δf. The results had a typical appearance of a psychometric curve of a 2AFC experiment, where 'increasing frequency' responses were almost random around the origin of Δf axis, and tended to 100% for strongly increasing frequency changes and to 0% for strongly decreasing ones (Figure 48). Since modulation of the parameters of vibro-tactile stimulation are well reflected in subject perception, with a monotonic mapping between stimuli difference and discrimination performance, the system

can be used to provide meaningful sensory feedback to a wearer by means of sensory substitution.

7.6. Discussion

Our study of the vibro-tactile glove shows that the volunteer subjects were able to successfully perceive stimuli. Our glove is easy to use and permits a wide range of haptic perception. Although multiple actuator identification is less precise, single activation are easily perceived. To address the non-ideal properties of this first generation glove, we aspire to develop an advanced high-density vibro-tactile glove that is exceptionally compact and formfitting, permitting more precise localization. We plan to increase perception using precise haptic actuators such as the Haptuator^{TM} Planar (TactileLabs). In addition, we plan to evaluate the capability of rendering multimodal tactile information using our second-generation glove. Analysis of the piezoelectric actuator to be integrated in the wristband showed with human subjects that the sequence of stimuli presentation could affect perception of frequency changes. Although preliminary results from psychophysical experiments showed that the single piezoelectric transducer is appropriate for the transmission of haptic information, further experiments must be performed to evaluate the

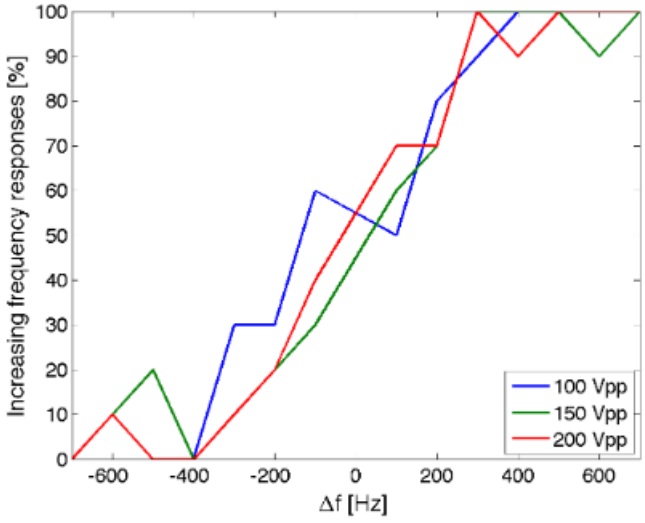

Figure 48 – Percentage of stimuli identified as having increasing frequency, as a function of the frequency variation Δ*f*. The colors of the curves represent three amplitudes of stimulation.

best configuration for the entire device, in terms of number and spatial distribution of the embedded transducers. We expect the device to be comfortable, able to effectively transmit information to the wrists and work in a complementary manner with the haptic glove.

Future studies will address the quantification of the information content that can be provided by means of this haptic interface, also jointly with the virtual reality environment.

Conclusions and perspectives

The work we have presented in this thesis is centred on the role of haptics for applications in medical robotics, rehabilitation and assistive technology for sensory substitution. What we have presented represents a further step towards remote palpation, remote control, communication and tactile perception.

Towards this objective, we have demonstrated a miniaturized tactile technology for capsule endoscopy. We have addressed two well-known problems in the field of endoscopy: *i)* pain and discomfort caused by poor manoeuvrability of standard endoscopes and absence of force sensing tools to monitor the pressure exerted against the colonic wall; *ii)* difficulty to detect non polypoid tumours (NPT) by visual inspection. Our experiments have demonstrated that our technology, in synergy with a robotic system for magnetic guidance, enables efficient locomotion and exerts a predefined pressure against the colonic wall. Furthermore, we have proved that this device allows a robust classification of non-protruding rubber hard inclusions in a soft silicone matrix. In particular, the device collects data while sliding on the tissue-under-test, and an algorithm, involving a kNN classifier, is able to discriminate different classes of tissues, based on hardness. In our tests, we discriminated six different classes of hard inclusions, with a 94 % precision.

In the second part of this thesis, we have presented our work on vibro-tactile devices. We have demonstrated a method for encapsulation of piezo-electric actuators, which is effective for delivering vibro-tactile information. Psychophysical tests based on a 2AFC (two-alternative forced-choice) protocol have shown that both a glove and a wrist-band embedding these vibrating elements allow precise discrimination of tactile information. We have outlined a virtual reality system involving our technology, and further tested our device for precise location discrimination.

Our studies in vibro-tactile stimulation go towards the development of a technology for fine haptic information communication. We believe that such technology can be useful for

applications such as sensory substitution for hearing or visually impaired people, communication and remote control in virtual reality environments, and tele-operated surgeries. Further studies are necessary for maturation of the technology. We need to conduct tests specifically designed for applications with impaired people and surgical operations.

The works regarding the tactile capsule consist of tests in synthetic environments, in order to prove the device capabilities. For the sake of simplicity and variables minimization, we decoupled the two problems of robotic tactile sensing and haptic feedback delivery to the endoscopist, proving: *i)* automated analysis of the forces exerted against the endoluminal wall, for improved locomotion and safety purposes; and *ii)* automatic detection of suspect abnormal tissues based on hardness classification. Further tests in *ex-vivo* and *in-vivo* conditions are fundamental to validate the technology. The device should be also re-designed to meet size constraints of colonoscopy. We also believe that the development of an accurate magnetic localization algorithm, which is in progress for the Endoo European project, is crucial and will potentially improve the capabilities of the tactile sensing algorithm.

Finally, the two proposed technologies can be joined to realize a system for remote palpation, involving the tactile probe for force reading and the vibro-tactile devices for delivering haptic feedback to the operator. It would be interesting to investigate whether a man-in-the-loop approach with tactile feedback or an automated classifier paired with standard imaging tools would be more convenient in the diagnosis of colonic tumours.

List of publications

Journal Publications

- **Caliò, R.***, Camboni, D.*, Massari, L., D'Abbraccio, J., Mazomenos, E., Stoyanov, D., Menciassi, A., Carrozza, M. C., Dario, P., Ciuti, G., & Oddo, C. M. (2018). Endoscopic tactile capsule for non-polypoid colorectal tumor detection through hardness and curvature classification. IEEE Transaction on Biomedical Engineering, TO BE SUBMITTED

- Sorgini, F., **Caliò, R.**, Carrozza, M. C., & Oddo, C. M. (2017). Haptic-assistive technologies for audition and vision sensory disabilities. Disability and Rehabilitation: Assistive Technology, 1-28.

- Sorgini, F., Mazzoni, A., Massari, L., **Caliò, R.**, Galassi, C., Kukreja, S. L., ... & Oddo, C. M. (2017). Encapsulation of piezoelectric transducers for sensory augmentation and substitution with wearable haptic devices. Micromachines, 8(9), 270.

- Ciuti, G., **Caliò, R.**, Camboni, D., Neri, L., Bianchi, F., Arezzo, A., ... & Magnani, B. (2016). Frontiers of robotic endoscopic capsules: a review. Journal of Micro-Bio Robotics, 11(1-4), 1-18.

- **Caliò, R.**, Rongala, U. B., Camboni, D., Milazzo, M., Stefanini, C., De Petris, G., & Oddo, C. M. (2014). Piezoelectric energy harvesting solutions. Sensors, 14(3), 4755-4790.

Conferences

- **Caliò, R.*,** Camboni, D.*, Ortega Alcaide, J., Oddo, C. M., Carrozza, M. C., Menciassi, A., Ciuti, G., Dario, P., Sensorized capsule endoscope for closed-loop magnetic navigation and safe tissue interaction. 29TH Conference of the international Society for Medical Innovation and Technology (SMIT 2017)

- **Caliò, R.*,** Camboni, D.*, Ortega Alcaide, J., Oddo, C. M., Carrozza, M. C., Menciassi, A., Ciuti, G., Dario, P., Robotic endoscopic capsule for

closed-loop force-based control and safety strategies. 2017 IEEE International Conference on Cyborg and Bionic Systems (CBS 2017)

- Camboni, D.*, **Caliò, R.***, Ortega Alcaide, J., Oddo, C. M., Carrozza, M. C., Menciassi, A., Ciuti, G., Dario, P., Tactile robotic endoscopic capsule for safe closed-loop force control. 7TH Joint Workshop on New Technologies for Computer/Robot ASssisted Surgery (CRAS 2017)
- Brandao, P., Mazomenos, E., Ciuti, G., **Caliò, R.**, Bianchi, F., Menciassi, A., ... & Stoyanov, D. (2017, March). Fully convolutional neural networks for polyp segmentation in colonoscopy. In Medical Imaging 2017: Computer-Aided Diagnosis (Vol. 10134, p. 101340F). International Society for Optics and Photonics.
- Sorgini, F., Ghosh, R., Huebotter, J. F., **Caliò, R.**, Galassi, C., Oddo, C. M., & Kukreja, S. L. (2016, June). Design and preliminary evaluation of haptic devices for upper limb stimulation and integration within a virtual reality cave. In Biomedical Robotics and Biomechatronics (BioRob), 2016 6th IEEE International Conference on (pp. 464-469). IEEE.
- Mazzoni, A.; Johnson, S.; Camboni, D.; **Caliò, R.**; Sorgini, F.; Rongala, U.B.; Spigler, G.; Oddo, C.M., Precise spike timing with an array of biomimetic mechanosensors performs optimal discrimination of sensory stimuli, Dynamics of Neural Circuits, NETT 2014

Patents

- **Caliò, R.**, Menciassi, A., Ciuti, G., Oddo, C. M., Camboni, D., Bianchi, F., Dario, P., Carrozza, M. C., (102017000103200) *"Dispositivo sondante per l'analisi di una superficie"*, Filing date: 14/09/2017. Status: pending.
- Galassi, C., Sorgini, F., **Caliò, R.**, Cipriani, C., Carrozza, M.C., Oddo, C.M., (102016000002346) "*Metodo per la realizzazione di trasduttori integrabili per applicazioni aptiche*" Filing date: 13/01/2016.

Bibliography

[1] L. D. Harmon, "Touch-sensing technology- A review," *Society of Manufacturing Engineers, 1980. 58,* 1980.

[2] L. D. Harmon, "Automated tactile sensing," *The International Journal of Robotics Research,* vol. 1, pp. 3-32, 1982.

[3] M. I. Tiwana, S. J. Redmond, and N. H. Lovell, "A review of tactile sensing technologies with applications in biomedical engineering," *Sensors and Actuators A: physical,* vol. 179, pp. 17-31, 2012.

[4] R. S. Johansson, "Tactile sensibility in the human hand: receptive field characteristics of mechanoreceptive units in the glabrous skin area," *The Journal of physiology,* vol. 281, pp. 101-125, 1978.

[5] R. S. Johansson and A. B. Vallbo, "Tactile Sensibility in the Human Hand - Relative and Absolute Densities of 4 Types of Mechanoreceptive Units in Glabrous Skin," *Journal of Physiology-London,* vol. 286, pp. 283-300, 1979.

[6] R. S. Johansson and A. B. Vallbo, "Tactile Sensory Coding in the Glabrous Skin of the Human Hand," *Trends in Neurosciences,* vol. 6, pp. 27-32, 1983.

[7] A. Vallbo and R. S. Johansson, "Properties of cutaneous mechanoreceptors in the human hand related to touch sensation," *Hum Neurobiol,* vol. 3, pp. 3-14, 1984.

[8] A. Iggo and A. R. Muir, "The structure and function of a slowly adapting touch corpuscle in hairy skin," *The Journal of physiology,* vol. 200, pp. 763-796, 1969.

[9] U. Lindblom, "Properties of touch receptors in distal glabrous skin of the monkey," *Journal of Neurophysiology,* vol. 28, pp. 966-985, 1965.

[10] M. R. Chambers, K. Andres, M. v. Duering, and A. Iggo, "The structure and function of the slowly adapting type II mechanoreceptor in hairy skin," *Experimental Physiology,* vol. 57, pp. 417-445, 1972.

[11] R. S. Johansson and I. Birznieks, "First spikes in ensembles of human tactile afferents code complex spatial fingertip events," *Nature neuroscience,* vol. 7, p. 170, 2004.

[12] R. S. Johansson and J. R. Flanagan, "Coding and use of tactile signals from the fingertips in object manipulation tasks," *Nature Reviews Neuroscience,* vol. 10, p. 345, 2009.

[13] P. Jenmalm, I. Birznieks, A. W. Goodwin, and R. S. Johansson, "Influence of object shape on responses of human tactile afferents under conditions characteristic of manipulation," *European journal of neuroscience,* vol. 18, pp. 164-176, 2003.

[14] M. C. Carrozza, G. Cappiello, S. Micera, B. B. Edin, L. Beccai, and C. Cipriani, "Design of a cybernetic hand for perception and action," *Biological cybernetics,* vol. 95, p. 629, 2006.

[15] M. S. Johannes, J. D. Bigelow, J. M. Burck, S. D. Harshbarger, M. V. Kozlowski, and T. Van Doren, "An overview of the developmental process for the modular prosthetic limb," *Johns Hopkins APL Technical Digest,* vol. 30, pp. 207-216, 2011.

[16] C. Connolly, "Prosthetic hands from touch bionics," *Industrial Robot: An International Journal,* vol. 35, pp. 290-293, 2008.

[17] S. Raspopovic, M. Capogrosso, F. M. Petrini, M. Bonizzato, J. Rigosa, G. Di Pino*, et al.*, "Restoring natural sensory feedback in real-time bidirectional hand prostheses," *Science translational medicine,* vol. 6, pp. 222ra19-222ra19, 2014.

[18] R. Bashir, "BioMEMS: state-of-the-art in detection, opportunities and prospects," *Advanced drug delivery reviews,* vol. 56, pp. 1565-1586, 2004.

[19] C. Lucarotti, C. M. Oddo, N. Vitiello, and M. C. Carrozza, "Synthetic and bio-artificial tactile sensing: A review," *Sensors,* vol. 13, pp. 1435-1466, 2013.

[20] J.-j. Cabibihan, M. C. Carrozza, P. Dario, S. Pattofatto, M. Jomaa, and A. Benallal, "The uncanny valley and the search for human skin-like materials for a prosthetic fingertip," in *Humanoid Robots, 2006 6th IEEE-RAS International Conference on*, 2006, pp. 474-477.

[21] R. S. Dahiya, G. Metta, M. Valle, and G. Sandini, "Tactile sensing—from humans to humanoids," *IEEE transactions on robotics,* vol. 26, pp. 1-20, 2010.

[22] V. Maheshwari and R. Saraf, "Tactile devices to sense touch on a par with a human finger," *Angewandte Chemie International Edition,* vol. 47, pp. 7808-7826, 2008.

[23] H. Yousef, M. Boukallel, and K. Althoefer, "Tactile sensing for dexterous in-hand manipulation in robotics—A review," *Sensors and Actuators A: physical,* vol. 167, pp. 171-187, 2011.

[24] K. Hosoda, Y. Tada, and M. Asada, "Anthropomorphic robotic soft fingertip with randomly distributed receptors," *Robotics and Autonomous Systems,* vol. 54, pp. 104-109, 2006.

[25] V. A. Ho, D. V. Dao, S. Sugiyama, and S. Hirai, "Development and analysis of a sliding tactile soft fingertip embedded with a microforce/moment sensor," *IEEE Transactions on Robotics,* vol. 27, pp. 411-424, 2011.

[26] K. V. D. S. Chathuranga and S. Hirai, "A bio-mimetic fingertip that detects force and vibration modalities and its application to surface identification," in *Robotics and Biomimetics (ROBIO), 2012 IEEE International Conference on*, 2012, pp. 575-581.

[27] D.-K. Kim, J.-H. Kim, Y.-T. Kim, M.-S. Kim, Y.-K. Park, and Y.-H. Kwon, "Robot fingertip tactile sensing module with a 3D-curved shape using molding technique," *Sensors and Actuators A: Physical,* vol. 203, pp. 421-429, 2013.

[28] J. Park, M. Kim, Y. Lee, H. S. Lee, and H. Ko, "Fingertip skin–inspired microstructured ferroelectric skins discriminate static/dynamic pressure and temperature stimuli," *Science advances,* vol. 1, p. e1500661, 2015.

[29] R. S. Johansson, G. E. Loeb, N. Wettels, D. Popovic, and V. J. Santos, "Biomimetic tactile sensor for control of grip," ed: Google Patents, 2011.

[30] N. Wettels, V. J. Santos, R. S. Johansson, and G. E. Loeb, "Biomimetic tactile sensor array," *Advanced Robotics,* vol. 22, pp. 829-849, 2008.

[31] C. H. Lin, T. W. Erickson, J. A. Fishel, N. Wettels, and G. E. Loeb, "Signal processing and fabrication of a biomimetic tactile sensor array with thermal, force and microvibration modalities," in *Robotics and Biomimetics (ROBIO), 2009 IEEE International Conference on*, 2009, pp. 129-134.

[32] L. Beccai, S. Roccella, A. Arena, F. Valvo, P. Valdastri, A. Menciassi*, et al.*, "Design and fabrication of a hybrid silicon three-axial force sensor for biomechanical applications," *Sensors and Actuators A: Physical,* vol. 120, pp. 370-382, 2005.

[33] C. M. Oddo, L. Beccai, M. Felder, F. Giovacchini, and M. C. Carrozza, "Artificial roughness encoding with a bio-inspired MEMS-based tactile sensor array," *Sensors,* vol. 9, pp. 3161-3183, 2009.

[34] C. M. Oddo, L. Beccai, J. Wessberg, H. B. Wasling, F. Mattioli, and M. C. Carrozza, "Roughness encoding in human and biomimetic artificial touch: Spatiotemporal frequency modulation and structural anisotropy of fingerprints," *Sensors,* vol. 11, pp. 5596-5615, 2011.

[35] C. M. Oddo, M. Controzzi, L. Beccai, C. Cipriani, and M. C. Carrozza, "Roughness encoding for discrimination of surfaces in artificial active-touch," *IEEE Transactions on Robotics,* vol. 27, pp. 522-533, 2011.

[36] C. M. Oddo, S. Raspopovic, F. Artoni, A. Mazzoni, G. Spigler, F. Petrini*, et al.*, "Intraneural stimulation elicits discrimination of textural features by artificial fingertip in intact and amputee humans," *Elife,* vol. 5, 2016.

[37] G. Ciuti, R. Caliò, D. Camboni, L. Neri, F. Bianchi, A. Arezzo*, et al.*, "Frontiers of robotic endoscopic capsules: a review," *Journal of micro-bio robotics,* vol. 11, pp. 1-18, 2016.

[38] X. Wang, C. Di Natali, M. Beccani, M. Kern, P. Valdastri, and M. Rentschler, "Novel medical wired palpation device: A validation study of material properties," in *Solid-State Sensors, Actuators and Microsystems (TRANSDUCERS & EUROSENSORS XXVII), 2013 Transducers & Eurosensors XXVII: The 17th International Conference on*, 2013, pp. 1653-1658.

[39] P. Armaroli, P. Villain, E. Suonio, M. Almonte, A. Anttila, W. S. Atkin*, et al.*, "European code against cancer: cancer screening," *Cancer epidemiology,* vol. 39, pp. S139-S152, 2015.

[40] C. Hassan, P. G. Rossi, L. Camilloni, D. Rex, B. Jimenez-Cendales, E. Ferroni*, et al.*, "Meta-analysis: adherence to colorectal cancer screening and the detection rate for advanced neoplasia, according to the type of screening test," *Alimentary pharmacology & therapeutics,* vol. 36, pp. 929-940, 2012.

[41] C. Senore, J. Inadomi, N. Segnan, C. Bellisario, and C. Hassan, "Optimising colorectal cancer screening acceptance: a review," *Gut,* vol. 64, pp. 1158-1177, 2015.

[42] W. Leung, C. Foo, T. Chan, M. Chiang, A. Lam, H. Chan*, et al.*, "Alternatives to colonoscopy for population-wide colorectal cancer screening," *Hong Kong Medical Journal,* 2016.

[43] L. Trevisani, A. Zelante, and S. Sartori, "Colonoscopy, pain and fears: Is it an indissoluble trinomial?," *World journal of gastrointestinal endoscopy,* vol. 6, p. 227, 2014.

[44] G. Iddan, G. Meron, A. Glukhovsky, and P. Swain, "Wireless capsule endoscopy," *Nature,* vol. 405, p. 417, 2000.

[45] A. Koulaouzidis, D. K. Iakovidis, A. Karargyris, and E. Rondonotti, "Wireless endoscopy in 2020: Will it still be a capsule?," *World journal of gastroenterology: WJG,* vol. 21, p. 5119, 2015.

[46] G. Ciuti, A. Menciassi, and P. Dario, "Capsule endoscopy: from current achievements to open challenges," *IEEE reviews in biomedical engineering,* vol. 4, pp. 59-72, 2011.

[47] A. Loeve, P. Breedveld, and J. Dankelman, "Scopes too flexible... and too stiff," *IEEE pulse,* vol. 1, pp. 26-41, 2010.

[48] L. J. Sliker and G. Ciuti, "Flexible and capsule endoscopy for screening, diagnosis and treatment," *Expert review of medical devices,* vol. 11, pp. 649-666, 2014.
[49] D. Cater, A. Vyas, and D. Vyas, "Robotics in colonoscopy," *American journal of robotic surgery,* vol. 1, pp. 48-54, 2014.
[50] B. P. M. Yeung and P. W. Y. Chiu, "Application of robotics in gastrointestinal endoscopy: A review," *World journal of gastroenterology,* vol. 22, p. 1811, 2016.
[51] C. Spada, C. Hassan, and G. Costamagna, "Colon capsule endoscopy in colorectal cancer screening: a rude awakening from a beautiful dream?," *Clinical Gastroenterology and Hepatology,* vol. 13, pp. 2302-2304, 2015.
[52] A. auTHOrSVan Gossum and D. O. INTErESTS, "Colon capsule endoscopy for detection of polyps and cancers: a step closer to non-invasive colon screening?," *JR Coll Physicians Edinb,* vol. 41, pp. 124-5, 2011.
[53] I. M. Gralnek, "Emerging technological advancements in colonoscopy: Third Eye® Retroscope® and Third Eye® PanoramicTM, Fuse® Full Spectrum Endoscopy® colonoscopy platform, Extra-Wide-Angle-View colonoscope, and NaviAidTM G-EYETM balloon colonoscope," *Digestive Endoscopy,* vol. 27, pp. 223-231, 2015.
[54] F. J. van den Broek, J. B. Reitsma, W. L. Curvers, P. Fockens, and E. Dekker, "Systematic review of narrow-band imaging for the detection and differentiation of neoplastic and nonneoplastic lesions in the colon (with videos)," *Gastrointestinal endoscopy,* vol. 69, pp. 124-135, 2009.
[55] M. R. Banks, R. Haidry, M. A. Butt, L. Whitley, J. Stein, L. Langmead*, et al.*, "High resolution colonoscopy in a bowel cancer screening program improves polyp detection," *World journal of gastroenterology: WJG,* vol. 17, p. 4308, 2011.
[56] R. Kiesslich, L. Gossner, M. Goetz, A. Dahlmann, M. Vieth, M. Stolte*, et al.*, "In vivo histology of Barrett's esophagus and associated neoplasia by confocal laser endomicroscopy," *Clinical Gastroenterology and Hepatology,* vol. 4, pp. 979-987, 2006.
[57] K. B. Dunbar, P. Okolo, E. Montgomery, and M. I. Canto, "Confocal laser endomicroscopy in Barrett's esophagus and endoscopically inapparent Barrett's neoplasia: a prospective, randomized, double-blind, controlled, crossover trial," *Gastrointestinal endoscopy,* vol. 70, pp. 645-654, 2009.
[58] M. A. Kara, F. P. Peters, F. J. ten Kate, S. J. van Deventer, P. Fockens, and J. J. Bergman, "Endoscopic video autofluorescence imaging may improve the detection of early neoplasia in patients with Barrett's esophagus," *Gastrointestinal endoscopy,* vol. 61, pp. 679-685, 2005.
[59] L. Seebach, P. Bauerfeind, and C. Gubler, "'"Sparing the surgeon": clinical experience with over-the-scope clips for gastrointestinal perforation," *Endoscopy,* vol. 42, pp. 1108-1111, 2010.
[60] A. Schmidt, P. Bauerfeind, C. Gubler, M. Damm, M. Bauder, and K. Caca, "Endoscopic full-thickness resection in the colorectum with a novel over-the-scope device: first experience," *Endoscopy,* vol. 47, pp. 719-725, 2015.
[61] A. Wang, S. Banerjee, B. A. Barth, Y. M. Bhat, S. Chauhan, K. T. Gottlieb*, et al.*, "Wireless capsule endoscopy," *Gastrointestinal endoscopy,* vol. 78, pp. 805-815, 2013.

[62] A. Koulaouzidis, E. Rondonotti, and A. Karargyris, "Small-bowel capsule endoscopy: a ten-point contemporary review," *World journal of gastroenterology: WJG,* vol. 19, p. 3726, 2013.

[63] D. Lomanto, S. Wijerathne, L. K. Y. Ho, and L. S. J. Phee, "Flexible endoscopic robot," *Minimally Invasive Therapy & Allied Technologies,* vol. 24, pp. 37-44, 2015.

[64] M. Quirini, A. Menciassi, S. Scapellato, C. Stefanini, and P. Dario, "Design and fabrication of a motor legged capsule for the active exploration of the gastrointestinal tract," *IEEE/ASME transactions on mechatronics,* vol. 13, pp. 169-179, 2008.

[65] G. Tortora, P. Valdastri, E. Susilo, A. Menciassi, P. Dario, F. Rieber*, et al.*, "Propeller-based wireless device for active capsular endoscopy in the gastric district," *Minimally Invasive Therapy & Allied Technologies,* vol. 18, pp. 280-290, 2009.

[66] I. De Falco, G. Tortora, P. Dario, and A. Menciassi, "An integrated system for wireless capsule endoscopy in a liquid-distended stomach," *IEEE transactions on biomedical engineering,* vol. 61, pp. 794-804, 2014.

[67] G. Kósa, P. Jakab, G. Székely, and N. Hata, "MRI driven magnetic microswimmers," *Biomedical microdevices,* vol. 14, pp. 165-178, 2012.

[68] P. Valdastri, E. Sinibaldi, S. Caccavaro, G. Tortora, A. Menciassi, and P. Dario, "A novel magnetic actuation system for miniature swimming robots," *IEEE Transactions on Robotics,* vol. 27, pp. 769-779, 2011.

[69] R. Caprara, K. L. Obstein, G. Scozzarro, C. Di Natali, M. Beccani, D. R. Morgan*, et al.*, "A platform for gastric cancer screening in low-and middle-income countries," *IEEE Transactions on Biomedical Engineering,* vol. 62, pp. 1324-1332, 2015.

[70] B. Kim, S. Lee, J. H. Park, and J.-O. Park, "Design and fabrication of a locomotive mechanism for capsule-type endoscopes using shape memory alloys (SMAs)," *IEEE/ASME Transactions On Mechatronics,* vol. 10, pp. 77-86, 2005.

[71] B. Kim, S. Park, C. Y. Jee, and S.-J. Yoon, "An earthworm-like locomotive mechanism for capsule endoscopes," in *Intelligent Robots and Systems, 2005.(IROS 2005). 2005 IEEE/RSJ International Conference on*, 2005, pp. 2997-3002.

[72] W. Li, W. Guo, M. Li, and Y. Zhu, "A novel locomotion principle for endoscopic robot," in *Mechatronics and Automation, Proceedings of the 2006 IEEE International Conference on*, 2006, pp. 1658-1662.

[73] S. Park, H. Park, S. Park, and B. Kim, "A paddling based locomotive mechanism for capsule endoscopes," *Journal of mechanical science and technology,* vol. 20, pp. 1012-1018, 2006.

[74] L. J. Sliker, M. D. Kern, J. A. Schoen, and M. E. Rentschler, "Surgical evaluation of a novel tethered robotic capsule endoscope using micro-patterned treads," *Surgical endoscopy,* vol. 26, pp. 2862-2869, 2012.

[75] M. Quirini, A. Menciassi, S. Scapellato, P. Dario, F. Rieber, C.-N. Ho*, et al.*, "Feasibility proof of a legged locomotion capsule for the GI tract," *Gastrointestinal endoscopy,* vol. 67, pp. 1153-1158, 2008.

[76] E. Buselli, P. Valdastri, M. Quirini, A. Menciassi, and P. Dario, "Superelastic leg design optimization for an endoscopic capsule with active locomotion," *Smart materials and structures,* vol. 18, p. 015001, 2008.

[77] P. Valdastri, R. J. Webster III, C. Quaglia, M. Quirini, A. Menciassi, and P. Dario, "A new mechanism for mesoscale legged locomotion in compliant tubular environments," *IEEE Transactions on Robotics,* vol. 25, pp. 1047-1057, 2009.

[78] S. Gorini, M. Quirini, A. Menciassi, G. Pernorio, C. Stefanini, and P. Dario, "A novel SMA-based actuator for a legged endoscopic capsule," in *Biomedical Robotics and Biomechatronics, 2006. BioRob 2006. The First IEEE/RAS-EMBS International Conference on*, 2006, pp. 443-449.

[79] H.-J. Park, J.-H. Lee, Y.-K. Moon, Y.-H. Yoon, C.-H. Won, H.-C. Choi*, et al.*, "New method of moving control for wireless endoscopic capsule using electrical stimuli," *IEICE Transactions on Fundamentals of Electronics, Communications and Computer Sciences,* vol. 88, pp. 1476-1480, 2005.

[80] C. A. Mosse, T. N. Mills, M. N. Appleyard, S. S. Kadirkamanathan, and C. P. Swain, "Electrical stimulation for propelling endoscopes," *Gastrointestinal endoscopy,* vol. 54, pp. 79-83, 2001.

[81] J. Keller, C. Fibbe, F. Volke, J. Gerber, A. C. Mosse, M. Reimann-Zawadzki*, et al.*, "Inspection of the human stomach using remote-controlled capsule endoscopy: a feasibility study in healthy volunteers (with videos)," *Gastrointestinal endoscopy,* vol. 73, pp. 22-28, 2011.

[82] F. Carpi, N. Kastelein, M. Talcott, and C. Pappone, "Magnetically controllable gastrointestinal steering of video capsules," *IEEE Transactions on Biomedical Engineering,* vol. 58, pp. 231-234, 2011.

[83] F. Carpi and C. Pappone, "Magnetic maneuvering of endoscopic capsules by means of a robotic navigation system," *IEEE Transactions on Biomedical Engineering,* vol. 56, pp. 1482-1490, 2009.

[84] G. Ciuti, P. Valdastri, A. Menciassi, and P. Dario, "Robotic magnetic steering and locomotion of capsule endoscope for diagnostic and surgical endoluminal procedures," *Robotica,* vol. 28, pp. 199-207, 2010.

[85] G. Ciuti, R. Donlin, P. Valdastri, A. Arezzo, A. Menciassi, M. Morino*, et al.*, "Robotic versus manual control in magnetic steering of an endoscopic capsule," *Endoscopy,* vol. 42, pp. 148-152, 2010.

[86] A. Arezzo, A. Menciassi, P. Valdastri, G. Ciuti, G. Lucarini, M. Salerno*, et al.*, "Experimental assessment of a novel robotically-driven endoscopic capsule compared to traditional colonoscopy," *Digestive and Liver Disease,* vol. 45, pp. 657-662, 2013.

[87] C. Di Natali, M. Beccani, and P. Valdastri, "Real-Time Pose Detection for Magnetic Medical Devices," *Ieee Transactions on Magnetics,* vol. 49, pp. 3524-3527, Jul 2013.

[88] P. Valdastri, G. Ciuti, A. Verbeni, A. Menciassi, P. Dario, A. Arezzo*, et al.*, "Magnetic air capsule robotic system: proof of concept of a novel approach for painless colonoscopy," *Surgical endoscopy,* vol. 26, pp. 1238-1246, 2012.

[89] G. Ciuti, N. Pateromichelakis, M. Sfakiotakis, P. Valdastri, A. Menciassi, D. Tsakiris*, et al.*, "A wireless module for vibratory motor control and inertial sensing in capsule endoscopy," *Sensors and Actuators A: Physical,* vol. 186, pp. 270-276, 2012.

[90] A. W. Mahoney, S. E. Wright, and J. J. Abbott, "Managing the attractive magnetic force between an untethered magnetically actuated tool and a rotating permanent

magnet," in *Robotics and Automation (ICRA), 2013 IEEE International Conference on*, 2013, pp. 5366-5371.

[91] A. W. Mahoney and J. J. Abbott, "Five-degree-of-freedom manipulation of an untethered magnetic device in fluid using a single permanent magnet with application in stomach capsule endoscopy," *The International Journal of Robotics Research,* vol. 35, pp. 129-147, 2016.

[92] J.-F. Rey, H. Ogata, N. Hosoe, K. Ohtsuka, N. Ogata, K. Ikeda*, et al.*, "Blinded nonrandomized comparative study of gastric examination with a magnetically guided capsule endoscope and standard videoendoscope," *Gastrointestinal endoscopy,* vol. 75, pp. 373-381, 2012.

[93] A. Bicchi and G. Tonietti, "Fast and" soft-arm" tactics [robot arm design]," *IEEE Robotics & Automation Magazine,* vol. 11, pp. 22-33, 2004.

[94] G. Lucarini, G. Ciuti, M. Mura, R. Rizzo, and A. Menciassi, "A new concept for magnetic capsule colonoscopy based on an electromagnetic system," *International Journal of Advanced Robotic Systems,* vol. 12, p. 25, 2015.

[95] J. L. Gorlewicz, S. Battaglia, B. F. Smith, G. Ciuti, J. Gerding, A. Menciassi*, et al.*, "Wireless insufflation of the gastrointestinal tract," *IEEE Transactions on Biomedical Engineering,* vol. 60, pp. 1225-1233, 2013.

[96] M. Simi, P. Valdastri, C. Quaglia, A. Menciassi, and P. Dario, "Design, fabrication, and testing of a capsule with hybrid locomotion for gastrointestinal tract exploration," *IEEe/ASME Transactions on Mechatronics,* vol. 15, pp. 170-180, 2010.

[97] T. D. Than, G. Alici, H. Zhou, and W. Li, "A review of localization systems for robotic endoscopic capsules," *IEEE transactions on biomedical engineering,* vol. 59, pp. 2387-2399, 2012.

[98] B. Z. Steinberg and I. Bettesh, "Localization of capsule with a synthetic source of quadrupoles and dipoles," ed: Google Patents, 2013.

[99] H. B. Shim, J. J. Hwang, K. S. Kim, Y. D. Seo, B. H. Kim, Y. W. Lee*, et al.*, "Endoscope and a method for finding its location," ed: Google Patents, 2010.

[100] K. Duda, T. Zielinski, R. Fraczek, J. Bulat, and M. Duplaga, "Localization of endoscopic capsule in the GI tract based on MPEG-7 visual descriptors," in *Imaging Systems and Techniques, 2007. IST'07. IEEE International Workshop on*, 2007, pp. 1-4.

[101] E. Spyrou and D. K. Iakovidis, "Video-based measurements for wireless capsule endoscope tracking," *Measurement Science and Technology,* vol. 25, p. 015002, 2013.

[102] C. Hu, M. Li, S. Song, R. Zhang, and M. Q.-H. Meng, "A cubic 3-axis magnetic sensor array for wirelessly tracking magnet position and orientation," *IEEE Sensors Journal,* vol. 10, pp. 903-913, 2010.

[103] N. Atuegwu and R. Galloway, "Volumetric characterization of the Aurora magnetic tracker system for image-guided transorbital endoscopic procedures," *Physics in Medicine & Biology,* vol. 53, p. 4355, 2008.

[104] D. Roetenberg, C. T. Baten, and P. H. Veltink, "Estimating body segment orientation by applying inertial and magnetic sensing near ferromagnetic materials," *IEEE Transactions on Neural Systems and Rehabilitation Engineering,* vol. 15, pp. 469-471, 2007.

[105] W. Liu, C. Hu, Q. He, M. Q.-H. Meng, and L. Liu, "An hybrid localization system based on optics and magnetics," in *Robotics and Biomimetics (ROBIO), 2010 IEEE International Conference on*, 2010, pp. 1165-1169.
[106] W. Weitschies, R. Kötitz, D. Cordini, and L. Trahms, "High-resolution monitoring of the gastrointestinal transit of a magnetically marked capsule," *Journal of pharmaceutical sciences,* vol. 86, pp. 1218-1222, 1997.
[107] W. Weitschies, J. Wedemeyer, R. Stehr, and L. Trahms, "Magnetic markers as a noninvasive tool to monitor gastrointestinal transit," *IEEE transactions on biomedical engineering,* vol. 41, pp. 192-195, 1994.
[108] X. Wu, W. Hou, C. Peng, X. Zheng, X. Fang, and J. He, "Wearable magnetic locating and tracking system for MEMS medical capsule," *Sensors and Actuators A: Physical,* vol. 141, pp. 432-439, 2008.
[109] A. Plotkin and E. Paperno, "3-D magnetic tracking of a single subminiature coil with a large 2-D array of uniaxial transmitters," *IEEE Transactions on Magnetics,* vol. 39, pp. 3295-3297, 2003.
[110] X. Guo, G. Yan, and W. He, "A novel method of three-dimensional localization based on a neural network algorithm," *Journal of medical engineering & technology,* vol. 33, pp. 192-198, 2009.
[111] I. Aoki, A. Uchiyama, K. Arai, K. Ishiyama, and S. Yabukami, "Detecting system of position and posture of capsule medical device," ed: Google Patents, 2010.
[112] M.-G. Kim, Y.-S. Hong, and E.-J. Lim, "Position and orientation detection of capsule endoscopes in spiral motion," *International Journal of Precision Engineering and Manufacturing,* vol. 11, pp. 31-37, 2010.
[113] M. Salerno, F. Mulana, R. Rizzo, A. Landi, and A. Menciassi, "Magnetic and inertial sensor fusion for the localization of endoluminal diagnostic devices," *INTERNATIONAL JOURNAL OF COMPUTER ASSISTED RADIOLOGY AND SURGERY,* vol. 7, pp. 3-4, 2012.
[114] C. Di Natali, M. Beccani, P. Valdastri, and K. L. Obstein, "Real-time pose and magnetic force detection for wireless magnetic capsule," ed: Google Patents, 2015.
[115] C. Di Natali, M. Beccani, N. Simaan, and P. Valdastri, "Jacobian-based iterative method for magnetic localization in robotic capsule endoscopy," *IEEE Transactions on Robotics,* vol. 32, pp. 327-338, 2016.
[116] K. Yu, I. Sharp, and Y. J. Guo, *Ground-based wireless positioning* vol. 5: John Wiley & Sons, 2009.
[117] D. Fischer, R. Schreiber, D. Levi, and R. Eliakim, "Capsule endoscopy: the localization system," *Gastrointestinal Endoscopy Clinics,* vol. 14, pp. 25-31, 2004.
[118] I. Wilding, P. Hirst, and A. Connor, "Development of a new engineering-based capsule for human drug absorption studies," *Pharmaceutical science & technology today,* vol. 3, pp. 385-392, 2000.
[119] C. L. Dumoulin, S. Souza, and R. Darrow, "Real-time position monitoring of invasive devices using magnetic resonance," *Magnetic resonance in medicine,* vol. 29, pp. 411-415, 1993.
[120] C. Van de Bruaene, D. De Looze, and P. Hindryckx, "Small bowel capsule endoscopy: Where are we after almost 15 years of use?," *World journal of gastrointestinal endoscopy,* vol. 7, p. 13, 2015.

[121] N. Hosoe, M. Naganuma, and H. Ogata, "Current status of capsule endoscopy through a whole digestive tract," *Digestive Endoscopy,* vol. 27, pp. 205-215, 2015.
[122] L. R. Fisher and W. L. Hasler, "New vision in video capsule endoscopy: current status and future directions," *Nature Reviews Gastroenterology and Hepatology,* vol. 9, p. 392, 2012.
[123] Z. Li, Z. Liao, and M. McAlindon, *Handbook of capsule endoscopy*: Springer, 2014.
[124] D. Filip, "Self–stabilizing capsule endoscope for early detection and biopsy of colonic polyps," University of Calgary, 2013.
[125] M.-J. Sheu, C.-W. Chiang, W.-S. Sun, J.-J. Wang, and J.-W. Pan, "Dual view capsule endoscopic lens design," *Optics express,* vol. 23, pp. 8565-8575, 2015.
[126] M. D. Goldstein, A. Yaron, and S. Ghilai, "Optical device," ed: Google Patents, 2002.
[127] A. Koulaouzidis and K. J. Dabos, "Looking forwards: not necessarily the best in capsule endoscopy?," *Annals of Gastroenterology: Quarterly Publication of the Hellenic Society of Gastroenterology,* vol. 26, p. 365, 2013.
[128] R. Shrestha, X. Zhang, Z. Gias, and K. Wahid, "Adaptive illumination in wireless capsule endoscopy system," in *Circuits and Systems (ISCAS), 2015 IEEE International Symposium on*, 2015, pp. 778-781.
[129] J. Aisenberg, "Gastrointestinal endoscopy nears “the molecular era”," *Gastrointestinal endoscopy,* vol. 68, pp. 528-530, 2008.
[130] M. A. Al-Rawhani, D. Chitnis, J. Beeley, S. Collins, and D. R. Cumming, "Design and implementation of a wireless capsule suitable for autofluorescence intensity detection in biological tissues," *IEEE Transactions on Biomedical Engineering,* vol. 60, pp. 55-62, 2013.
[131] P. R. Slawinski, K. L. Obstein, and P. Valdastri, "Emerging issues and future developments in capsule endoscopy," *Techniques in gastrointestinal endoscopy,* vol. 17, pp. 40-46, 2015.
[132] P. R. Slawinski, K. L. Obstein, and P. Valdastri, "Capsule endoscopy of the future: What’s on the horizon?," *World Journal of Gastroenterology: WJG,* vol. 21, p. 10528, 2015.
[133] L.-R. Dung and Y.-Y. Wu, "A wireless narrowband imaging chip for capsule endoscope," *IEEE transactions on biomedical circuits and systems,* vol. 4, pp. 462-468, 2010.
[134] A. Kolar, O. Romain, J. Ayoub, S. Viateur, and B. Granado, "Prototype of video endoscopic capsule with 3-d imaging capabilities," *IEEE transactions on biomedical circuits and systems,* vol. 4, pp. 239-249, 2010.
[135] A. Koulaouzidis, D. K. Iakovidis, A. Karargyris, and J. N. Plevris, "Optimizing lesion detection in small-bowel capsule endoscopy: from present problems to future solutions," *Expert review of gastroenterology & hepatology,* vol. 9, pp. 217-235, 2015.
[136] E. Rondonotti, A. Koulaouzidis, A. Karargyris, A. Giannakou, L. Fini, M. Soncini*, et al.*, "Utility of 3-dimensional image reconstruction in the diagnosis of small-bowel masses in capsule endoscopy (with video)," *Gastrointestinal endoscopy,* vol. 80, pp. 642-651, 2014.
[137] D. K. Iakovidis and A. Koulaouzidis, "Software for enhanced video capsule endoscopy: challenges for essential progress," *Nature Reviews Gastroenterology and Hepatology,* vol. 12, p. 172, 2015.

[138] M. Simi, M. Silvestri, C. Cavallotti, M. Vatteroni, P. Valdastri, A. Menciassi*, et al.*, "Magnetically activated stereoscopic vision system for laparoendoscopic single-site surgery," *IEEE/ASME Transactions on Mechatronics,* vol. 18, pp. 1140-1151, 2013.
[139] Y. Qiu, J. V. Gigliotti, M. Wallace, F. Griggio, C. E. Demore, S. Cochran*, et al.*, "Piezoelectric micromachined ultrasound transducer (PMUT) arrays for integrated sensing, actuation and imaging," *Sensors,* vol. 15, pp. 8020-8041, 2015.
[140] M. Keuchel, F. Hagenmüller, and H. Tajiri, *Video capsule endoscopy: a reference guide and atlas*: Springer, 2015.
[141] S. Bang, J. Y. Park, S. Jeong, Y. H. Kim, H. B. Shim, T. S. Kim*, et al.*, "First clinical trial of the "MiRo" capsule endoscope by using a novel transmission technology: electric-field propagation," *Gastrointestinal endoscopy,* vol. 69, pp. 253-259, 2009.
[142] M. R. Yuce and T. Dissanayake, "Easy-to-swallow wireless telemetry," *IEEE Microwave magazine,* vol. 13, pp. 90-101, 2012.
[143] K. M. Thotahewa, J.-M. Redouté, and M. R. Yuce, "A UWB wireless capsule endoscopy device," in *Engineering in Medicine and Biology Society (EMBC), 2014 36th Annual International Conference of the IEEE*, 2014, pp. 6977-6980.
[144] E. Atashpanjeh and A. Pirhadi, "Design of wideband monopole antenna loaded with small spiral for using in wireless capsule endoscopy systems," *Prog Electromagn Res C,* vol. 59, pp. 71-78, 2015.
[145] K. M. Thotahewa, J.-M. Redoutè, and M. R. Yuce, "Propagation, power absorption, and temperature analysis of UWB wireless capsule endoscopy devices operating in the human body," *IEEE Transactions on Microwave Theory and Techniques,* vol. 63, pp. 3823-3833, 2015.
[146] K. Kim, S. Yun, S. Lee, S. Nam, Y. J. Yoon, and C. Cheon, "A design of a high-speed and high-efficiency capsule endoscopy system," *IEEE Transactions on Biomedical Engineering,* vol. 59, pp. 1005-1011, 2012.
[147] D. X. Lioe, S. Shafie, H. Ramiah, N. Sulaiman, and I. A. Halin, "Low power transmitter for capsule endoscope," in *Recent Trends in Physics of Material Science and Technology*, ed: Springer, 2015, pp. 111-122.
[148] S. Rao and J.-C. Chiao, "Body electric: Wireless power transfer for implant applications," *IEEE Microwave Magazine,* vol. 16, pp. 54-64, 2015.
[149] R. Puers, R. Carta, and J. Thoné, "Wireless power and data transmission strategies for next-generation capsule endoscopes," *Journal of Micromechanics and Microengineering,* vol. 21, p. 054008, 2011.
[150] Y. Shi, G. Yan, B. Zhu, and G. Liu, "A portable wireless power transmission system for video capsule endoscopes," *Bio-medical materials and engineering,* vol. 26, pp. S1721-S1730, 2015.
[151] G. Tortora, F. Mulana, G. Ciuti, P. Dario, and A. Menciassi, "Inductive-based wireless power recharging system for an innovative endoscopic capsule," *Energies,* vol. 8, pp. 10315-10334, 2015.
[152] M. R. Basar, M. Y. Ahmad, J. Cho, and F. Ibrahim, "Performance evaluation of power transmission coils for powering endoscopic wireless capsules," in *Engineering in Medicine and Biology Society (EMBC), 2015 37th Annual International Conference of the IEEE*, 2015, pp. 2263-2266.

[153] A. Karargyris and N. Bourbakis, "Three-dimensional reconstruction of the digestive wall in capsule endoscopy videos using elastic video interpolation," *IEEE transactions on Medical Imaging,* vol. 30, pp. 957-971, 2011.

[154] Q. Zhao and M. Q.-H. Meng, "3D reconstruction of GI tract texture surface using Capsule Endoscopy Images," in *Automation and Logistics (ICAL), 2012 IEEE International Conference on*, 2012, pp. 277-282.

[155] B. Li and M. Q.-H. Meng, "Automatic polyp detection for wireless capsule endoscopy images," *Expert Systems with Applications,* vol. 39, pp. 10952-10958, 2012.

[156] Y. Yuan, B. Li, and M. Q.-H. Meng, "Improved bag of feature for automatic polyp detection in wireless capsule endoscopy images," *IEEE Transactions on Automation Science and Engineering,* vol. 13, pp. 529-535, 2016.

[157] A. V. Mamonov, I. N. Figueiredo, P. N. Figueiredo, and Y.-H. R. Tsai, "Automated polyp detection in colon capsule endoscopy," *IEEE transactions on medical imaging,* vol. 33, pp. 1488-1502, 2014.

[158] M. S. Imtiaz and K. A. Wahid, "Color enhancement in endoscopic images using adaptive sigmoid function and space variant color reproduction," *Computational and mathematical methods in medicine,* vol. 2015, 2015.

[159] H. R. Roth, J. R. McClelland, D. J. Boone, M. Modat, M. Jorge Cardoso, T. E. Hampshire*, et al.*, "Registration of the endoluminal surfaces of the colon derived from prone and supine CT colonography," *Medical Physics,* vol. 38, pp. 3077-3089, 2011.

[160] M. L. Halling, T. Nathan, J. Kjeldsen, and M. D. Jensen, "High sensitivity of quick view capsule endoscopy for detection of small bowel Crohn's disease," *Journal of gastroenterology and hepatology,* vol. 29, pp. 992-996, 2014.

[161] Y.-S. Kwon, Y.-S. Cho, T.-J. Yoon, H.-S. Kim, and M.-G. Choi, "Recent advances in targeted endoscopic imaging: Early detection of gastrointestinal neoplasms," *World journal of gastrointestinal endoscopy,* vol. 4, p. 57, 2012.

[162] J. L. Gonzalez-Guillaumin, D. C. Sadowski, K. V. Kaler, and M. P. Mintchev, "Ingestible capsule for impedance and pH monitoring in the esophagus," *IEEE Transactions on Biomedical Engineering,* vol. 54, pp. 2231-2236, 2007.

[163] E. A. Johannessen, L. Wang, L. Cui, T. B. Tang, M. Ahmadian, A. Astaras*, et al.*, "Implementation of multichannel sensors for remote biomedical measurements in a microsystems format," *IEEE Transactions on Biomedical Engineering,* vol. 51, pp. 525-535, 2004.

[164] B. Chander, N. Hanley-Williams, Y. Deng, and A. Sheth, "24 versus 48-hour bravo pH monitoring," *Journal of clinical gastroenterology,* vol. 46, pp. 197-200, 2012.

[165] S. S. C. Rao, M. Camilleri, W. Hasler, A. Maurer, H. Parkman, R. Saad*, et al.*, "Evaluation of gastrointestinal transit in clinical practice: position paper of the American and European Neurogastroenterology and Motility Societies," *Neurogastroenterology & Motility,* vol. 23, pp. 8-23, 2011.

[166] R. Niedermann, E. Wyss, S. Annaheim, A. Psikuta, S. Davey, and R. M. Rossi, "Prediction of human core body temperature using non-invasive measurement methods," *International journal of biometeorology,* vol. 58, pp. 7-15, 2014.

[167] C. M. Jacquot, L. Schellen, B. R. Kingma, M. A. van Baak, and W. D. van Marken Lichtenbelt, "Influence of thermophysiology on thermal behavior: the essentials of categorization," *Physiology & behavior,* vol. 128, pp. 180-187, 2014.
[168] H. Chatrath and D. K. Rex, "Potential screening benefit of a colorectal imaging capsule that does not require bowel preparation," *Journal of clinical gastroenterology,* vol. 48, pp. 52-54, 2014.
[169] S. Schostek, M. Zimmermann, J. Keller, M. Fode, M. Melbert, M. O. Schurr*, et al.*, "Telemetric real-time sensor for the detection of acute upper gastrointestinal bleeding," *Biosensors and Bioelectronics,* vol. 78, pp. 524-529, 2016.
[170] P. Valdastri, C. Quaglia, E. Susilo, A. Menciassi, P. Dario, C. Ho*, et al.*, "Wireless therapeutic endoscopic capsule: in vivo experiment," *Endoscopy,* vol. 40, p. 979, 2008.
[171] K.-C. Kong, J. Cha, D. Jeon, and D.-i. D. Cho, "A rotational micro biopsy device for the capsule endoscope," in *Intelligent Robots and Systems, 2005.(IROS 2005). 2005 IEEE/RSJ International Conference on*, 2005, pp. 1839-1843.
[172] K. Kong, S. Yim, S. Choi, and D. Jeon, "A robotic biopsy device for capsule endoscopy," *Journal of Medical Devices,* vol. 6, p. 031004, 2012.
[173] M. Simi, G. Gerboni, A. Menciassi, and P. Valdastri, "Magnetic torsion spring mechanism for a wireless biopsy capsule," *Journal of Medical Devices,* vol. 7, p. 041009, 2013.
[174] S. Yim, E. Gultepe, D. H. Gracias, and M. Sitti, "Biopsy using a magnetic capsule endoscope carrying, releasing, and retrieving untethered microgrippers," *IEEE Transactions on Biomedical Engineering,* vol. 61, pp. 513-521, 2014.
[175] C. Quaglia, S. Tognarelli, E. Sinibaldi, N. Funaro, P. Dario, and A. Menciassi, "Wireless robotic capsule for releasing bioadhesive patches in the gastrointestinal tract," *Journal of Medical Devices,* vol. 8, p. 014503, 2014.
[176] S. P. Woods and T. G. Constandinou, "Wireless capsule endoscope for targeted drug delivery: mechanics and design considerations," *IEEE Transactions on Biomedical Engineering,* vol. 60, pp. 945-953, 2013.
[177] F. Munoz, G. Alici, and W. Li, "A review of drug delivery systems for capsule endoscopy," *Advanced drug delivery reviews,* vol. 71, pp. 77-85, 2014.
[178] G. Tortora, B. Orsini, P. Pecile, A. Menciassi, F. Fusi, and G. Romano, "An ingestible capsule for the photodynamic therapy of helicobacter pylori infection," *IEEE/ASME Transactions on Mechatronics,* vol. 21, pp. 1935-1942, 2016.
[179] P. Saccomandi, E. Schena, C. M. Oddo, L. Zollo, S. Silvestri, and E. Guglielmelli, "Microfabricated tactile sensors for biomedical applications: a review," *Biosensors,* vol. 4, pp. 422-448, 2014.
[180] D. W. Tan, M. A. Schiefer, M. W. Keith, J. R. Anderson, J. Tyler, and D. J. Tyler, "A neural interface provides long-term stable natural touch perception," *Science translational medicine,* vol. 6, pp. 257ra138-257ra138, 2014.
[181] M. Ortiz-Catalan, B. Håkansson, and R. Brånemark, "An osseointegrated human-machine gateway for long-term sensory feedback and motor control of artificial limbs," *Science translational medicine,* vol. 6, pp. 257re6-257re6, 2014.

[182] U. B. Rongala, A. Mazzoni, and C. M. Oddo, "Neuromorphic artificial touch for categorization of naturalistic textures," *IEEE transactions on neural networks and learning systems,* vol. 28, pp. 819-829, 2017.
[183] A. M. Okamura, "Methods for haptic feedback in teleoperated robot-assisted surgery," *Industrial Robot: An International Journal,* vol. 31, pp. 499-508, 2004.
[184] B. Maurin, J. Gangloff, B. Bayle, M. de Mathelin, O. Piccin, P. Zanne*, et al.*, "A parallel robotic system with force sensors for percutaneous procedures under CT-guidance," in *International Conference on Medical Image Computing and Computer-Assisted Intervention*, 2004, pp. 176-183.
[185] F. L. Hammond, R. K. Kramer, Q. Wan, R. D. Howe, and R. J. Wood, "Soft tactile sensor arrays for force feedback in micromanipulation," *IEEE Sensors Journal,* vol. 14, pp. 1443-1452, 2014.
[186] M. S. Arian, C. A. Blaine, G. E. Loeb, and J. A. Fishel, "Using the BioTac as a tumor localization tool," in *Haptics Symposium (HAPTICS), 2014 IEEE*, 2014, pp. 443-448.
[187] Y. Tanaka, T. Nagai, M. Fujiwara, and A. Sano, "Lump detection with tactile sensing system including haptic bidirectionality," in *World Automation Congress (WAC), 2014*, 2014, pp. 77-82.
[188] C. Ledermann, H. Alagi, H. Woern, R. Schirren, and S. Reiser, "Biomimetic tactile sensor based on Fiber Bragg Gratings for tumor detection—Prototype and results," in *Medical Measurements and Applications (MeMeA), 2014 IEEE International Symposium on*, 2014, pp. 1-6.
[189] M. Beccani, C. Di Natali, M. E. Rentschler, and P. Valdastri, "Wireless tissue palpation: Proof of concept for a single degree of freedom," in *Robotics and Automation (ICRA), 2013 IEEE International Conference on*, 2013, pp. 711-717.
[190] S. Schostek, C. N. Ho, D. Kalanovic, and M. O. Schurr, "Artificial tactile sensing in minimally invasive surgery–a new technical approach," *Minimally invasive therapy & allied technologies,* vol. 15, pp. 296-304, 2006.
[191] B. Winstone, C. Melhuish, S. Dogramadzi, T. Pipe, and M. Callaway, "A novel bio-inspired tactile tumour detection concept for capsule endoscopy," in *Conference on Biomimetic and Biohybrid Systems*, 2014, pp. 442-445.
[192] A. Moglia, A. Menciassi, and P. Dario, "Recent patents on wireless capsule endoscopy," *Recent Patents on Biomedical Engineering,* vol. 1, pp. 24-33, 2008.
[193] S. N. Itoua, "Spherical capsule video endoscopy," ed: Google Patents, 2012.
[194] A. W. Mahoney and J. J. Abbott, "Control of magnetically actuated tools in any position using a rotating magnetic source," ed: Google Patents, 2014.
[195] G. J. Tearney, M. G. Lee, S. Bhagatual, R. W. Carruth, and M. Gora, "Apparatus, system and method for providing image-guided in-vivo biopsy with at least one capsule," ed: Google Patents, 2014.
[196] D. K. Iakovidis, R. Sarmiento, J. S. Silva, A. Histace, O. Romain, A. Koulaouzidis*, et al.*, "Towards intelligent capsules for robust wireless endoscopic imaging of the gut," in *IEEE International Conference on Imaging Systems and Techniques*, 2014, pp. 95-100.
[197] A. Tozzi, G. Ciuti, G. Lucarini, M. Mura, C. Quaglia, A. Menciassi*, et al.*, "Supcam european project: Preliminary prototyping and test of a new generation active endoscopic colon capsule," *European: UEG Week,* 2014.

[198] G. Ciuti, R. Caliò, D. Camboni, L. Neri, F. Bianchi, A. Arezzo*, et al.*, "Frontiers of robotic endoscopic capsules: a review," *JMBR,* vol. 11, pp. 1-18, 2016.
[199] L. Liu, S. Towfighian, and A. Hila, "A review of locomotion systems for capsule endoscopy," *IEEE Rev. Biomed. Eng.,* vol. 8, pp. 138-151, 2015.
[200] M. Salerno, G. Ciuti, G. Lucarini, R. Rizzo, P. Valdastri, A. Menciassi*, et al.*, "A discrete-time localization method for capsule endoscopy based on on-board magnetic sensing," *Measurement Science and Technology,* vol. 23, Jan 2012.
[201] H. Mateen, M. R. Basar, A. U. Ahmed, and M. Y. Ahmad, "Localization of Wireless Capsule Endoscope: A Systematic Review," *Ieee Sensors Journal,* vol. 17, pp. 1197-1206, Mar 1 2017.
[202] H. Mateen, M. R. Basar, A. U. Ahmed, and M. Y. Ahmad, "Localization of Wireless Capsule Endoscope: A Systematic Review," *IEEE Sensors J.,* vol. 17, pp. 1197-1206, Mar 1 2017.
[203] L. Beccai, S. Roccella, A. Arena, F. Valvo, P. Valdastri, A. Menciassi*, et al.*, "Design and fabrication of a hybrid silicon three-axial force sensor for biomechanical applications," *Sensors and Actuators a-Physical,* vol. 120, pp. 370-382, May 17 2005.
[204] C. M. Oddo, L. Beccai, G. G. Muscolo, and M. C. Carrozza, "A Biomimetic MEMS-based Tactile Sensor Array with Fingerprints integrated in a Robotic Fingertip for Artificial Roughness Encoding," *Robio 2009,* vol. 1-4, pp. 894-900, 2009.
[205] E. A. M. Heijnsdijk, M. van der Voort, H. de Visser, J. Dankelman, and D. J. Gouma, "Inter- and intraindividual variabilities of perforation forces of human and pig bowel tissue," *SURG ENDOSC,* vol. 17, pp. 1923-1926, 2003.
[206] B. Winstone, C. Melhuish, T. Pipe, M. Callaway, and S. Dogramadzi, "Toward Bio-Inspired Tactile Sensing Capsule Endoscopy for Detection of Submucosal Tumors," *IEEE Sensors Journal,* vol. 17, pp. 848-857, 2017.
[207] A. Facciorusso, M. Antonino, M. Di Maso, M. Barone, and N. Muscatiello, "Non-polypoid colorectal neoplasms: Classification, therapy and follow-up," *World J Gastroenterol,* vol. 21, pp. 5149-57, May 07 2015.
[208] S. Kawano, M. Kojima, Y. Higuchi, M. Sugimoto, K. Ikeda, N. Sakuyama*, et al.*, "Assessment of elasticity of colorectal cancer tissue, clinical utility, pathological and phenotypical relevance," *Cancer Sci,* vol. 106, pp. 1232-9, Sep 2015.
[209] S. Kudo, S. Tamura, T. Nakajima, H. Yamano, H. Kusaka, and H. Watanabe, "Diagnosis of colorectal tumorous lesions by magnifying endoscopy," *Gastrointest Endosc,* vol. 44, pp. 8-14, Jul 1996.
[210] J. East, N. Suzuki, P. Bassett, M. Stavrinidis, H. Thomas, T. Guenther*, et al.*, "Narrow band imaging with magnification for the characterization of small and diminutive colonic polyps: pit pattern and vascular pattern intensity," *Endoscopy,* vol. 40, pp. 811-817, 2008.
[211] J. Tischendorf, H. Wasmuth, A. Koch, H. Hecker, C. Trautwein, and R. Winograd, "Value of magnifying chromoendoscopy and narrow band imaging (NBI) in classifying colorectal polyps: a prospective controlled study," *Endoscopy,* vol. 39, pp. 1092-1096, 2007.
[212] S. Trolier-McKinstry, F. Griggio, C. Yaeger, P. Jousse, D. Zhao, S. S. Bharadwaja*, et al.*, "Designing piezoelectric films for micro electromechanical systems," *IEEE transactions on ultrasonics, ferroelectrics, and frequency control,* vol. 58, 2011.

[213] M. Baumhauer, M. Feuerstein, H. P. Meinzer, and J. Rassweiler, "Navigation in endoscopic soft tissue surgery: Perspectives and limitations," *Journal of Endourology,* vol. 22, pp. 751-766, Apr 2008.

[214] S. Schostek, M. J. Binser, F. Rieber, C. N. Ho, M. O. Schurr, and G. F. Buess, "Artificial tactile feedback can significantly improve tissue examination through remote palpation," *Surgical Endoscopy and Other Interventional Techniques,* vol. 24, pp. 2299-2307, Sep 2010.

[215] V. Sadovnichy, R. Gabidullina, M. Sokolov, V. Galatenko, V. Budanov, and E. Nakashidze, "Haptic device in endoscopy," in *MMVR*, 2014, pp. 365-368.

[216] A. Bicchi, G. Canepa, D. De Rossi, P. Iacconi, and E. P. Scillingo, "A sensor-based minimally invasive surgery tool for detecting tissutal elastic properties (003) 5323219," in *Robotics and Automation, 1996. Proceedings., 1996 IEEE International Conference on*, 1996, pp. 884-888.

[217] P. Puangmali, K. Althoefer, L. D. Seneviratne, D. Murphy, and P. Dasgupta, "State-of-the-art in force and tactile sensing for minimally invasive surgery," *Ieee Sensors Journal,* vol. 8, pp. 371-381, Mar-Apr 2008.

[218] J. Konstantinova, A. Jiang, K. Althoefer, P. Dasgupta, and T. Nanayakkara, "Implementation of tactile sensing for palpation in robot-assisted minimally invasive surgery: A review," *IEEE Sensors Journal,* vol. 14, pp. 2490-2501, 2014.

[219] C. Pacchierotti, D. Prattichizzo, and K. J. Kuchenbecker, "Cutaneous feedback of fingertip deformation and vibration for palpation in robotic surgery," *IEEE Transactions on Biomedical Engineering,* vol. 63, pp. 278-287, 2016.

[220] P. Polygerinos, A. Ataollahi, T. Schaeffter, R. Razavi, L. D. Seneviratne, and K. Althoefer, "MRI-Compatible Intensity-Modulated Force Sensor for Cardiac Catheterization Procedures," *IEEE Transactions on Biomedical Engineering,* vol. 58, pp. 721-726, 2011.

[221] P. Puangmali, H. Liu, L. D. Seneviratne, P. Dasgupta, and K. Althoefer, "Miniature 3-axis distal force sensor for minimally invasive surgical palpation," *IEEE/ASME Transactions On Mechatronics,* vol. 17, pp. 646-656, 2012.

[222] H. Xie, H. Liu, L. D. Seneviratne, and K. Althoefer, "An optical tactile array probe head for tissue palpation during minimally invasive surgery," *IEEE Sensors Journal,* vol. 14, pp. 3283-3291, 2014.

[223] J. C. Gwilliam, Z. Pezzementi, E. Jantho, A. M. Okamura, and S. Hsiao, "Human vs. robotic tactile sensing: Detecting lumps in soft tissue," in *Haptics Symposium, 2010 IEEE*, 2010, pp. 21-28.

[224] B. Ahn, Y. Kim, C. K. Oh, and J. Kim, "Robotic palpation and mechanical property characterization for abnormal tissue localization," *Medical & biological engineering & computing,* vol. 50, pp. 961-971, 2012.

[225] R. Ahmadi, S. Arbatani, M. Packirisamy, and J. Dargahi, "Micro-optical force distribution sensing suitable for lump/artery detection," *Biomedical microdevices,* vol. 17, p. 10, 2015.

[226] X. Jia, R. Li, M. A. Srinivasan, and E. H. Adelson, "Lump detection with a gelsight sensor," in *World Haptics Conference (WHC), 2013*, 2013, pp. 175-179.

[227] E. Heijnsdijk, M. Van Der Voort, H. De Visser, J. Dankelman, and D. Gouma, "Inter-and intraindividual variabilities of perforation forces of human and pig bowel tissue,"

Surgical Endoscopy and other interventional Techniques, vol. 17, pp. 1923-1926, 2003.

[228] C. Chuang, T. Li, I. Chou, and Y. Teng, "Piezoelectric tactile sensor for submucosal tumor hardness detection in endoscopy," in *Solid-State Sensors, Actuators and Microsystems (TRANSDUCERS), 2015 Transducers-2015 18th International Conference on*, 2015, pp. 871-875.

[229] C.-H. Chuang, T.-H. Li, I.-C. Chou, and Y.-J. Teng, "Piezoelectric tactile sensor for submucosal tumor detection in endoscopy," *Sensors and Actuators A: Physical,* vol. 244, pp. 299-309, 2016.

[230] M. Beccani, C. Di Natali, L. J. Sliker, J. A. Schoen, M. E. Rentschler, and P. Valdastri, "Wireless tissue palpation for intraoperative detection of lumps in the soft tissue," *IEEE Transactions on Biomedical Engineering,* vol. 61, pp. 353-361, 2014.

[231] K. A. Nichols and A. M. Okamura, "Methods to segment hard inclusions in soft tissue during autonomous robotic palpation," *IEEE Transactions on Robotics,* vol. 31, pp. 344-354, 2015.

[232] J. C. Hui, A. E. Block, C. J. Taylor, and K. J. Kuchenbecker, "Robust tactile perception of artificial tumors using pairwise comparisons of sensor array readings," in *Haptics Symposium (HAPTICS), 2016 IEEE*, 2016, pp. 305-312.

[233] B. Winstone, G. Griffiths, T. Pipe, C. Melhuish, and J. Rossiter, "TACTIP - Tactile Fingertip Device, Texture Analysis through Optical Tracking of Skin Features," Berlin, Heidelberg, 2013, pp. 323-334.

[234] B. Winstone, T. Pipe, C. Melhuish, S. Dogramadzi, and M. Callaway, "Biomimetic tactile sensing capsule," in *Conference on Biomimetic and Biohybrid Systems*, 2015, pp. 113-122.

[235] R. Caliò, D. Camboni, J. O. Alcaide, C. M. Oddo, M. C. Carrozza, A. Menciassi*, et al.*, "Robotic endoscopic capsule for closed-loop force-based control and safety strategies," in *Cyborg and Bionic Systems (CBS), 2017 IEEE International Conference on*, 2017, pp. 253-256.

[236] P. Valdastri, K. Harada, A. Menciassi, L. Beccai, C. Stefanini, M. Fujie*, et al.*, "Integration of a miniaturised triaxial force sensor in a minimally invasive surgical tool," *IEEE transactions on biomedical engineering,* vol. 53, pp. 2397-2400, 2006.

[237] L. J. Sliker, G. Ciuti, M. E. Rentschler, and A. Menciassi, "Frictional resistance model for tissue-capsule endoscope sliding contact in the gastrointestinal tract," *Tribology International,* vol. 102, pp. 472-484, 2016.

[238] C. M. Oddo, L. Beccai, G. G. Muscolo, and M. C. Carrozza, "A Biomimetic MEMS-based Tactile Sensor Array with Fingerprints integrated in a Robotic Fingertip for Artificial Roughness Encoding," *2009 Ieee International Conference on Robotics and Biomimetics (Robio 2009), Vols 1-4,* pp. 894-900, 2009.

[239] I. D. Johnston, D. K. McCluskey, C. K. L. Tan, and M. C. Tracey, "Mechanical characterization of bulk Sylgard 184 for microfluidics and microengineering," *Journal of Micromechanics and Microengineering,* vol. 24, Mar 2014.

[240] M. Clerc and J. Kennedy, "The particle swarm - Explosion, stability, and convergence in a multidimensional complex space," *Ieee Transactions on Evolutionary Computation,* vol. 6, pp. 58-73, Feb 2002.

[241] F. Sorgini, R. Caliò, M. C. Carrozza, and C. M. Oddo, "Haptic-assistive technologies for audition and vision sensory disabilities," *Disability and Rehabilitation: Assistive Technology,* pp. 1-28, 2017.
[242] K. Ziegler-Graham, E. J. MacKenzie, P. L. Ephraim, T. G. Travison, and R. Brookmeyer, "Estimating the prevalence of limb loss in the United States: 2005 to 2050," *Archives of physical medicine and rehabilitation,* vol. 89, pp. 422-429, 2008.
[243] Z. O. Abu-Faraj, *Handbook of research on biomedical engineering education and advanced bioengineering learning: interdisciplinary concepts: interdisciplinary concepts* vol. 2: IGI Global, 2012.
[244] M. Auer-Grumbach, P. De Jonghe, K. Verhoeven, V. Timmerman, K. Wagner, H.-P. Hartung*, et al.*, "Autosomal dominant inherited neuropathies with prominent sensory loss and mutilations: a review," *Archives of neurology,* vol. 60, pp. 329-334, 2003.
[245] P. Rasmussen, "The congenital insensitivity-to-pain syndrome (analgesia congenita): report of a case," *International journal of paediatric dentistry,* vol. 6, pp. 117-122, 1996.
[246] M. Wickremaratchi and J. Llewelyn, "Effects of ageing on touch," *Postgraduate medical journal,* vol. 82, pp. 301-304, 2006.
[247] G. G. Celesia and G. Hickok, *The human auditory system: fundamental organization and clinical disorders* vol. 129: Elsevier, 2015.
[248] R. F. Canalis and P. R. Lambert, *The ear comprehensive otology*: Lippincott Williams & Wilkins, 2000.
[249] D. T. Hartong, E. L. Berson, and T. P. Dryja, "Retinitis pigmentosa," *The Lancet,* vol. 368, pp. 1795-1809, 2006.
[250] M. Schalock and R. Bull, "The 2014 National child count of children and youth who are deaf-blind," 2015.
[251] J. Robertson and E. Emerson, "Estimating the number of people with co-occurring vision and hearing impairments in the UK," 2010.
[252] K. A. Kaczmarek, "Sensory augmentation and substitution," *CRC handbook of biomedical engineering,* pp. 2100-2109, 1995.
[253] J. M. Allen, P. K. Asselin, and R. Foulds, "American Sign Language finger spelling recognition system," in *Bioengineering Conference, 2003 IEEE 29th Annual, Proceedings of*, 2003, pp. 285-286.
[254] J. G. Kyle and B. Woll, *Sign language: The study of deaf people and their language*: Cambridge University Press, 1988.
[255] S. Wall and S. Brewster, "Feeling what you hear: tactile feedback for navigation of audio graphs," in *Proceedings of the SIGCHI conference on Human Factors in computing systems*, 2006, pp. 1123-1132.
[256] C. Moore and I. Murray, "An electronic design of a low cost braille typewriter," in *Intelligent Information Systems Conference, The Seventh Australian and New Zealand 2001*, 2001, pp. 153-157.
[257] C. M. Reed, W. M. Rabinowitz, N. I. Durlach, L. D. Braida, S. Conway-Fithian, and M. C. Schultz, "Research on the Tadoma method of speech communication," *The Journal of the Acoustical society of America,* vol. 77, pp. 247-257, 1985.

[258] U. Gollner, T. Bieling, and G. Joost, "Mobile Lorm Glove: introducing a communication device for deaf-blind people," in *Proceedings of the sixth international conference on tangible, embedded and embodied interaction*, 2012, pp. 127-130.
[259] N. Caporusso, "A wearable Malossi alphabet interface for deafblind people," in *Proceedings of the working conference on Advanced visual interfaces*, 2008, pp. 445-448.
[260] M. Miyagi, M. Nishida, Y. Horiuchi, and A. Ichikawa, "Analysis of prosody in finger braille using electromyography," in *Engineering in Medicine and Biology Society, 2006. EMBS'06. 28th Annual International Conference of the IEEE*, 2006, pp. 4901-4904.
[261] Y. Matsuda and T. Isomura, "Finger Braille recognition system," in *Advances in Character Recognition*, ed: InTech, 2012.
[262] L. A. Jones and N. B. Sarter, "Tactile displays: Guidance for their design and application," *Human factors,* vol. 50, pp. 90-111, 2008.
[263] S. Brewster and L. M. Brown, "Tactons: structured tactile messages for non-visual information display," in *Proceedings of the fifth conference on Australasian user interface-Volume 28*, 2004, pp. 15-23.
[264] K. Pisanski, V. Cartei, C. McGettigan, J. Raine, and D. Reby, "Voice modulation: a window into the origins of human vocal control?," *Trends in cognitive sciences,* vol. 20, pp. 304-318, 2016.
[265] F. A. Geldard, "Adventures in tactile literacy," *American Psychologist,* vol. 12, p. 115, 1957.
[266] G. M. O'donoghue, T. P. Nikolopoulos, and S. M. Archbold, "Determinants of speech perception in children after cochlear implantation," *The Lancet,* vol. 356, pp. 466-468, 2000.
[267] S. Engelmann and R. Rosov, "Tactual hearing experiment with deaf and hearing subjects," *Exceptional Children,* vol. 41, pp. 243-253, 1975.
[268] K. Rakowski, C. Brenner, and J. M. Weisenberger, "Evaluation of a 32-channel electrotactile vocoder," *The Journal of the Acoustical Society of America,* vol. 86, pp. S83-S83, 1989.
[269] C. E. Sherrick, "Basic and applied research on tactile aids for deaf people: Progress and prospects," *The Journal of the Acoustical Society of America,* vol. 75, pp. 1325-1342, 1984.
[270] R. H. Gault and G. W. Crane, "Tactual patterns from certain vowel qualities instrumentally communicated from a speaker to a subject's fingers," *The Journal of General Psychology,* vol. 1, pp. 353-359, 1928.
[271] R. Guelke and R. Huyssen, "Development of apparatus for the analysis of sound by the sense of touch," *The Journal of the Acoustical Society of America,* vol. 31, pp. 799-809, 1959.
[272] M. Kringlebotn, "Experiments with some visual and vibrotactile aids for the deaf," *American annals of the deaf,* pp. 311-317, 1968.
[273] J. Pickett and B. H. Pickett, "Communication of speech sounds by a tactual vocoder," *Journal of Speech, Language, and Hearing Research,* vol. 6, pp. 207-222, 1963.
[274] R. H. Gault, "Touch as a substitute for hearing in the interpretation and control of speech," *Archives of Otolaryngology,* vol. 3, pp. 121-135, 1926.

[275] K. Schulte, "Fonator system: Speech stimulation and speech feed-back by technically amplified one-channel vibrations," in *International Symposium on Speech Communication Ability and Profound Deafness. Washington, DC: AG Bell Association for the Deaf, Paper*, 1972.
[276] T. R. Willemain and F. F. Lee, "Tactile pitch feedback for deaf speakers," *The Volta Review,* 1971.
[277] W. D. Stratton, "Intonation feedback for the deaf through a tactile display," *The Volta Review,* 1974.
[278] P. Brooks and B. J. Frost, "Evaluation of a tactile vocoder for word recognition," *The Journal of the Acoustical Society of America,* vol. 74, pp. 34-39, 1983.
[279] G. H. Yeni-Komshian and M. H. Goldstein Jr, "Identification of speech sounds displayed on a vibrotactile vocoder," *The Journal of the Acoustical Society of America,* vol. 62, pp. 194-198, 1977.
[280] D. W. Sparks, P. K. Kuhl, A. E. Edmonds, and G. P. Gray, "Investigating the MESA (Multipoint Electrotactile Speech Aid): The transmission of segmental features of speech," *The Journal of the Acoustical Society of America,* vol. 63, pp. 246-257, 1978.
[281] M. H. Goldstein Jr and A. Proctor, "Tactile aids for profoundly deaf children," *The Journal of the Acoustical Society of America,* vol. 77, pp. 258-265, 1985.
[282] K. L. Galvin, G. Mavrias, A. Moore, R. S. Cowan, P. J. Blamey, and G. M. Clark, "A comparison of tactaid ii and tactaid 7 use by adults with a profound hearing impairment," *Ear and hearing,* vol. 20, pp. 471-482, 1999.
[283] A. Risberg, "A critical review of work on speech analyzing hearing aids," *IEEE Transactions on Audio and Electroacoustics,* vol. 17, pp. 290-297, 1969.
[284] E. Biondi and L. Biondi, "The sampling of sounds as a new means of making speech intelligible to the profoundly deaf," *Alta. Frequenza,* vol. 37, pp. 180-191, 1968.
[285] B. Johansson, "A new coding amplifier system for the severely hard of hearing," in *Proc. 3rd ICA*, 1961, pp. 655-657.
[286] A. Risberg and K. Spens, "Teaching machine for training experiments in speech perception," *Speech Technol. Lab. Quart. Report,* vol. 2, p. 72, 1967.
[287] N. Guttman and J. R. Nelson, "An instrument that creates some artificial speech spectra for the severely hard of hearing," *American annals of the deaf,* pp. 295-302, 1968.
[288] D. Ling and W. S. Druz, "Transposition of high frequency sounds by partial vocoding of the speech spectrum: Its use by deaf children," *J Aud Res,* vol. 7, p. 133Á144, 1967.
[289] L. Pimonow, "La parole synthétique et son application dans la correction auditive," in *Annales des Télécommunications*, 1965, pp. 151-171.
[290] K. Spens, C. Huss, M. Dahlqvist, and E. Agelfors, "A hand held two-channel vibro-tactile speech communication aid for the deaf: characteristics and results," *Scandinavian audiology. Supplementum,* vol. 47, pp. 7-13, 1997.
[291] A. Mazzoni and N. Bryan-Kinns, "Mood glove: A haptic wearable prototype system to enhance mood music in film," *Entertainment Computing,* vol. 17, pp. 9-17, 2016.
[292] A. Boothroyd, "Wearable tactile sensory aid providing information on voice pitch and intonation patterns," ed: Google Patents, 1986.
[293] A. Boothroyd, "A wearable tactile intonation display for the deaf," *IEEE transactions on acoustics, speech, and signal processing,* vol. 33, pp. 111-117, 1985.

[294] G. A. Gescheider, "Cutaneous sound localization," *Journal of Experimental Psychology,* vol. 70, p. 617, 1965.
[295] G. A. Gescheider, "Some comparisons between touch and hearing," *IEEE Transactions on Man-Machine Systems,* vol. 11, pp. 28-35, 1970.
[296] G. v. Békésy, "Human skin perception of traveling waves similar to those on the cochlea," *The Journal of the Acoustical Society of America,* vol. 27, pp. 830-841, 1955.
[297] B. Richardson, D. Wuillemin, and F. Saunders, "Tactile discrimination of competing sounds," *Perception & psychophysics,* vol. 24, pp. 546-550, 1978.
[298] A. Baijal, J. Kim, C. Branje, F. Russo, and D. I. Fels, "Composing vibrotactile music: A multi-sensory experience with the emoti-chair," in *Haptics Symposium (HAPTICS), 2012 IEEE*, 2012, pp. 509-515.
[299] C. Wada, S. Ino, and T. Ifukube, "Proposal and evaluation of the sweeping display of speech spectrum for a tactile vocoder used by the profoundly hearing impaired," *Electronics and Communications in Japan (Part III: Fundamental Electronic Science),* vol. 79, pp. 56-66, 1996.
[300] K. O. Johnson and J. R. Phillips, "Tactile spatial resolution. I. Two-point discrimination, gap detection, grating resolution, and letter recognition," *Journal of neurophysiology,* vol. 46, pp. 1177-1192, 1981.
[301] M. Sakajiri, S. Miyoshi, K. Nakamura, S. Fukushima, and T. Ifukube, "Voice pitch control using tactile feedback for the deafblind or the hearing impaired persons to assist their singing," in *Systems Man and Cybernetics (SMC), 2010 IEEE International Conference on*, 2010, pp. 1483-1487.
[302] M. Sakajiri, S. Miyoshi, J. Onishi, T. Ono, and T. Ifukube, "Tactile pitch feedback system for deafblind or hearing impaired persons singing accuracy of hearing persons under conditions of added noise," in *Computational Intelligence in Robotic Rehabilitation and Assistive Technologies (CIR2AT), 2014 IEEE Symposium on*, 2014, pp. 31-35.
[303] M. Sakajiri, K. Nakamura, S. Fukushima, S. Miyoshi, and T. Ifukube, "Effect of voice pitch control training using a two-dimensional tactile feedback display system," in *Systems, Man, and Cybernetics (SMC), 2012 IEEE International Conference on*, 2012, pp. 2943-2947.
[304] M. Sakajiri, S. Miyoshi, K. Nakamura, S. Fukushima, and T. Ifukube, "Voice pitch control ability of hearing persons with or without tactile feedback using a two-dimensional tactile display system," in *Systems, Man, and Cybernetics (SMC), 2011 IEEE International Conference on*, 2011, pp. 1069-1073.
[305] S. Nanayakkara, L. Wyse, and E. A. Taylor, "The haptic chair as a speech training aid for the deaf," in *Proceedings of the 24th Australian Computer-Human Interaction Conference*, 2012, pp. 405-410.
[306] S. Nanayakkara, L. Wyse, and E. A. Taylor, "Effectiveness of the haptic chair in speech training," in *Proceedings of the 14th international ACM SIGACCESS conference on Computers and accessibility*, 2012, pp. 235-236.
[307] M. Karam, G. Nespoli, F. Russo, and D. I. Fels, "Modelling perceptual elements of music in a vibrotactile display for deaf users: A field study," in *Advances in Computer-Human Interactions, 2009. ACHI'09. Second International Conferences on*, 2009, pp. 249-254.

[308] M. P. Saba, D. Filippo, F. R. Pereira, and P. L. P. De Souza, "Hey yaa: A haptic warning wearable to support deaf people communication," in *International Conference on Collaboration and Technology*, 2011, pp. 215-223.
[309] J. Harkins, P. E. Tucker, N. Williams, and J. Sauro, "Vibration signaling in mobile devices for emergency alerting: A study with deaf evaluators," *Journal of deaf studies and deaf education,* vol. 15, pp. 438-445, 2010.
[310] J. S. Kim and C. H. Kim, "A review of assistive listening device and digital wireless technology for hearing instruments," *Korean journal of audiology,* vol. 18, p. 105, 2014.
[311] R. I. Damper and M. D. Evans, "A multifunction domestic alert system for the deaf-blind," *IEEE Transactions on Rehabilitation Engineering,* vol. 3, pp. 354-359, 1995.
[312] H. Yuan, C. M. Reed, and N. I. Durlach, "Tactual display of consonant voicing as a supplement to lipreading," *The Journal of the Acoustical society of America,* vol. 118, pp. 1003-1015, 2005.
[313] Y. Wang and K. J. Kuchenbecker, "HALO: Haptic alerts for low-hanging obstacles in white cane navigation," in *Haptics Symposium (HAPTICS), 2012 IEEE*, 2012, pp. 527-532.
[314] D. Dakopoulos and N. G. Bourbakis, "Wearable obstacle avoidance electronic travel aids for blind: a survey," *IEEE Transactions on Systems, Man, and Cybernetics, Part C (Applications and Reviews),* vol. 40, pp. 25-35, 2010.
[315] S. Ram and J. Sharf, "The people sensor: a mobility aid for the visually impaired," in *Wearable Computers, 1998. Digest of Papers. Second International Symposium on*, 1998, pp. 166-167.
[316] S. Kammoun, C. Jouffrais, T. Guerreiro, H. Nicolau, and J. Jorge, "Guiding blind people with haptic feedback," *Frontiers in Accessibility for Pervasive Computing (Pervasive 2012),* vol. 3, 2012.
[317] S. Mann, J. Huang, R. Janzen, R. Lo, V. Rampersad, A. Chen*, et al.*, "Blind navigation with a wearable range camera and vibrotactile helmet," in *Proceedings of the 19th ACM international conference on Multimedia*, 2011, pp. 1325-1328.
[318] D. Dakopoulos, S. K. Boddhu, and N. Bourbakis, "A 2D vibration array as an assistive device for visually impaired," in *Bioinformatics and Bioengineering, 2007. BIBE 2007. Proceedings of the 7th IEEE International Conference on*, 2007, pp. 930-937.
[319] M. Adjouadi, "A man-machine vision interface for sensing the environment," *Journal of rehabilitation research and development,* vol. 29, pp. 57-76, 1992.
[320] K. A. Kaczmarek, J. G. Webster, P. Bach-y-Rita, and W. J. Tompkins, "Electrotactile and vibrotactile displays for sensory substitution systems," *IEEE Transactions on Biomedical Engineering,* vol. 38, pp. 1-16, 1991.
[321] S. Akhter, J. Mirsalahuddin, F. Marquina, S. Islam, and S. Sareen, "A Smartphone-based Haptic Vision Substitution system for the blind," in *Bioengineering Conference (NEBEC), 2011 IEEE 37th Annual Northeast*, 2011, pp. 1-2.
[322] F. Gemperle, N. Ota, and D. Siewiorek, "Design of a wearable tactile display," in *Wearable Computers, 2001. Proceedings. Fifth International Symposium on*, 2001, pp. 5-12.
[323] L. A. Jones, B. Lockyer, and E. Piateski, "Tactile display and vibrotactile pattern recognition on the torso," *Advanced Robotics,* vol. 20, pp. 1359-1374, 2006.

[324] H. Van Veen and J. B. Van Erp, "Providing directional information with tactile torso displays," in *Proceedings of EuroHaptics*, 2003, pp. 471-474.
[325] T. McDaniel, S. Krishna, V. Balasubramanian, D. Colbry, and S. Panchanathan, "Using a haptic belt to convey non-verbal communication cues during social interactions to individuals who are blind," in *Haptic Audio visual Environments and Games, 2008. HAVE 2008. IEEE International Workshop on*, 2008, pp. 13-18.
[326] J. B. Van Erp, H. A. Van Veen, C. Jansen, and T. Dobbins, "Waypoint navigation with a vibrotactile waist belt," *ACM Transactions on Applied Perception (TAP),* vol. 2, pp. 106-117, 2005.
[327] C. Rose, D. Pierce, and A. Sherman, "Interactive Navigation System for the Visually Impaired with Auditory and Haptic Cues in Crosswalks, Indoors and Urban Areas," in *International Conference on Human-Computer Interaction*, 2015, pp. 539-545.
[328] G. Flores, S. Kurniawan, R. Manduchi, E. Martinson, L. M. Morales, and E. A. Sisbot, "Vibrotactile guidance for wayfinding of blind walkers," *IEEE transactions on haptics,* vol. 8, pp. 306-317, 2015.
[329] S. Gilson, S. Gohil, F. Khan, and V. Nagaonkar, "A Wireless Navigation System For the Visually Impaired," 2015.
[330] K. Tsukada and M. Yasumura, "Activebelt: Belt-type wearable tactile display for directional navigation," in *International Conference on Ubiquitous Computing*, 2004, pp. 384-399.
[331] S. K. Nagel, C. Carl, T. Kringe, R. Märtin, and P. König, "Beyond sensory substitution—learning the sixth sense," *Journal of neural engineering,* vol. 2, p. R13, 2005.
[332] J. Wu, Z. Song, W. Wu, A. Song, and D. Constantinescu, "A vibro-tactile system for image contour display," in *VR Innovation (ISVRI), 2011 IEEE International Symposium on*, 2011, pp. 145-150.
[333] L. A. Johnson and C. M. Higgins, "A navigation aid for the blind using tactile-visual sensory substitution," in *Engineering in Medicine and Biology Society, 2006. EMBS'06. 28th Annual International Conference of the IEEE*, 2006, pp. 6289-6292.
[334] R. Velázquez, O. Bazán, C. Alonso, and C. Delgado-Mata, "Vibrating insoles for tactile communication with the feet," in *Advanced Robotics (ICAR), 2011 15th International Conference on*, 2011, pp. 118-123.
[335] R. Velãzquez, O. Bazán, and M. Magaña, "A shoe-integrated tactile display for directional navigation," in *Intelligent Robots and Systems, 2009. IROS 2009. IEEE/RSJ International Conference on*, 2009, pp. 1235-1240.
[336] R. Velázquez and O. Bazán, "Preliminary evaluation of podotactile feedback in sighted and blind users," in *Engineering in Medicine and Biology Society (EMBC), 2010 Annual International Conference of the IEEE*, 2010, pp. 2103-2106.
[337] J. Zhang, C. W. Lip, S.-K. Ong, and A. Y. Nee, "A multiple sensor-based shoe-mounted user interface designed for navigation systems for the visually impaired," in *Wireless Internet Conference (WICON), 2010 The 5th Annual ICST*, 2010, pp. 1-8.
[338] Z. O. Abu-Faraj, E. Jabbour, P. Ibrahim, and A. Ghaoui, "Design and development of a prototype rehabilitative shoes and spectacles for the blind," in *Biomedical Engineering and Informatics (BMEI), 2012 5th International Conference on*, 2012, pp. 795-799.

[339] L. Lobo, D. Travieso, A. Barrientos, and D. M. Jacobs, "Stepping on obstacles with a sensory substitution device on the lower leg: practice without vision is more beneficial than practice with vision," *PloS one,* vol. 9, p. e98801, 2014.

[340] G. Ghiani, B. Leporini, and F. Paternò, "Vibrotactile feedback as an orientation aid for blind users of mobile guides," in *Proceedings of the 10th international conference on Human computer interaction with mobile devices and services*, 2008, pp. 431-434.

[341] Y. Kim, M. Harders, and R. Gassert, "Identification of vibrotactile patterns encoding obstacle distance information," *IEEE transactions on haptics,* vol. 8, pp. 298-305, 2015.

[342] S. Gallo, D. Chapuis, L. Santos-Carreras, Y. Kim, P. Retornaz, H. Bleuler*, et al.*, "Augmented white cane with multimodal haptic feedback," in *Biomedical Robotics and Biomechatronics (BioRob), 2010 3rd IEEE RAS and EMBS International Conference on*, 2010, pp. 149-155.

[343] L. Fanucci, R. Roncella, F. Iacopetti, M. Donati, A. Calabro, B. Leporini*, et al.*, "Improving mobility of pedestrian visually-impaired users," *Assistive Technol. Res. Ser,* vol. 29, pp. 595-603, 2011.

[344] L. Scalise, V. M. Primiani, D. Shahu, A. De Leo, P. Russo, V. Di Mattia*, et al.*, "Electromagnetic aids for visually impaired users," *ICEmB II Convegno Nazionale,"Interazioni fra campi elettromagnetici e biosistemi," Bologna,* 2012.

[345] D. J. Calder, "Ecological solutions for the blind," in *Digital Ecosystems and Technologies (DEST), 2010 4th IEEE International Conference on*, 2010, pp. 625-630.

[346] T. Amemiya and H. Sugiyama, "Design of a haptic direction indicator for visually impaired people in emergency situations," in *International Conference on Computers for Handicapped Persons*, 2008, pp. 1141-1144.

[347] L. Ortigoza-Ayala, L. Ruiz-Huerta, A. Caballero-Ruiz, and E. Kussul, "Artificial vision for the human blind," *Revista medica del Instituto Mexicano del Seguro Social,* vol. 47, pp. 393-398, 2009.

[348] L. Ortigoza-Ayala, L. Ruiz-Huerta, A. Caballero-Ruiz, and E. Kussul, "Prótesis de substitución sensorial visual para pacientes ciegos," *Rev Mex Oftalmol,* vol. 83, pp. 235-238, 2009.

[349] J. Zelek, R. Audette, J. Balthazaar, and C. Dunk, "A stereo-vision system for the visually impaired," *University of Guelph,* vol. 1999, 1999.

[350] J. Oliveira, T. Guerreiro, H. Nicolau, J. Jorge, and D. Gonçalves, "BrailleType: unleashing braille over touch screen mobile phones," in *IFIP Conference on Human-Computer Interaction*, 2011, pp. 100-107.

[351] S. Azenkot and E. Fortuna, "Improving public transit usability for blind and deaf-blind people by connecting a braille display to a smartphone," in *Proceedings of the 12th international ACM SIGACCESS conference on Computers and accessibility*, 2010, pp. 317-318.

[352] M. Nakamura and L. Jones, "An actuator for the tactile vest-a torso-based haptic device," in *Haptic Interfaces for Virtual Environment and Teleoperator Systems, 2003. HAPTICS 2003. Proceedings. 11th Symposium on*, 2003, pp. 333-339.

[353] L. A. Jones, M. Nakamura, and B. Lockyer, "Development of a tactile vest," in *Haptic Interfaces for Virtual Environment and Teleoperator Systems, 2004. HAPTICS'04. Proceedings. 12th International Symposium on*, 2004, pp. 82-89.

[354] R. Velazquez, E. Fontaine, and E. Pissaloux, "Coding the environment in tactile maps for real-time guidance of the visually impaired," in *Micro-NanoMechatronics and Human Science, 2006 International Symposium on*, 2006, pp. 1-6.

[355] P. Arcara, L. Di Stefano, S. Mattoccia, C. Melchiorri, and G. Vassura, "Perception of depth information by means of a wire-actuated haptic interface," in *Robotics and Automation, 2000. Proceedings. ICRA'00. IEEE International Conference on*, 2000, pp. 3443-3448.

[356] J. Akita, T. Komatsu, K. Ito, T. Ono, and M. Okamoto, "CyARM: Haptic sensing device for spatial localization on basis of exploration by arms," *Advances in Human-Computer Interaction,* vol. 2009, p. 6, 2009.

[357] D. Yuan and R. Manduchi, "A tool for range sensing and environment discovery for the blind," in *Computer Vision and Pattern Recognition Workshop, 2004. CVPRW'04. Conference on*, 2004, pp. 39-39.

[358] C. H. Park, E.-S. Ryu, and A. M. Howard, "Telerobotic haptic exploration in art galleries and museums for individuals with visual impairments," *IEEE transactions on Haptics,* vol. 8, pp. 327-338, 2015.

[359] C. Loscos, F. Tecchia, A. Frisoli, M. Carrozzino, H. R. Widenfeld, D. Swapp*, et al.*, "The Museum of Pure Form: touching real statues in an immersive virtual museum," in *VAST*, 2004, pp. 271-279.

[360] A. Russomanno, S. O'Modhrain, R. B. Gillespie, and M. W. Rodger, "Refreshing refreshable braille displays," *IEEE transactions on haptics,* vol. 8, pp. 287-297, 2015.

[361] P. Bach-y-Rita, "Neurophysiological basis of a tactile vision-substitution system," *IEEE Transactions on Man-Machine Systems,* vol. 11, pp. 108-110, 1970.

[362] P. Bach-y-Rita, C. C. Collins, F. A. Saunders, B. White, and L. Scadden, "Vision substitution by tactile image projection," *Nature,* vol. 221, p. 963, 1969.

[363] P. Bach-y-Rita, M. E. Tyler, and K. A. Kaczmarek, "Seeing with the brain," *International journal of human-computer interaction,* vol. 15, pp. 285-295, 2003.

[364] E. P. Gardner and C. I. Palmer, "Simulation of motion on the skin. I. Receptive fields and temporal frequency coding by cutaneous mechanoreceptors of OPTACON pulses delivered to the hand," *Journal of Neurophysiology,* vol. 62, pp. 1410-1436, 1989.

[365] L. H. Goldish and H. E. Taylor, "The Optacon: A Valuable Device for Blind Persons," *New Outlook for the Blind,* vol. 68, pp. 49-56, 1974.

[366] P. Smithmaitrie, J. Kanjantoe, and P. Tandayya, "Touching force response of the piezoelectric Braille cell," *Disability and Rehabilitation: Assistive Technology,* vol. 3, pp. 360-365, 2008.

[367] V. Lévesque, J. Pasquero, V. Hayward, and M. Legault, "Display of virtual braille dots by lateral skin deformation: feasibility study," *ACM Transactions on Applied Perception (TAP),* vol. 2, pp. 132-149, 2005.

[368] V. Hayward and M. Cruz-Hernandez, "Tactile display device using distributed lateral skin stretch," in *Proceedings of the haptic interfaces for virtual environment and teleoperator systems symposium*, 2000, pp. 1309-1314.

[369] V. Hayward, A. V. Terekhov, S.-C. Wong, P. Geborek, F. Bengtsson, and H. Jörntell, "Spatio-temporal skin strain distributions evoke low variability spike responses in cuneate neurons," *Journal of the Royal Society Interface,* vol. 11, p. 20131015, 2014.

[370] H. Jörntell, F. Bengtsson, P. Geborek, A. Spanne, A. V. Terekhov, and V. Hayward, "Segregation of tactile input features in neurons of the cuneate nucleus," *Neuron,* vol. 83, pp. 1444-1452, 2014.

[371] J. Pasquero and V. Hayward, "STReSS: A practical tactile display system with one millimeter spatial resolution and 700 Hz refresh rate," in *Proc. Eurohaptics*, 2003, pp. 94-110.

[372] J. C. Bliss, M. H. Katcher, C. H. Rogers, and R. P. Shepard, "Optical-to-tactile image conversion for the blind," *IEEE Transactions on Man-Machine Systems,* vol. 11, pp. 58-65, 1970.

[373] M. Kobayashi and T. Watanabe, "A tactile display system equipped with a pointing device—MIMIZU," in *International Conference on Computers for Handicapped Persons*, 2002, pp. 527-534.

[374] T. Homma, S. Ino, H. Kuroki, T. Izumi, and T. Ifukube, "Development of a piezoelectric actuator for presentation of various tactile stimulation patterns to fingerpad skin," in *Engineering in Medicine and Biology Society, 2004. IEMBS'04. 26th Annual International Conference of the IEEE*, 2004, pp. 4960-4963.

[375] V. G. Chouvardas, A. N. Miliou, and M. K. Hatalis, "Tactile display applications: A state of the art survey," in *Proceedings of the 2nd Balkan Conference in Informatics*, 2005, pp. 290-303.

[376] S. O'Modhrain, N. A. Giudice, J. A. Gardner, and G. E. Legge, "Designing media for visually-impaired users of refreshable touch displays: Possibilities and pitfalls," *IEEE transactions on haptics,* vol. 8, pp. 248-257, 2015.

[377] I. M. Koo, K. Jung, J. C. Koo, J.-D. Nam, Y. K. Lee, and H. R. Choi, "Development of soft-actuator-based wearable tactile display," *IEEE Transactions on Robotics,* vol. 24, pp. 549-558, 2008.

[378] Y. Haga, W. Makishi, K. Iwami, K. Totsu, K. Nakamura, and M. Esashi, "Dynamic Braille display using SMA coil actuator and magnetic latch," *Sensors and Actuators A: Physical,* vol. 119, pp. 316-322, 2005.

[379] L. Yobas, D. M. Durand, G. G. Skebe, F. J. Lisy, and M. A. Huff, "A novel integrable microvalve for refreshable Braille display system," *Journal of microelectromechanical systems,* vol. 12, pp. 252-263, 2003.

[380] J. S. Lee and S. Lucyszyn, "A micromachined refreshable Braille cell," *Journal of Microelectromechanical Systems,* vol. 14, pp. 673-682, 2005.

[381] J. C. da Cunha, L. A. Bordignon, and P. Nohama, "Tactile communication using a CO 2 flux stimulation for blind or deafblind people," in *Engineering in Medicine and Biology Society (EMBC), 2010 Annual International Conference of the IEEE*, 2010, pp. 5871-5874.

[382] J. Cunha and P. Nohama, "A Novel Instrumentation to Investigate the Alternative Tactile Communication through Mechanical Stimulation Using CO 2 Jets," in *VI Latin American Congress on Biomedical Engineering CLAIB 2014, Paraná, Argentina 29, 30 & 31 October 2014*, 2015, pp. 35-38.

[383] Y. Visell, "Tactile sensory substitution: Models for enaction in HCI," *Interacting with Computers,* vol. 21, pp. 38-53, 2008.

[384] C. Garland, "Sensory devices for the blind," *Journal of medical engineering & technology,* vol. 1, pp. 319-323, 1977.

[385] H. Minagawa, N. Ohnishi, and N. Sugie, "Tactile-audio diagram for blind persons," *IEEE Transactions on Rehabilitation Engineering,* vol. 4, pp. 431-437, 1996.
[386] B. Plimmer, P. Reid, R. Blagojevic, A. Crossan, and S. Brewster, "Signing on the tactile line: A multimodal system for teaching handwriting to blind children," *ACM Transactions on Computer-Human Interaction (TOCHI),* vol. 18, p. 17, 2011.
[387] D. W. Schloerb, O. Lahav, J. G. Desloge, and M. A. Srinivasan, "BlindAid: Virtual environment system for self-reliant trip planning and orientation and mobility training," in *Haptics Symposium, 2010 IEEE*, 2010, pp. 363-370.
[388] K. A. Johnsor and S. K. Semwal, "Shapes: A multi-sensory environment for the B/VI and hearing impaired community," in *Virtual and Augmented Assistive Technology (VAAT), 2014 2nd Workshop on*, 2014, pp. 1-6.
[389] H. N. Schwerdt, J. Tapson, and R. Etienne-Cummings, "A color detection glove with haptic feedback for the visually disabled," in *Information Sciences and Systems, 2009. CISS 2009. 43rd Annual Conference on*, 2009, pp. 681-686.
[390] L. Cappelletti, M. Ferri, and G. Nicoletti, "Vibrotactile color rendering for the visually impaired within the VIDET project," in *Telemanipulator and Telepresence Technologies V*, 1998, pp. 92-97.
[391] C. C. Collins, "Tactile television-mechanical and electrical image projection," *IEEE Transactions on man-machine systems,* vol. 11, pp. 65-71, 1970.
[392] D. Klein, D. Rensink, H. Freimuth, G. Monkman, S. Egersdörfer, H. Böse*, et al.*, "Modelling the response of a tactile array using electrorheological fluids," *Journal of Physics D: Applied Physics,* vol. 37, p. 794, 2004.
[393] V. G. Chouvardas, A. N. Miliou, and M. K. Hatalis, "Tactile displays: Overview and recent advances," *Displays,* vol. 29, pp. 185-194, 2008.
[394] C. Xu, A. Israr, I. Poupyrev, O. Bau, and C. Harrison, "Tactile display for the visually impaired using TeslaTouch," in *CHI'11 Extended Abstracts on Human Factors in Computing Systems*, 2011, pp. 317-322.
[395] B. Schmitz and T. Ertl, "Making digital maps accessible using vibrations," in *International Conference on Computers for Handicapped Persons*, 2010, pp. 100-107.
[396] C. Shah, M. Bouzit, M. Youssef, and L. Vasquez, "Evaluation of RU-netra-tactile feedback navigation system for the visually impaired," in *Virtual Rehabilitation, 2006 International Workshop on*, 2006, pp. 72-77.
[397] M. Bouzit, A. Chaibi, K. De Laurentis, and C. Mavroidis, "Tactile feedback navigation handle for the visually impaired," in *ASME 2004 International Mechanical Engineering Congress and Exposition*, 2004, pp. 1171-1177.
[398] C. Vincent, F. Routhier, V. Martel, M.-E. Mottard, F. Dumont, L. Côté*, et al.*, "Field testing of two electronic mobility aid devices for persons who are deaf-blind," *Disability and Rehabilitation: Assistive Technology,* vol. 9, pp. 414-420, 2014.
[399] M. Hersh and M. A. Johnson, *Assistive technology for visually impaired and blind people*: Springer Science & Business Media, 2010.
[400] M. L. Max and J. R. Gonzalez, "Blind persons navigate in virtual reality (VR); hearing and feeling communicates" reality"," *Studies in health technology and informatics,* vol. 39, pp. 54-59, 1997.

[401] M. Ogrinc, I. Farkhatdinov, R. Walker, and E. Burdet, "Deaf-blind can practise horse riding with the help of haptics," in *International Conference on Human Haptic Sensing and Touch Enabled Computer Applications*, 2016, pp. 452-461.
[402] S. Cardin, D. Thalmann, and F. Vexo, "A wearable system for mobility improvement of visually impaired people," *The Visual Computer,* vol. 23, pp. 109-118, 2007.
[403] A. J. Spiers and A. M. Dollar, "Design and evaluation of shape-changing haptic interfaces for pedestrian navigation assistance," *IEEE transactions on haptics,* vol. 10, pp. 17-28, 2017.
[404] T. Amemiya, J. Yamashita, K. Hirota, and M. Hirose, "Virtual leading blocks for the deaf-blind: A real-time way-finder by verbal-nonverbal hybrid interface and high-density RFID tag space," in *Virtual Reality, 2004. Proceedings. IEEE*, 2004, pp. 165-287.
[405] M. Hirose and T. Amemiya, "Wearable finger-braille interface for navigation of deaf-blind in ubiquitous barrier-free space," in *Proceedings of the HCI International*, 2003, pp. 1417-1421.
[406] D. A. Ross and B. B. Blasch, "Wearable interfaces for orientation and wayfinding," in *Proceedings of the fourth international ACM conference on Assistive technologies*, 2000, pp. 193-200.
[407] K. Murphy and M. Darrah, "Haptics-based apps for middle school students with visual impairments," *IEEE transactions on haptics,* vol. 8, pp. 318-326, 2015.
[408] L. O. Russo, G. A. Farulla, D. Pianu, A. R. Salgarella, M. Controzzi, C. Cipriani*, et al.*, "PARLOMA–a novel human-robot interaction system for deaf-blind remote communication," *International Journal of Advanced Robotic Systems,* vol. 12, p. 57, 2015.
[409] G. A. Farulla, L. O. Russo, C. Pintor, D. Pianu, G. Micotti, A. R. Salgarella*, et al.*, "Real-time single camera hand gesture recognition system for remote deaf-blind communication," in *International Conference on Augmented and Virtual Reality*, 2014, pp. 35-52.
[410] R. Sarkar, S. Das, and D. Rudrapal, "A low cost microelectromechanical Braille for blind people to communicate with blind or deaf blind people through SMS subsystem," in *Advance Computing Conference (IACC), 2013 IEEE 3rd International*, 2013, pp. 1529-1532.
[411] C. Jayant, C. Acuario, W. Johnson, J. Hollier, and R. Ladner, "V-braille: haptic braille perception using a touch-screen and vibration on mobile phones," in *Proceedings of the 12th international ACM SIGACCESS conference on Computers and accessibility*, 2010, pp. 295-296.
[412] F. Ramirez-Garibay, C. M. Olivarria, A. F. E. Aguilera, and J. C. Huegel, "MyVox—Device for the communication between people: blind, deaf, deaf-blind and unimpaired," in *Global Humanitarian Technology Conference (GHTC), 2014 IEEE*, 2014, pp. 506-509.
[413] V. Khambadkar and E. Folmer, "A tactile-proprioceptive communication aid for users who are deafblind," in *Haptics Symposium (HAPTICS), 2014 IEEE*, 2014, pp. 239-245.
[414] T. Choudhary, S. Kulkarni, and P. Reddy, "A Braille-based mobile communication and translation glove for deaf-blind people," in *Pervasive Computing (ICPC), 2015 International Conference on*, 2015, pp. 1-4.

[415] H. Nicolau, J. Guerreiro, T. Guerreiro, and L. Carriço, "UbiBraille: designing and evaluating a vibrotactile Braille-reading device," in *Proceedings of the 15th International ACM SIGACCESS Conference on Computers and Accessibility*, 2013, p. 23.

[416] S. Ohtsuka, S. Hasegawa, N. Sasaki, and T. Harakawa, "Communication system between deaf-blind people and non-disabled people using body-braille and infrared communication," in *Consumer Communications and Networking Conference (CCNC), 2010 7th IEEE*, 2010, pp. 1-2.

[417] S. P. Eberhardt, L. E. Bernstein, D. C. Coulter, and L. A. Hunckler, "OMAR a haptic display for speech perception by deaf and deaf-blind individuals," in *Virtual Reality Annual International Symposium, 1993., 1993 IEEE*, 1993, pp. 195-201.

[418] J. P. Kramer, P. Lindener, and W. R. George, "Communication system for deaf, deaf-blind, or non-vocal individuals using instrumented glove," ed: Google Patents, 1991.

[419] R. Sarkar, S. Das, and S. Roy, "SPARSHA: A Low Cost Refreshable Braille for Deaf-Blind People for Communication with Deaf-Blind and Non-disabled Persons," in *International Conference on Distributed Computing and Internet Technology*, 2013, pp. 465-475.

[420] F. Sorgini, A. Mazzoni, L. Massari, R. Caliò, C. Galassi, S. L. Kukreja*, et al.*, "Encapsulation of piezoelectric transducers for sensory augmentation and substitution with wearable haptic devices," *Micromachines,* vol. 8, p. 270, 2017.

[421] N. Caporusso, L. Mkrtchyan, and L. Badia, "A multimodal interface device for online board games designed for sight-impaired people," *IEEE Transactions on Information Technology in Biomedicine,* vol. 14, pp. 248-254, 2010.

[422] R. W. Van Boven, R. H. Hamilton, T. Kauffman, J. P. Keenan, and A. Pascual–Leone, "Tactile spatial resolution in blind Braille readers," *Neurology,* vol. 54, pp. 2230-2236, 2000.

[423] R. Heinrichs and J. Moorhouse, "Touch-perception thresholds in blind diabetic subjects in relation to the reading of Braille type," *New England Journal of Medicine,* vol. 280, pp. 72-75, 1969.

[424] J. C. Stevens, E. Foulke, and M. Q. Patterson, "Tactile acuity, aging, and braille reading in long-term blindness," *Journal of experimental psychology: applied,* vol. 2, p. 91, 1996.

[425] A. C. Grant, M. C. Thiagarajah, and K. Sathian, "Tactile perception in blind Braille readers: a psychophysical study of acuity and hyperacuity using gratings and dot patterns," *Perception & psychophysics,* vol. 62, pp. 301-312, 2000.

[426] M. Hollins, *Understanding blindness: An integrative approach*: Lawrence Erlbaum Associates, Inc, 1989.

[427] M. Goldstein, A. Proctor, L. Bulle, H. Shimuzu, I. Hochberg, H. Levitt*, et al.*, "Tactile stimulation in speech reception: Experience with a nonauditory child," *Speech of the hearing impaired: Research training and personal preparation,* pp. 147-166, 1983.

[428] J. Pickett, "Speech communication for the deaf: visual, tactile, and cochlear-implant," *Journal of rehabilitation research and development,* vol. 23, pp. 95-99, 1986.

[429] S. Reinfeldt, B. Håkansson, H. Taghavi, and M. Eeg-Olofsson, "New developments in bone-conduction hearing implants: a review," *Medical Devices (Auckland, NZ),* vol. 8, p. 79, 2015.

[430] A. Hagr, "BAHA: bone-anchored hearing aid," *International journal of health sciences,* vol. 1, p. 265, 2007.
[431] R. Yawn, J. B. Hunter, A. D. Sweeney, and M. L. Bennett, "Cochlear implantation: a biomechanical prosthesis for hearing loss," *F1000prime reports,* vol. 7, 2015.
[432] R. Biran, D. C. Martin, and P. A. Tresco, "Neuronal cell loss accompanies the brain tissue response to chronically implanted silicon microelectrode arrays," *Experimental neurology,* vol. 195, pp. 115-126, 2005.
[433] D. J. Edell, V. Toi, V. M. McNeil, and L. Clark, "Factors influencing the biocompatibility of insertable silicon microshafts in cerebral cortex," *IEEE Transactions on Biomedical Engineering,* vol. 39, pp. 635-643, 1992.
[434] E. Azemi, C. F. Lagenaur, and X. T. Cui, "The surface immobilization of the neural adhesion molecule L1 on neural probes and its effect on neuronal density and gliosis at the probe/tissue interface," *Biomaterials,* vol. 32, pp. 681-692, 2011.
[435] G. C. McConnell, H. D. Rees, A. I. Levey, C.-A. Gutekunst, R. E. Gross, and R. V. Bellamkonda, "Implanted neural electrodes cause chronic, local inflammation that is correlated with local neurodegeneration," *Journal of neural engineering,* vol. 6, p. 056003, 2009.
[436] D. McCreery, V. Pikov, and P. R. Troyk, "Neuronal loss due to prolonged controlled-current stimulation with chronically implanted microelectrodes in the cat cerebral cortex," *Journal of neural engineering,* vol. 7, p. 036005, 2010.
[437] E. Zrenner, "Will retinal implants restore vision?," *Science,* vol. 295, pp. 1022-1025, 2002.
[438] R. T. Miyamoto, A. M. Robbins, M. J. Osberger, S. L. Todd, A. I. Riley, and K. I. Kirk, "Comparison of multichannel tactile aids and multichannel cochlear implants in children with profound hearing impairments," *The American journal of otology,* vol. 16, pp. 8-13, 1995.
[439] M. N. Somers, "Speech perception abilities in children with cochlear implants or hearing aids," *The American journal of otology,* vol. 12, pp. 174-178, 1991.
[440] H. Tang and D. J. Beebe, "An oral tactile interface for blind navigation," *IEEE Transactions on Neural Systems and Rehabilitation Engineering,* vol. 14, pp. 116-123, 2006.
[441] S. J. Bolanowski Jr, G. A. Gescheider, R. T. Verrillo, and C. M. Checkosky, "Four channels mediate the mechanical aspects of touch," *The Journal of the Acoustical society of America,* vol. 84, pp. 1680-1694, 1988.
[442] S. Weinstein, "Intensive and extensive aspects of tactile sensitivity as a function of body part, sex and laterality," in *the First Int'l symp. on the Skin Senses, 1968*, 1968.
[443] C. C. Collins, "On mobility aids for the blind," in *Electronic spatial sensing for the blind*, ed: Springer, 1985, pp. 35-64.
[444] M. Gori, G. Cappagli, A. Tonelli, G. Baud-Bovy, and S. Finocchietti, "Devices for visually impaired people: High technological devices with low user acceptance and no adaptability for children," *Neuroscience & Biobehavioral Reviews,* vol. 69, pp. 79-88, 2016.
[445] G. H. Saunders and K. V. Echt, "An overview of dual sensory impairment in older adults: perspectives for rehabilitation," *Trends in amplification,* vol. 11, pp. 243-258, 2007.

[446] M. Hersh, "Deafblind people, stigma and the use of communication and mobility assistive devices," *Technology and Disability,* vol. 25, pp. 245-261, 2013.
[447] H.-K. Lee, J. Chung, S.-I. Chang, and E. Yoon, "Normal and shear force measurement using a flexible polymer tactile sensor with embedded multiple capacitors," *Journal of Microelectromechanical Systems,* vol. 17, pp. 934-942, 2008.
[448] T. Ninomiya, Y. Okayama, Y. Matsumoto, X. Arouette, K. Osawa, and N. Miki, "MEMS-based hydraulic displacement amplification mechanism with completely encapsulated liquid," *Sensors and Actuators A: Physical,* vol. 166, pp. 277-282, 2011.
[449] M. Kawazoe, Y. Kosemura, and N. Miki, "Encoding and presentation of surface textures using a mechanotactile display," *Sensors and Actuators A: Physical,* vol. 261, pp. 30-39, 2017.
[450] I. Johnston, D. McCluskey, C. Tan, and M. Tracey, "Mechanical characterization of bulk Sylgard 184 for microfluidics and microengineering," *Journal of Micromechanics and Microengineering,* vol. 24, p. 035017, 2014.
[451] P. Du, I.-K. Lin, H. Lu, and X. Zhang, "Extension of the beam theory for polymer bio-transducers with low aspect ratios and viscoelastic characteristics," *Journal of Micromechanics and Microengineering,* vol. 20, p. 095016, 2010.
[452] E. Gunther and S. O'Modhrain, "Cutaneous grooves: composing for the sense of touch," *Journal of New Music Research,* vol. 32, pp. 369-381, 2003.
[453] R. T. Verrillo, "Psychophysics of vibrotactile stimulation," *The Journal of the Acoustical Society of America,* vol. 77, pp. 225-232, 1985.
[454] A. Grinsted, J. C. Moore, and S. Jevrejeva, "Application of the cross wavelet transform and wavelet coherence to geophysical time series," *Nonlinear processes in geophysics,* vol. 11, pp. 561-566, 2004.
[455] F. Sorgini, R. Ghosh, J. F. Huebotter, R. Caliò, C. Galassi, C. M. Oddo*, et al.*, "Design and preliminary evaluation of haptic devices for upper limb stimulation and integration within a virtual reality cave," in *Biomedical Robotics and Biomechatronics (BioRob), 2016 6th IEEE International Conference on*, 2016, pp. 464-469.
[456] R. Bogacz, E. Brown, J. Moehlis, P. Holmes, and J. D. Cohen, "The physics of optimal decision making: a formal analysis of models of performance in two-alternative forced-choice tasks," *Psychological review,* vol. 113, p. 700, 2006.
[457] C. Pacchierotti, S. Sinclair, M. Solazzi, A. Frisoli, V. Hayward, and D. Prattichizzo, "Wearable haptic systems for the fingertip and the hand: Taxonomy, review, and perspectives," *IEEE transactions on haptics,* vol. 10, pp. 580-600, 2017.
[458] C. Cipriani, J. L. Segil, F. Clemente, and B. Edin, "Humans can integrate feedback of discrete events in their sensorimotor control of a robotic hand," *Experimental brain research,* vol. 232, pp. 3421-3429, 2014.
[459] C. Antfolk, M. D'Alonzo, B. Rosén, G. Lundborg, F. Sebelius, and C. Cipriani, "Sensory feedback in upper limb prosthetics," *Expert review of medical devices,* vol. 10, pp. 45-54, 2013.
[460] C. Antfolk, M. D'Alonzo, M. Controzzi, G. Lundborg, B. Rosén, F. Sebelius*, et al.*, "Artificial redirection of sensation from prosthetic fingers to the phantom hand map on transradial amputees: vibrotactile versus mechanotactile sensory feedback," *IEEE transactions on neural systems and rehabilitation engineering,* vol. 21, pp. 112-120, 2013.

[461] G. Sziebig, B. Solvang, C. Kiss, and P. Korondi, "Vibro-tactile feedback for VR systems," in *Human System Interactions, 2009. HSI'09. 2nd Conference on*, 2009, pp. 406-410.
[462] A. Alahakone and S. A. Senanayake, "Vibrotactile feedback systems: Current trends in rehabilitation, sports and information display," in *Advanced Intelligent Mechatronics, 2009. AIM 2009. IEEE/ASME International Conference on*, 2009, pp. 1148-1153.
[463] T. Yamamoto, N. Abolhassani, S. Jung, A. M. Okamura, and T. N. Judkins, "Augmented reality and haptic interfaces for robot-assisted surgery," *The International Journal of Medical Robotics and Computer Assisted Surgery,* vol. 8, pp. 45-56, 2012.
[464] S. Choi and K. J. Kuchenbecker, "Vibrotactile display: Perception, technology, and applications," *Proceedings of the IEEE,* vol. 101, pp. 2093-2104, 2013.
[465] J. Sibert, J. Cooper, C. Covington, A. Stefanovski, D. Thompson, and R. W. Lindeman, "Vibrotactile feedback for enhanced control of urban search and rescue robots," in *Proc. of the IEEE Symp. on Safety, Security and Rescue Robots*, 2006, pp. 22-24.
[466] G. Burdea and J. Zhuang, "Dextrous telerobotics with force feedback–an overview. Part 1: Human factors," *Robotica,* vol. 9, pp. 171-178, 1991.
[467] M. Slater and S. Wilbur, "A framework for immersive virtual environments (FIVE): Speculations on the role of presence in virtual environments," *Presence: Teleoperators & Virtual Environments,* vol. 6, pp. 603-616, 1997.
[468] A. Amer and P. Peralez, "Affordable altered perspectives: Making augmented and virtual reality technology accessible," in *Global Humanitarian Technology Conference (GHTC), 2014 IEEE*, 2014, pp. 603-608.
[469] C. Cruz-Neira, D. J. Sandin, T. A. DeFanti, R. V. Kenyon, and J. C. Hart, "The CAVE: audio visual experience automatic virtual environment," *Communications of the ACM,* vol. 35, pp. 64-73, 1992.
[470] S. Jeon and S. Choi, "Haptic augmented reality: Taxonomy and an example of stiffness modulation," *Presence: Teleoperators and Virtual Environments,* vol. 18, pp. 387-408, 2009.
[471] A. S. Mathur, "Low cost virtual reality for medical training," in *Virtual Reality (VR), 2015 IEEE*, 2015, pp. 345-346.
[472] J. Nishida, K. Nakai, A. Matsushita, and K. Suzuki, "Haptic Augmentation of Surgical Operation Using a Passive Hand Exoskeleton," in *Haptic Interaction*, ed: Springer, 2015, pp. 237-243.
[473] A. S. Merians and G. G. Fluet, "Rehabilitation applications using virtual reality for persons with residual impairments following stroke," in *Virtual Reality for Physical and Motor Rehabilitation*, ed: Springer, 2014, pp. 119-144.
[474] R. B. Hellman, E. Chang, J. Tanner, S. I. Helms Tillery, and V. J. Santos, "A robot hand testbed designed for enhancing embodiment and functional neurorehabilitation of body schema in subjects with upper limb impairment or loss," *Frontiers in human neuroscience,* vol. 9, p. 26, 2015.
[475] S. Jeon and M. Harders, "Haptic tumor augmentation: exploring multi-point interaction," *IEEE transactions on haptics,* vol. 7, pp. 477-485, 2014.
[476] C. Strub, F. Wörgötter, H. Ritter, and Y. Sandamirskaya, "Using haptics to extract object shape from rotational manipulations," in *Intelligent Robots and Systems (IROS 2014), 2014 IEEE/RSJ International Conference on*, 2014, pp. 2179-2186.

[477] G. Luo and E. Peli, "Use of an augmented-vision device for visual search by patients with tunnel vision," *Investigative ophthalmology & visual science,* vol. 47, pp. 4152-4159, 2006.
[478] M. A. Muhanna, "Virtual reality and the CAVE: Taxonomy, interaction challenges and research directions," *Journal of King Saud University-Computer and Information Sciences,* vol. 27, pp. 344-361, 2015.
[479] P. Galambos and P. Baranyi, "Vibrotactile force feedback for telemanipulation: Concept and applications," in *Cognitive Infocommunications (CogInfoCom), 2011 2nd International Conference on*, 2011, pp. 1-6.
[480] M. Bouzit, G. Burdea, G. Popescu, and R. Boian, "The Rutgers Master II-new design force-feedback glove," *IEEE/ASME Transactions on mechatronics,* vol. 7, pp. 256-263, 2002.
[481] J. Wither, S. DiVerdi, and T. Höllerer, "Annotation in outdoor augmented reality," *Computers & Graphics,* vol. 33, pp. 679-689, 2009.
[482] R. Rosenholtz, Y. Li, and L. Nakano, "Measuring visual clutter," *Journal of vision,* vol. 7, pp. 17-17, 2007.
[483] W. Lu, H. B.-L. Duh, S. Feiner, and Q. Zhao, "Attributes of subtle cues for facilitating visual search in augmented reality," *IEEE transactions on visualization and computer graphics,* vol. 20, pp. 404-412, 2014.
[484] G. Airò Farulla, D. Pianu, M. Cempini, M. Cortese, L. O. Russo, M. Indaco*, et al.*, "Vision-based pose estimation for robot-mediated hand telerehabilitation," *Sensors,* vol. 16, p. 208, 2016.
[485] P. Lichtsteiner, C. Posch, and T. Delbruck, "A 128× 128 120 dB 15 μs Latency Asynchronous Temporal Contrast Vision Sensor," *IEEE Journal of Solid-State Circuits,* vol. 43, pp. 566-576, 2008.